1967

Kilocycle range dislocation damping in dilute magnesium alloy single crystals

Robert Ray Nothdurft

Department: Physics

KILOCYCLE RANGE DISLOCATION DAMPING IN DILUTE MAGNESIUM ALLOY SINGLE CRYSTALS

by

ROBERT RAY NOTHDURFT, 1931

A DISSERTATION

Presented to the Faculty of the Graduate School of the

UNIVERSITY OF MISSOURI AT ROLLA

In Partial Fulfillment of the Requirements for the Degree

DOCTOR OF PHILOSOPHY

1967

Harry B. Brown
Advisor

Harold Q. Fuller

O. W. Johnson

LeRoy R. Furlong

Lauri V. Gund

ABSTRACT

The kilocycle range dislocation damping and Young's modulus of single crystals of magnesium and single crystals of magnesium containing small additions of lithium, zinc, or aluminum have been studied as a function of strain amplitude, temperature, and time during annealing and following a high strain amplitude vibration.

The data are compared to the Granato-Lücke theory of dislocation damping, the Granato-Hikata-Lücke theory for the recovery of damping following plastic deformation, and the Yamafuji-Bauer theory for the recovery of damping following a high strain amplitude vibration.

Reasonable qualitative agreement is obtained between the Granato-Lücke theory and the observed dependence of the damping and modulus on strain amplitude and temperature. Reasonable quantitative values for the dislocation density, network node loop length, and activation energy for the migration of vacancies in magnesium are obtained.

It is found that in order to get agreement with the decay of the damping during annealing at high temperature, it is necessary to modify the Granato-Hikata-Lücke theory. This is accomplished by replacing the Cottrell-Bilby expression for the segregation of pinning points to dislocations by an expression suggested by Harper to account for longer times.

The observed dependence of the damping on composition does not agree with the Granato-Lücke predictions. A possible explanation for this discrepancy is offered.

Several new phenomena that were observed are described and discussed.

ACKNOWLEDGEMENTS

The author wishes to express his gratitude to the United States Department of the Interior, Bureau of Mines and the University of Missouri at Rolla for providing him the fellowship for the entire investigation.

Special appreciation is expressed to the Rolla Metallurgy Research Center, Rolla, Missouri for providing the space, equipment, supplies and services necessary for the research. In particular, he wishes to thank the following service groups at the Rolla Metallurgy Research Center: The Machine Shop, the X-ray Diffraction Laboratory, the Analytical Laboratory, and the Metallographic Laboratory.

He is also indebted to the following individuals:

Dr. Robert Gerson, Dr. H. P. Leighly Jr. and Dr. LeRoy Furlong for reading the thesis and providing helpful suggestions;

Mr. Alfred E. Schwaneke, for constant guidance, stimulating discussions and unfailing encouragement;

Mr. James W. Jensen, who supervised the investigation;

Mr. Robert W. Nash, who provided helpful suggestions, assisted in the maintenance of the electronic equipment and was a constant source of encouragement;

and Dr. A. V. Granato, for helpful suggestions and discussions.

The author is especially indebted to his wife for her patience, endurance, encouragement, and help in typing the manuscript.

Finally, the author wishes to dedicate this thesis to his parents, Mr. and Mrs. Burton H. Nothdurft.

TABLE OF CONTENTS

LIST OF FIGURES

LIST OF TABLES

LIST OF SYMBOLS

A parameter related to the force between a solute atom and a dislocation; defined completely in the Appendix.

A_1 pre-exponential constant in the expression for the dependence of the damping on strain amplitude and equal to the intercept of a G-L plot; defined completely on page 8.

A_2 constant in the exponential of the expression for the dependence of the damping on strain amplitude and equal to the absolute value of the slope of a G-L plot; defined completely on page 8.

A_3 constant in the expression for the independent decrement; defined completely on page 9.

A_4 constant in the expression for the independent modulus change; defined completely on page 9.

A_q constant in the equation for the decrement of the composite oscillator as a function of strain amplitude and temperature; see page 22.

a basal plane lattice parameter or Burger's vector; see Appendix.

B damping constant for the moving dislocation; defined completely in the Appendix.

B_q constant in the equation for the decrement of the composite oscillator as a function of strain amplitude and temperature; see page 22.

C total local concentration of minor pinning points on the dislocation lines after equilibrium is established, or when time equals infinity; equal to a/L_c .

C_o overall concentration of point defects in the lattice.

C_1 local concentration of type 1 point defects on the dislocations after equilibrium is established, or when time equals infinity.

C_2 local concentration of type 2 point defects on the dislocations after equilibrium is established, or when time equals infinity.

C_{10} overall concentration of type 1 point defects in the lattice.

C_{20} overall concentration of type 2 point defects in the lattice.

C_{44} elastic stiffness constant for magnesium.

$C(t)$ total local concentration of minor pinning points on the dislocations at any time (t).

$C_1(t)$ local concentration of type 1 point defects on the dislocations at any time (t).

$C_2(t)$ local concentration of type 2 point defects on the dislocations at any time (t).

C_q constant in the equation for the decrement of the composite oscillator as a function of strain amplitude and temperature; see page 22.

C' dislocation line tension; defined completely in the Appendix.

$\bar{c}$ Fermi velocity of electrons; defined completely in the Appendix.

c_p specific heat at constant pressure.

c_v specific heat at constant volume.

D diffusion coefficient for point defect diffusion.

D_o frequency factor for point defect diffusion.

D^d pipe diffusion coefficient for point defect diffusion along dislocations.

D_o^d frequency factor or pre-exponential term in the expression for the pipe diffusion coefficient.

D_q constant in the expression for the frequency of the composite oscillator as a function of temperature; see page

d atomic diameter of the magnesium atom.

d_o atomic diameter of solute atom.

E measured Young's modulus.

E_e true elastic Young's modulus.

E_I measured Young's modulus at low strain amplitude.

$E(\theta)$ Young's modulus for a particular orientation (θ) in magnesium.

E' internal energy calculated from the Debye theory; see Appendix.

$\Delta E/E$ total fractional change in Young's modulus; equal to $(E_e-E)/E_e$

$(\Delta E/E)_H$ strain amplitude dependent fractional modulus change equal to $(E-E_I)/E$

$(\Delta E/E)_I$ strain amplitude independent fractional modulus change equal to $(E_e-E_I)/E_e$

Q interaction energy between a point defect and a dislocation.

Q_1 interaction energy between a type 1 point defect and a dislocation.

Q_2 interaction energy between a type 2 point defect and a dislocation.

R resolved shear stress factor = $\sin\theta\cos\theta\cos\phi$.

R_i resolved shear stress factor for the ith slip system.

r constant of proportionality between $(\Delta E/E)_H$ and Δ_H ; of the order unity.

r_o atomic radius of solvent (magnesium) atom.

S experimental absolute value of the slope of a G-L plot.

S_B vibrational entropy of a pinned dislocation.

S_{44} elastic compliance constant for magnesium.

T absolute temperature: in some cases, centigrade temperature where designated.

t time.

U activation energy for the migration of point defects in the lattice.

U^d activation energy for the migration of point defects along dislocations.

U_B binding potential energy between a solute atom and a dislocation; $= -Q$.

v_s shear wave velocity = $(C_{44}/\rho)^{1/2}$

X_b distance the solute atom is away from the dislocation line when breakaway occurs.

x represents the quantity in the exponential term in the Harper modified G-H-L equation; $= -\lambda$, see page 47.

Z number of atoms per unit cell.

α constant = $3(\pi/2)^{1/2}$.

α_o coefficient of linear expansion.

β parameter in the Cottrell-Bilby form of the G-H-L equations equal to $(C_{10}\sqrt{2}\alpha/C_{20}a^2)(AD/kT)^{2/3}$.

β_o bulk modulus.

β' electronic heat capacity coefficient.

γ parameter in the Harper modified G-H-L equation given by $C_{10}\sqrt{2}/C_{20}a^2\Lambda$ and later equal to $C_1/(C_2+a/L_N)$.

Δ total specimen decrement equal to $\Delta_I + \Delta_H$.

Δ_b background decrement of the specimen.

Δ_H strain amplitude dependent part of the specimen decrement.

Δ_I strain amplitude independent part of the specimen decrement.

$\Delta_I(0)$ value of the independent decrement at time equal zero; equal to A_3a^4/C_{20}^4 and later equal to $A_3a^4/(C_2+a/L_N)^4$.

$\Delta_I(\infty)$ value of the independent decrement at time equal infinity; equal to $A_3a^4/C_{20}^4(1+\gamma)^4$ and later equal to $A_3a^4/(C_2+a/L_N)^4(1+\gamma)^4$.

Δ_q decrement of the composite oscillator with no specimen attached.

ε_o maximum strain amplitude in the specimen.

ε_b value of the strain amplitude when breakaway occurs and the decrement becomes dependent on strain amplitude.

ε_c value of the strain amplitude when the decrement suddenly jumps to a larger value; see page 31.

η misfit parameter or fractional change in the lattice constant with a change in solute concentration.

Θ Debye temperature.

θ angle between the normal to the basal plane of the hexagonal crystal structure and the cylinder axis of the specimen.

κ thermal diffusivity; see Appendix.

Λ dislocation density or total length of dislocation line per unit volume.

Λ_i dislocation density for the ith slip system.

λ parameter equal to the quantity in the exponential term in the modified G-H-L equation equal to $\alpha\Lambda(AD/kT)^{2/3}$.

ν Poisson's ratio.

ρ density of the specimen.

τ relaxation time in the Yamafuji-Bauer theory; see page 62.

ϕ angle between the slip direction and the projection of the cylinder axis on the basal plane of the hexagonal crystal structure.

χ parameter in the Harper modified G-H-L equation for the dependence of the independent modulus change on time and equal to $A_4a^2/2C_{20}^2$ and later equal to $A_4a^2/2(C_2+a/L_N)^2$.

Ω orientation factor; defined completely in the Appendix.

ω circular frequency of the specimen $= 2\pi f$

I. INTRODUCTION

A. Statement of Problem

Since the suggestion by T. A. Read[1] in 1940 that the dissipation of mechanical energy within a vibrating solid (internal friction) could be attributed to the motion of dislocations (now termed dislocation damping), research on dislocation damping has progressed from studies of the phenomenon itself to the use of damping as a tool in the study of defects in solids. This change was made possible largely by a successful theory of dislocation damping published in 1956 by Granato and Lücke.[2] This theory placed the interpretation of damping data on a quantitative basis. It is now possible to predict reasonable values of dislocation density, point defect concentration, diffusion coefficients and other parameters involved in dislocation point defect interactions from a measurement of the dislocation damping of the material.

In order to determine quantitative values for all of the parameters in the Granato-Lücke theory, it is necessary to measure the dislocation damping and Young's modulus as a function of strain amplitude, temperature and time for the same specimen. A comprehensive study of a single sample is desired because the damping is so sensitive to conditions that cannot be controlled or evaluated such as mechanical and thermal history, and handling.[3]

There is a general lack of experiments in the literature in which enough parameters were systematically varied for the same sample to provide a complete check of all the predictions of the theory. In most experiments, only a few parameters were varied and usually the range of variation of each parameter was small.

B. Purpose of the Investigation

The investigation reported in this thesis was undertaken with the above need for a comprehensive study of dislocation damping in mind. The specific objective of the research was to interpret the dislocation damping data quantitatively in terms of the Granato-Lücke theory to determine a) whether the theory was consistent with the data and b) whether the predicted values of dislocation density, impurity concentration, activation energy, and other constants were reasonable and in agreement with known values in the crystal. It was also hoped that the results might make it possible to identify the nature of the point defects involved in the dislocation damping.

C. Method Used to Meet Objectives

An ideal experiment would be one in which the dislocation damping of a single specimen is studied as a function of strain amplitude, temperature, impurity concentration, frequency, orientation, recovery time after plastic deformation and possibly irradiation. It is nearly impossible to achieve this ideal for several reasons. First, a measurement of the damping as a function of frequency from the 1 cycle per second range to the megacycle range for the same specimen is nearly prevented because of measuring techniques. In the 1 cycle per second range the torsion pendulum method is used. In the kilocycle range the resonant bar method is usually employed, while in the megacycle range the pulse-echo technique is used. The physical size and shape of the specimen vary for each of these three frequency ranges. Size and shape requirements also hinder the variation of the orientation for the same specimen, although it can be studied to some extent in the megacycle range. Variation of the impurity concentration for the same specimen over a very wide range would also present considerable difficulties.

As a compromise to the above ideal, it was decided to measure the dislocation damping and Young's modulus of magnesium single crystals at approximately 33 kilocycles per second as a function of strain amplitude from about 10^{-8} to 10^{-5}, as a function of temperature from approximately 25° C to 280° C, and as a function of annealing time and recovery time following a high strain amplitude vibration. Single crystals of magnesium containing small additions of aluminum, zinc, or lithium were also studied to determine the effect of known amounts of metal impurity atoms on the dislocation damping.

II. LITERATURE REVIEW

A. General Background

Damping in a solid containing dislocations results from a viscous drag on the dislocation as it moves through the lattice. In addition there is an effective decrease in the modulus of elasticity since the dislocation strain will add to the elastic lattice strain. The exact mechanism by which the dislocation is viscously damped is still somewhat obscure but recent evidence strongly indicates it is due to scattering of phonons by the moving dislocations.[4]

It was recognized early that the theoretically predicted damping would be much larger than that observed if the dislocation motion were not restricted in some manner. All of the existing dislocation damping theories assume some type of restrictive mechanism. The restrictive mechanisms vary from Peierls barriers in the theory of the Bordoni peak damping[5] in plastically deformed face-centered-cubic metals at low temperature, to point defects which pin the dislocation in the Granato-Lücke theory.

Although other dislocation damping theories have been advanced by Koehler[6], Nowick[7], and Weertman[8], none of these has received the wide acceptance that the Granato-Lücke theory has received. Also, some of their predictions are not substantiated by the experimental data. The Granato-Lücke theory has been successful in explaining nearly all of the dislocation damping data to date (other than the Bordoni peak damping) with the exception of data obtained from materials that were exceptionally pure or highly deformed. For this reason the review here will be limited to a brief description of the Granato-Lücke theory and its experimental consequences.

B. The Granato-Lücke Theory

1. The Model. A detailed review of the Granato-Lücke theory will not be presented here because several detailed reviews of the theory are available in the literature.[9,10,11] However, the results of the theory will be briefly summarized for the benefit of the reader.

The theory is based on an earlier model by Koehler[6] in which the dislocation is considered to be pinned by two types of pinning points. The first type are known as major pinning points and are caused by dislocation network nodes. The second type are known as minor pinning points and are presumably impurity atoms or vacancies in the lattice. When an oscillatory stress is applied to the sample, the dislocations vibrate between the pinning points much like a stretched string in a viscous medium. Figure 1(a) shows a dislocation of length L_N pinned by a number of minor pinning points separated by an average distance, L_c. If a small vibratory stress is applied, fig. 1(b), the dislocation will bow out slightly in the slip plane which is the plane of the paper in this figure. If the stress is reduced to zero at this point, the dislocation will return elastically to its unstressed position. However, if the maximum stress in the first quarter cycle is great enough to unpin the dislocation from one of the minor pinning points (fig. 1(c)), then the whole line will unpin catastrophically as shown in fig. 1(d). This catastrophic unpinning is designated as "breakaway". If the stress is now increased further, the dislocation will continue to bow out as shown in fig. 1(e). However, in this case it is pinned at its ends by the major pinning points (network nodes) and will therefore have a smaller restoring force. It is assumed that the stress is never

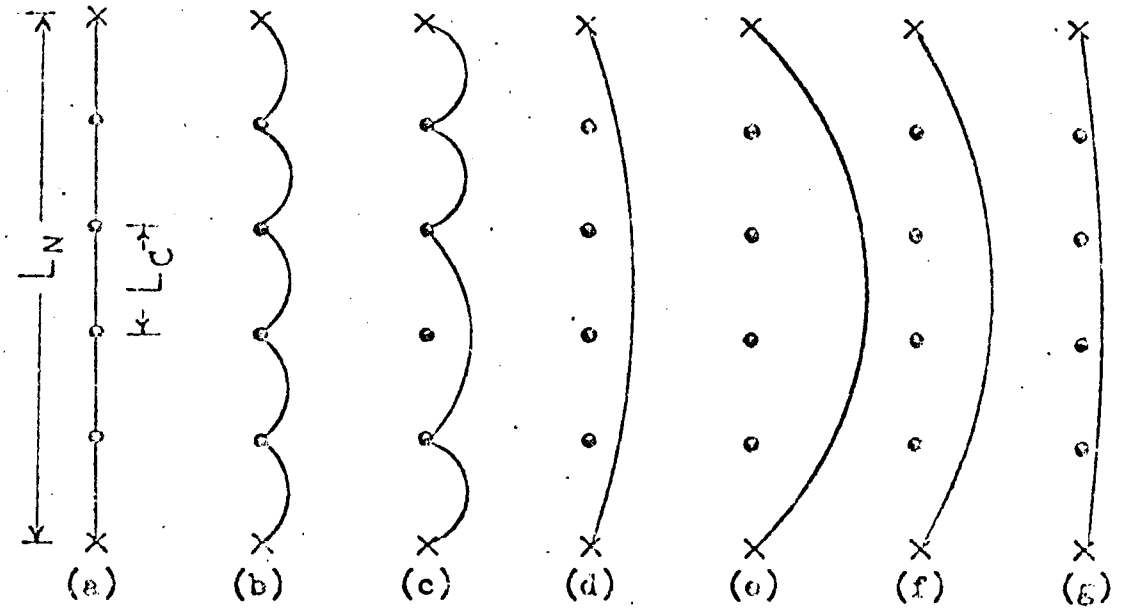

Figure 1. Schematic representation of the motion of a pinned dislocation under an increasing and decreasing stress

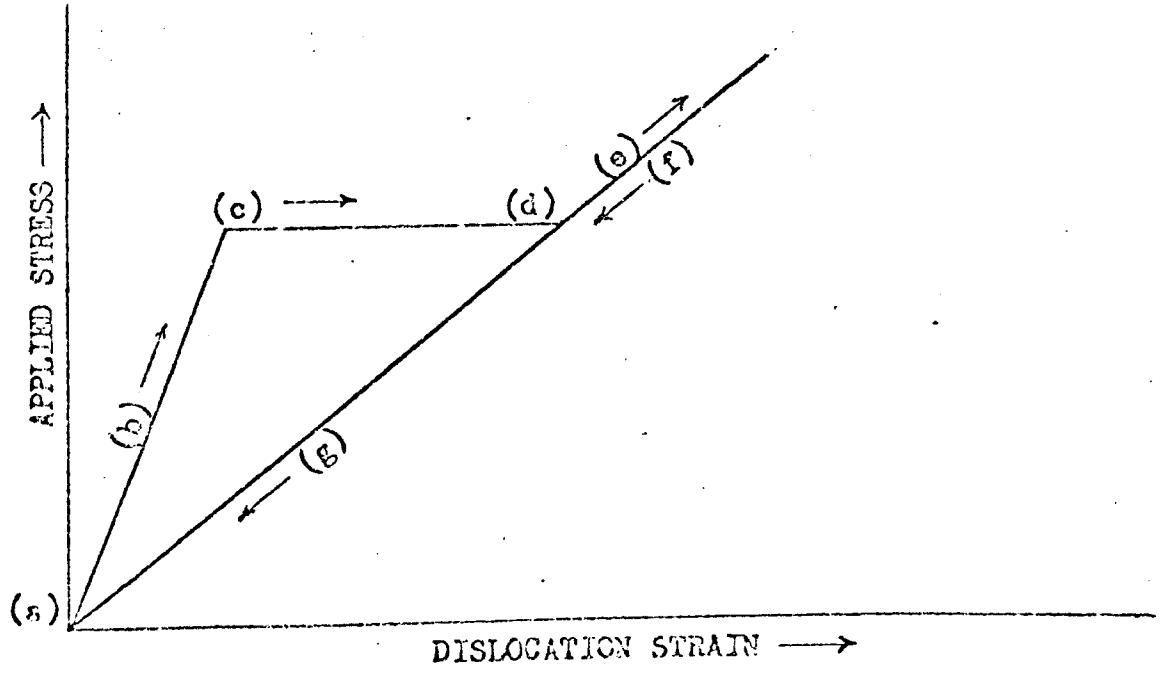

Figure 2. Approximate stress-strain curve resulting from the model of a pinned dislocation

sufficient to pull the dislocation away from the network nodes. If the stress is decreased to zero, the dislocation will return to its unstressed position in the manner of fig. 1 (f) and fig. 1 (g).

It is then assumed that the dislocation is repinned at zero stress and the process begins again on the third quarter cycle.

Figure 2 shows the approximate stress-strain curve resulting from the unpinning process illustrated in figs. 1 (a) to 1 (g). Each part of the graph in fig. 2 is labeled with the letter of the illustration in fig. 1 to which it corresponds. The curve follows different paths for increasing and decreasing stress due to the different restoring forces before and after unpinning. Only the dislocation strain is shown in fig. 2, the elastic lattice strain having been subtracted out.

This model predicts that the damping, Δ , and modulus change, $\Delta E/E$, will be of two types. The first loss results from the viscous damping of the dislocation as it moves while still being pinned by the minor pinning points. This loss is independent of the strain-amplitude but is frequency dependent. It is predicted that this strain-amplitude independent decrement (hereafter referred to as the independent decrement, Δ_I) will have a maximum value at the resonant frequency of the dislocation and it is estimated that this will occur in the megacycle range.[12] The second loss arises when the strain amplitude is sufficient to break the dislocation away from the minor pinning points. The large increase in strain at breakaway for no increase in stress results in a hysteresis loss that is dependent on the strain amplitude. This loss is referred to as the dependent decrement, Δ_H, and is proportional to the area

inside the stress-strain cycle shown in fig. 2. Thus the damping observed is given by the sum of these two losses, $\Delta = \Delta_I + \Delta_H$.

2. Predicted Dependence on Strain Amplitude. At kilocycle frequencies and for a specimen vibrating longitudinally in resonance, the dependence of the damping on strain amplitude is given by,[13]

$$\Delta_H = (A_1/\varepsilon_o^{1/2}) \exp(-A_2/\varepsilon_o) \qquad (1)$$

where $A_1 = (\Omega\Lambda L_N^3/\pi^2)(2K\eta a/\pi L_c^3)^{1/2}$ and $A_2 = K\eta a/L_c$

In the above expressions,

ε_o is the maximum strain amplitude,

Ω is an orientation factor,

Λ is the dislocation density,

L_N is the average distance between major pinning points or network nodes,

K is a parameter related to the force required to produce breakaway and is also dependent on orientation,

η is the misfit parameter,

a is the lattice parameter,

and L_c is the average distance between minor pinning points.

The associated strain amplitude dependent fractional modulus change is given by $(\Delta E/E)_H = r\,\Delta_H$ where $(\Delta E/E)_H$ is the ratio of the difference between the modulus measured at any strain amplitude and the modulus measured at low strain amplitudes to the modulus measured at any strain amplitude, and r is a constant of order unity.

The damping and modulus change observed at low strain amplitudes are independent of strain amplitude and at kilocycle frequencies are given by,[14]

$$\Delta_I = A_3 L^4 \qquad (2)$$

$$(\Delta E/E)_I = A_4 L^2 \qquad (3)$$

where $A_3 = 120\Omega\Lambda B\omega/\pi^3 C'$, and $A_4 = 6\Omega\Lambda/\pi^2$.

In the above equations, $(\Delta E/E)_I$ is the ratio of the difference between the true elastic modulus and the measured modulus to the true elastic modulus, L is the average loop length including both the major and minor pinning points and is given by $1/L = 1/L_c + 1/L_N$, B is the damping constant for dislocation motion, ω is equal to 2π times the resonant frequency of the specimen, and C' is the dislocation line tension.

An evaluation of the above constants, as well as the exact forms for Ω , K , and C', is presented in the Appendix for the case of magnesium single crystals.

The dependence of the damping on strain amplitude can be tested by writing equation (1) in the linear form;

$$\ln[(\Delta-\Delta_I)\varepsilon_o^{1/2}] = \ln(\Delta_H\varepsilon_o^{1/2}) = \ln A_1 - A_2(1/\varepsilon_o)$$

and a plot of $\ln(\Delta_H\varepsilon_o^{1/2})$ vs $1/\varepsilon_o$ should yield a straight line with slope of absolute value, $S = A_2$ and intercept, $I = \ln A_1$. This type of plot is known as a Granato-Lücke (G-L) plot. In general, quite good agreement is obtained for the strain amplitude dependence of the damping.[9] G-L plots are quite numerous in the literature and linear plots are obtained for materials that are not too pure and not highly deformed. However, curved plots have been noted for some dilute alloys.[15,16]

3. Predicted Dependence on Temperature. The temperature dependence of the damping can be predicted from the dependence of the population of pinning points on temperature. It is generally assumed that the dislocation is surrounded by a Cottrell atmosphere of pinning points that are in equilibrium at a temperature T and

given by the following equation,[17] $C = C_o \exp(Q/kT)$ where Q is the interaction energy between a pinning point and a dislocation, C_o is the overall point defect concentration in the sample, and kT has its usual meaning. The dislocation damping should depend on temperature through the loop length, L_c, which is related to the point defect concentration, C, by $C = a/L_c$.

Therefore, the slope of a G-L plot should depend on temperature in the following manner: $S = KnC_o \exp(Q/kT)$. Thus plots of $\ln S$ vs $1/T$ should be linear with slope Q/k and intercept $\ln KnC_o$. This has been verified by a number of people and values of Q range from 0.3 eV for lead[18] to 1.6 eV for aluminum.[19] The intercept of a plot like the above gives a value for the constant K if C_o is known.

If the temperature dependence of the major pinning points is neglected $(L = L_c)$, the temperature dependence of the independent decrement and fractional modulus change will be given by:

$$\Delta_1 = (A_3 a^4/C_o^4) \exp(-4Q/kT)$$

$$(\Delta E/E)_1 = (A_4 a^2/C_o^2) \exp(-2Q/kT)$$

A plot of $\ln \Delta_1$ vs $1/T$ should be linear with a slope, $-4Q/k$ and an intercept, $\ln(A_3 a^4/C_o^4)$. Also, a plot of $\ln (\Delta E/E)_1$ vs $1/T$ should be linear with a slope, $-2Q/k$ and an intercept, $\ln(A_4 a^2/C_o^2)$.

4. Predicted Dependence on Time. In 1958, Granato, Hikata and Lücke[14] (G-H-L) published a theory for the recovery of the dislocation damping and modulus change in a plastically deformed solid. The theory was based on the assumption that during plastic deformation the number of dislocations is increased, causing an increase in the damping and recovery occurs as point defects created by the deformation migrate to the dislocations, pinning them and therefore immobilizing them.

Other interpretations as to what occurs during recovery have also been advanced. Smith[20] assumes that the number of dislocations formed by the plastic deformation is reduced by mutual annihilation of the dislocations. Nowick[21] assumes the dislocations become immobilized by dislocation rearrangement. However no model has been constructed to permit experimental checks.

For the case of the G-H-L theory, the decrease in damping is described by the decrease in loop length L. The decrease of L with time is obtained from the Cottrell-Bilby strain aging law. This law, derived by Cottrell and Bilby[22] in 1949, gives the number of point defects that have diffused to the dislocations after a time, t, per unit dislocation length as:

$$n(t) = n_o \alpha \Lambda (ADt/kT)^{2/3} \tag{4}$$

where n_o is the number of point defects in the lattice per unit volume,

$\alpha = 3(\pi/2)^{1/2}$

Λ is the dislocation density,

A is a parameter related to the force between a pinning point and a dislocation,

and D is the diffusion coefficient given by $D = D_o \exp(-U/kT)$ where D_o is the frequency factor, and U is the activation energy.

In terms of concentrations, $n_o = C_o N$ where N is the number of atoms per unit volume, and $n(t) = \Lambda/L_c = C(t)\Lambda/a$. For ideal hcp structures, $N\sqrt{2}a^3 = 2$ where a is the basal plane lattice parameter. Therefore, $C(t) = (C_o \sqrt{2}\alpha/a^2)\ (ADt/kT)^{2/3}$.

G-H-L assume two types of defects, one mobile, whose concentration is given by $C_1(t)$, and the other immobile, whose concentration is

given by C_2 . The total loop length is given by,

$$1/L = 1/L_N + C_1(t)/a + C_2/a \tag{5}$$

If we substitute $C_1(t) = (C_{10}\sqrt{2}\alpha/a^2)(ADt/kT)^{2/3}$ and $C_2 = C_{20}$ in this expression for L and neglect the number of network node points we obtain:

$$L = a/[C_{20}(\ 1 + \beta t^{2/3})]$$

where C_{10} and C_{20} are the overall concentrations of type 1 and type 2 point defects, respectively, and $= (C_{10}\sqrt{2}\alpha/C_{20}a^2)(AD/kT)^{2/3}$. This expression for L may be substituted in equations (1), (2), and (3) to give the dependence of the damping and modulus change on time following a plastic deformation. We obtain:

$$\Delta_H = (A_1/\varepsilon_o^{1/2})\ \exp[-(Kn C_{20}/\varepsilon_o)(\ 1 + \beta t^{2/3})] \tag{6}$$

$$\Delta_1 = A_3 a^4/[C_{20}^4(\ 1 + \beta t^{2/3})]^4 \tag{7}$$

$$(\Delta E/E)_1 = A_4 a^2/[C_{20}^2(\ 1 + \beta t^{2/3})]^2 \tag{8}$$

In equation (6) the time dependence of A_1 is neglected with respect to that of the exponential. These equations were applied by G-H-L to recovery data on Na Cl by Gordon and Nowick,[23] on copper by Smith,[20] on zinc by Alers,[24] and on aluminum by Hikata et al,[25] Hikata and Truell,[26] and Köster.[27] Only the Na Cl data were complete enough to permit a full check of all the equations. Smith's data are for the recovery of the modulus only and not the damping, and Alers, Hikata et al, and Hikata and Truell did not report the modulus recovery. Köster reported the recovery of both the damping and modulus. However, the frequency of vibration was too low to consider the damping a dynamic loss. Also, insufficient data points points were reported to allow an accurate check.

In general, the above data agrees reasonably well with the theory except for recovery data obtained after an extremely small deformation for zinc, and a rather large (8.4%) deformation for copper.

III. EXPERIMENTAL CONSIDERATIONS

A. Crystal Preparation

1. Description of Equipment. The pure magnesium and magnesium base alloy single crystals were grown by the Bridgman technique in an apparatus described in detail previously.[28] The major components of the crystal growing apparatus are shown in fig. 3 and consist of two separate vertical furnaces, one placed on top of the other, a long alumina tube containing a graphite crucible at the bottom, and a mechanism for lowering the tube down through the furnaces.

2. Growing Procedure. The procedure followed to grow the pure magnesium crystals has been described in detail previously.[28] The alloy crystals were seeded so that all of them would possess the same orientation. The seeding was accomplished by using a special graphite crucible shown in fig. 4. The seed was obtained from a previously grown single crystal having the desired orientation. Each magnesium alloy rod stock was machined to fit the crucible exactly for filling purposes, and prior to each run the rod stock and the seed to be used were cleaned in dilute HCl, rinsed with acetone and air dried. The seed and rod stock were placed in the graphite crucible and this entire assembly was inserted into the alumina tube and evacuation begun. The assembly was kept under vacuum (10 microns) at 400° C for 8 hours before the crystal run began. At the start of each run, the furnace temperatures and position of the alumina tube were adjusted to permit partial melting of the seed. The tube was then lowered into the bottom furnace at the rate of .75 in/hr.

Because of the high vapor pressure of magnesium, the crystals were grown in helium at approximately atmospheric pressure. It was found that to obtain fonding between the melted portion of the seed

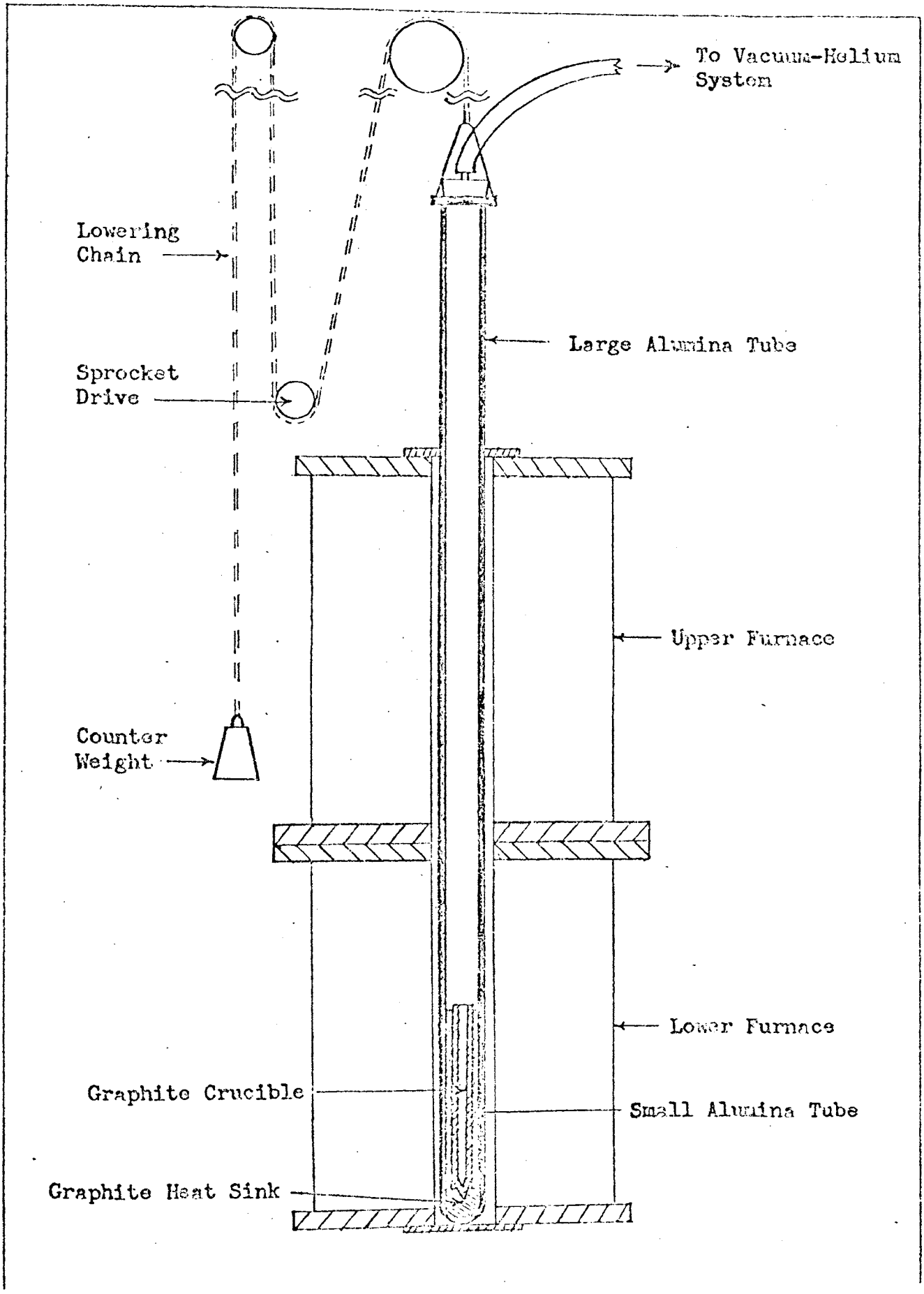

Figure 3. Functional diagram of the crystal growing apparatus

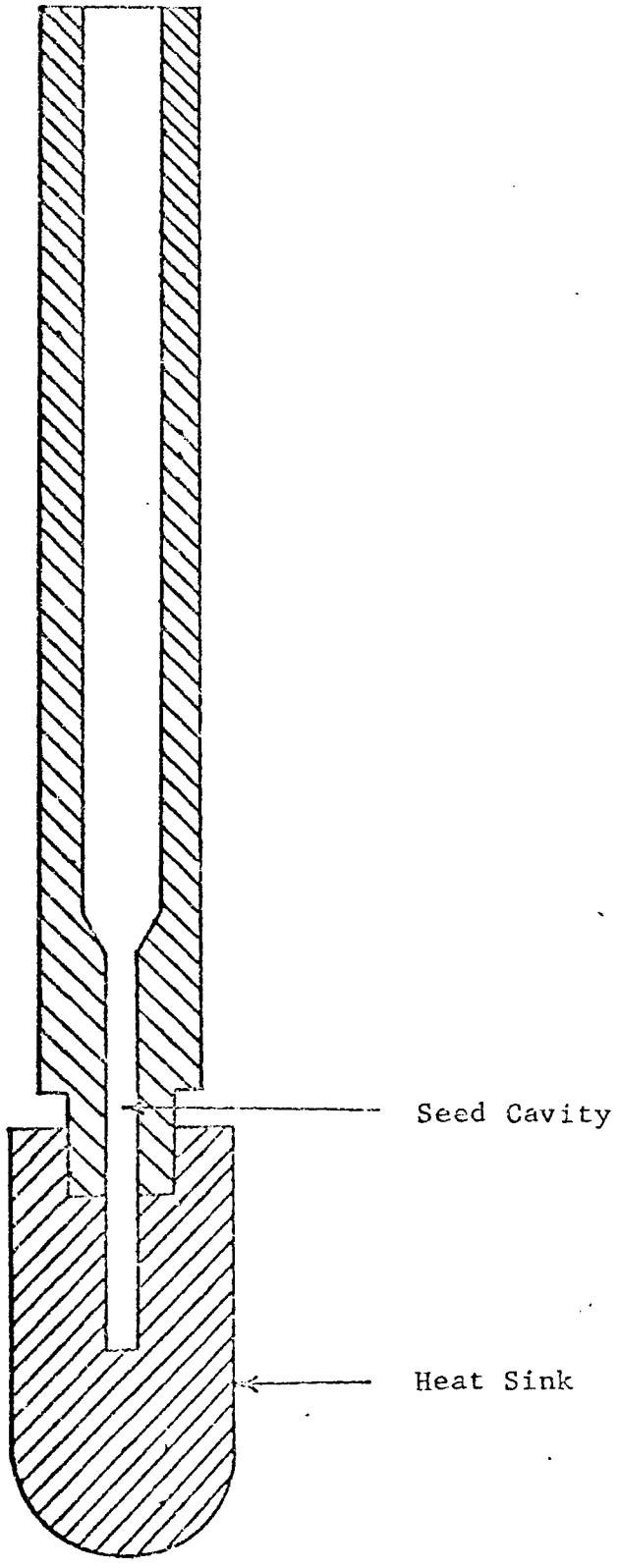

Figure 4. Graphite Crucible for Growing Seeded Crystals

and the rod stock, it was necessary to purify the helium. This was accomplished by passing the helium through a drying column and heated (900° C) titanium chips. Special care was also taken to avoid contamination of the crystal by the graphite crucible and alumina tube. The alumina tube was baked in air at 700° C for 8 hours prior to each crystal run to oxidize any impurities remaining in the tube. The graphite crucible was cleaned after each use in dilute HCl, then soaked in distilled water for 6-8 hours and finally soaked in acetone for 1-2 hours. It was then placed in a vacuum oven at 100° C and kept under vacuum (1-2 mm Hg) for approximately 8 hours.

3. Crystal Examination. After the crystal run was completed, the crystal was removed very carefully from the graphite crucible and the seed was sawed off with a jeweler's saw. The crystal was initially examined for grain boundaries usually by rotating in a strong light. If no grain boundaries were noticed, it was then etched in a manner described proviously.[28] The etchant was dilute HCl in every case except that of the Mg-Zn alloys, where dilute HNO_3 was employed. This was to prevent the darkening caused by the dilute HCl on Mg-Zn alloys.

After etching, the crystal was again visually examined for grain boundaries. If none were found, the orientation of the crystal was determined by the back reflection Laue method. Crystals possessing the desired orientation were etched to approximately 5/32 inch diameter cylinders by rotating in dilute HCl and then they were cut to length by a spark cutter. Each crystal was then reexamined by X-ray diffraction in several places along its length to insure that it was a single crystal.

Table I lists the crystals used in this investigation. The orientation is given for each crystal and is expressed as the angle, θ, between the normal to the basal plane (i.e., the [0001] axis) and the cylinder axis. The pure crystals are identified by their orientation and the alloy crystals by the type and approximate amount of added impurity.

4. Chemical Analysis. The ends of the alloy crystals and one pure crystal were analyzed qualitatively by spectrographic analysis and quantitatively by atomic absorption analysis. The average analysis for each crystal is given in Table I. The distribution of alloying elements along the crystal length was analyzed for each element by sampling a typical crystal that was not usable because of the wrong orientation or small grains. The results show that there was less than 10% variation in percentage of alloying elements along the length of the crystal. The possible segregation of alloying atoms into clusters was not investigated.

It is not known why no lithium was found in the Li doped crystals. However, Ueki[29] found that heating a sample of magnesium containing 1% Li to 750° C and holding it for 1 hour in a graphite crucible under an argon atmosphere yielded only .00005% Li upon analysis. It is possible that the lithium is reacting with the graphite crucible. Secrist and Wisnyi[30] produced LiC in an argon atmosphere by heating lithium and graphite to 700° C.

Lithium, aluminum and zinc were chosen as alloying elements because each is soluble in magnesium and the respective phase diagrams showed it is possible to grow single crystals of each alloy. All three alloying atoms possess a smaller atomic radius than the magnesium atom. Magnesium melts containing lead and calcium which possess a larger

TABLE I

Orientation and Chemical Analysis of Crystals

Crystal	θ	Fe	Cu	Ca	Li	Zn	Al
		Atomic Absorption Analysis At. %					
P10	10°						
P14.5	14.5°						
P38	38°	.004	.0011	.0012			
P44	44°						
P50	50°						
P57	57°						
P62.5	62.5°						
P68	68°						
P74	74°						
P84	84°						
Li	23°	.004	.0008	.0004	<.001	-	-
Zn	22°	.004	.0011	.0004	-	.048	-
.03 Al	24°	.008	.0008	.002	-	-	.027
.05 Al	22°	.004	.0004	.003	-	-	.045
.135 Al	23°	.004	.0004	.002	-	-	.16

atomic radius than magnesium were prepared, but time did not permit an investigation of crystals containing lead and calcium.

B. Modulus and Decrement Measurements

1. Description of the Oscillator. The decrement and Young's modulus were measured by the resonant bar technique using a Marx piezoelectric composite oscillator which employs a gauge crystal in addition to the driver crystal. Construction details of the oscillator have been given by Schwaneke[31] and the theory of operation was presented by Marx.[32]

Figure 5 is a functional diagram of the oscillator set-up. The basis function of the oscillator is to generate resonant longitudinal vibrations in a specimen and to provide a measure of the input and output energy. The oscillator consists of two identical quartz crystals and an extension rod of fused silica. Both quartz crystals and the extension rod possess approximately the same resonant frequency and are cemented together* to form a resonant unit. The unit is driven by applying an ac voltage to the driver crystal by a signal generator. The lower crystal, called the gauge crystal, serves to indicate the output voltage of the unit. The input and output voltages are measured by vacuum-tube voltmeters. The specimen to be measured is placed on the extension rod. The length of each specimen is adjusted so that the resonant frequency of the specimen is approximately equal to that of the oscillator unit. The frequency of the applied voltage is adjusted to equal the resonant frequency of the entire unit (oscillator plus specimen). The resonance condition is indicated by a peak in the output voltage, or by a 90 degree

---

* Eastman 910 adhesive was used for the cement.

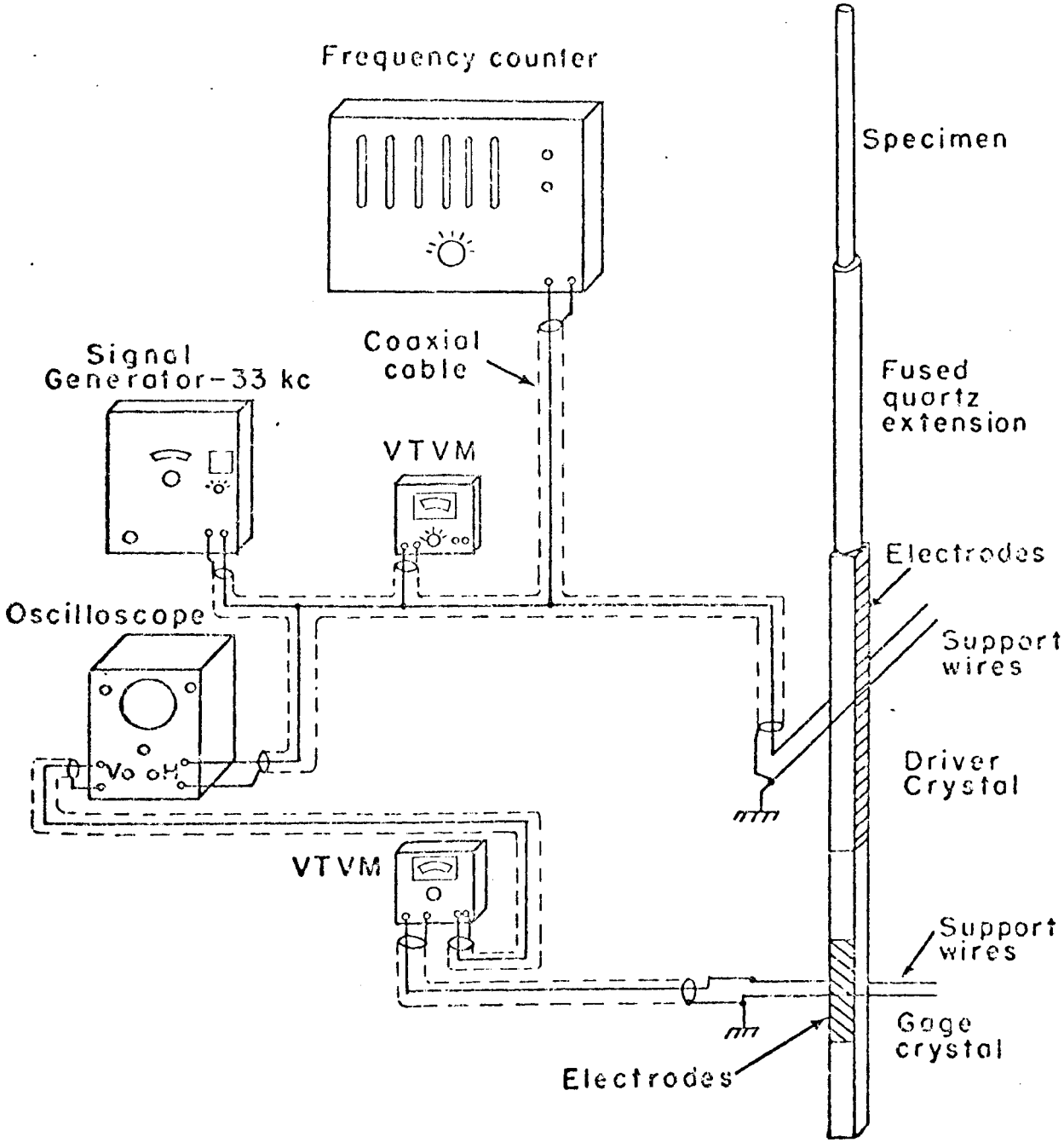

Figure 5. Functional diagram of the composite oscillator setup

phase difference between the input and ouput voltages. The latter method is facilitated by the use of an oscilloscope as shown in fig. 5. All of the decrement and modulus measurements are made at resonance.

The formulas for calculating the decrement, strain amplitude, and Young's modulus from the observed voltages and frequency have been given previously by the author.[28]

2. Oscillator Calibration. Three separate oscillators were employed to speed the measurements. The decrement of each oscillator was measured as a function of strain amplitude and temperature with no specimen attached. The results although non-linear were fitted with a straight line. For an oscillator with no specimen attached the general equation for the decrement, Δ_q, as a function of strain amplitude, ε_o, and temperature, T, in °C is: $\Delta_q = A_q + B_q\varepsilon_o + C_q(T-25)$, where A_q, B_q, and C_q are constants which vary slightly for each oscillator but are of the order of 4×10^{-6}, 10^{-8}, and 10^{-9} $°C^{-1}$ respectively. The resonant frequency of the oscillator alone, f_q, was found to be quite linear with temperature and is given by, $f_q = f_{qo} + D_q(T-25)$, where f_{qo} is the resonant frequency at 25 °C and is approximately 33.5 kilocycles and D_q is approximately .25 cps/°C for all three oscillators.

Since it is very difficult to obtain a material which has a known standard value of internal friction, the oscillators were not standardized. Therefore, while absolute values of the damping are questionable, relative values are comparable.

3. Accessory Equipment. Each oscillator was fitted with a long pyrex tube with a vacuum O-ring seal at the bottom end and a rubber stopper at the top. An aluminum heat shield which contained iron-

constantan thermocouples surrounded the crystal to provide an even distribution of heat. A large tube furnace surrounded the pyrex tube. The furnace temperature was controlled with a temperature controller and a powerstat. Temperature regulation was maintained in all cases to ±1° C.

Each oscillator was affixed with a stop-cock to permit evacuation of one, two, or all three oscillators by the same vacuum pump. The vacuum was maintained at approximately 15 microns during specimen tests. Measurement of the vacuum was made by a thermocouple vacuum gauge.

The resonant frequency of the oscillator was determined by measuring the period of 100,000 cycles with a frequency counter. This method permitted the frequency to be accurately known to within 0.1 cycle.

4. Special Modification. In making measurements at high strain amplitudes it was sometimes necessary to minimize the duration of the applied voltage to the oscillator. The reasons for this are given on page 70. Measurements of this type were made with a special set-up. The meter of the vacuum-tube voltmeter (VTVM) used to measure the output voltage was disconnected, and the meter voltage amplified and applied to an oscillograph. The oscillograph (trade name Visicorder) employs a light beam galvanometer and special light sensitive paper. The oscillograph was necessary since the inertia of the meter in the VTVM was too great to respond to the short pulses applied. The measurements were made by applying a series of short pulses of applied voltage to the oscillator while varying the frequency over a small range about resonance. The resonant frequency was read from the counter when the output pulse was maximum. This method of measurement permitted the duration of vibration time to be as short as 0.1

sec. Calibration of the oscillograph showed its accuracy to be the same as that for the VTVM which is about 1%.

It should be emphasized that this system was only used when it was necessary to keep the duration of the applied voltage as short as possible.

C. Experimental Procedure

The data reported in this thesis were obtained from measuring the damping and Young's modulus of the crystals listed in Table I as a function of strain amplitude, temperature, and time. Almost every crystal was mounted and measured several different times. The mounting number is included on each figure to distinguish the separate mountings. Table 5 on page 67 lists the different mountings for all the crystals. If a considerable time lapse occurred between successive mountings of a crystal, the specimen was etched in dilute HCl to remove any oxide layer which may have formed and to restore the bright surface.

All of the early data were taken in air, and both air and vacuum measurements were made in the later work. The symbol A or V before the mounting number indicates air and vacuum measurement respectively.

Although the procedure followed to obtain the damping data for each crystal varied somewhat depending on the behavior of the crystal, it was basically the following: The crystal to be measured was etched in dilute HCl and mounted with silicone vacuum grease on the end of the quartz extension rod of the composite oscillator. The tube furnace was then put into position and evacuated if vacuum measurements were to be made. The temperature was raised to approximately 280° C

to begin the anneal of the crystal. The crystal was usually annealed until no change in decrement vs time was observed. Measurement of decrement vs strain amplitude was taken periodically during the annealing. When fully annealed, the temperature was lowered about 50° and the decrement again measured as a function of strain amplitude. This was continued until room temperature was reached. It should be emphasized that the above was the "ideal" procedure and in many cases circumstances prevented following it exactly.

D. Experimental Errors

1. Specimen-Quartz Bond Error. The most significant error in the damping measurement was due to the specimen-quartz bond. Preliminary measurements at the beginning of the investigation showed that the type of bonding agent had little effect on the measured damping.[33] Beeswax, shellac, and silicone vacuum grease were some of the bonding agents tried. Others[1,34-36] have tried beeswax, beeswax and rosin, phenyl salicylate, and insulate. In all cases the effect of the bond was reported to be negligible. This is to be expected since the bond is located at a stress node.

As stated earlier, silicone vacuum grease was used exclusively for the specimen-to-quartz bond. However, a very serious problem associated with the use of this bond was unfortunately discovered rather late in the investigation. It was found that slight variations in the specimen position could cause large variations in the observed damping at room temperature. For one particular specimen, variations in the mounting position caused the independent decrement to vary from $.36 \times 10^{-3}$ to 2.5×10^{-3}. It should be emphasized that the changes in mounting position were very slight and usually involved a rotation

of the specimen about its axis or a tilt of the specimen axis 1 or 2° from the vertical. It is believed that the variation in damping is caused by a non-uniform attachment of the specimen to the quartz rod by the grease. It is also believed that the best mounting produces the lowest value of the damping, because obviously poor mountings always resulted in higher values for the damping. However, the position providing the lowest damping was not always the perfectly vertical position.

It was also discovered that the variation of damping with mounting positions was largest for specimens having diameters of the order of the quartz rod diameter,which is 5/32 inch. The damping variation for different mounting positions was less than 15% for specimens having diameters of 1/8 inch or less. However, several specimens had diameters of nearly 5/32 inch as did the one reported above. Therefore comparison of the absolute magnitude of the damping between different specimens is very unreliable.

2. Temperature Fluctuation. Another experimental error is due to temperature fluctuations. The temperature did not usually vary more than ±1° C, but the modulus was sensitive to variations of 0.1 degree. Figure 6 shows a typical variation of the specimen frequency with temperature. The damping was much less sensitive to thermal changes varying only about ±1% for a variation of ±1° C. Therefore measurements of the damping at a constant temperature are much more reliable than modulus measurements.

3. Pressure Variation. Variation in the system pressure affected both the modulus and damping. A variation in the vacuum of 100 microns could cause a change in the damping of 10%. This error could have been compensated for by measuring the damping of the

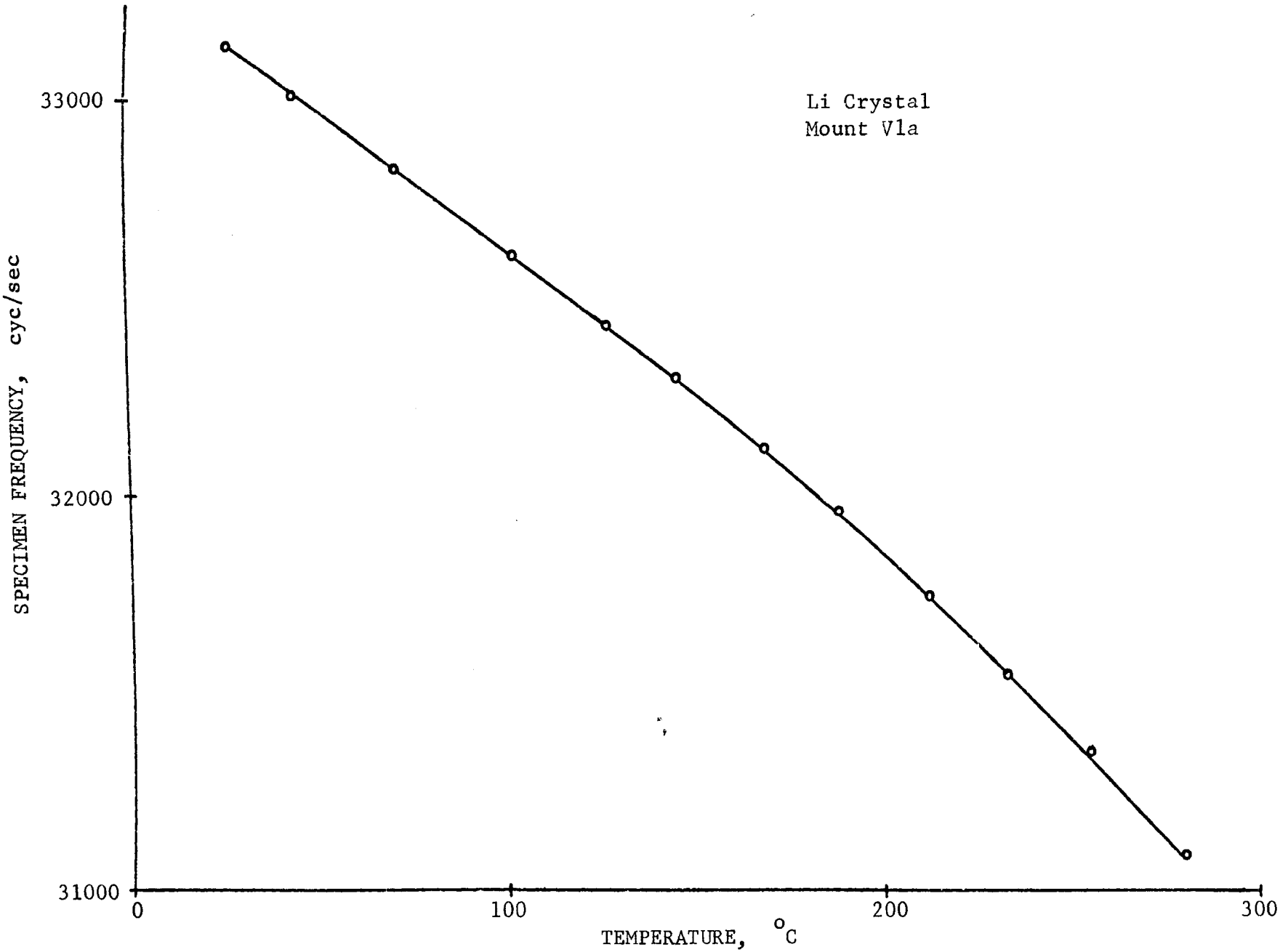

Figure 6. Variation of specimen frequency with temperature

oscillator with no specimen attached as a function of pressure. However, the oscillator was calibrated only at 15 microns and atmospheric pressure. Measurements were made with a vacuum of 15 microns whenever possible, but measurements at higher pressures were sometimes unavoidable.

IV. EXPERIMENTAL DATA AND ANALYSIS

A. Dependence on Strain Amplitude

In general, the damping for the pure crystals exhibited a well defined independent decrement up to a breakaway strain amplitude, ε_b , where amplitude dependence began. The dilute alloy specimens exhibited a less well defined region of amplitude independence and the damping was much less dependent on strain amplitude. In general, the dilute alloys exhibited smaller values for the independent decrement and larger values for the breakaway amplitude. This is shown in fig. 7.

G-L plots (see page 9) of the early pure crystal data showed very good straight lines and were reported earlier by the author.[28] However, occasionally curved G-L plots were obtained for some of these pure crystals and also for some of the dilute alloy crystals. Curved G-L plots are not unusual and have been reported by others.[15,16] It is not known why dilute alloys in general seem to give curved G-L plots. The problem seems to be that the G-L equation overestimates the rate of increase of the damping with the strain amplitude for these alloys. This problem needs additional theoretical consideration.

For the data giving curved plots, the values of I and S were not obtained from a linear least square fit to the curved data plot, but a generalized least squares fit of the actual G-L equation to the data. This results in a much closer fit of the data to the equation since the G-L plot exaggerates the deviations at low strain amplitude. A similar method to this has been employed by Hinton and Rider[37] to obtain the slope and intercept values for their curved G-L plots.

A graphical representation of all the G-L fits and the values of I and S obtained from them will not be given because there are a

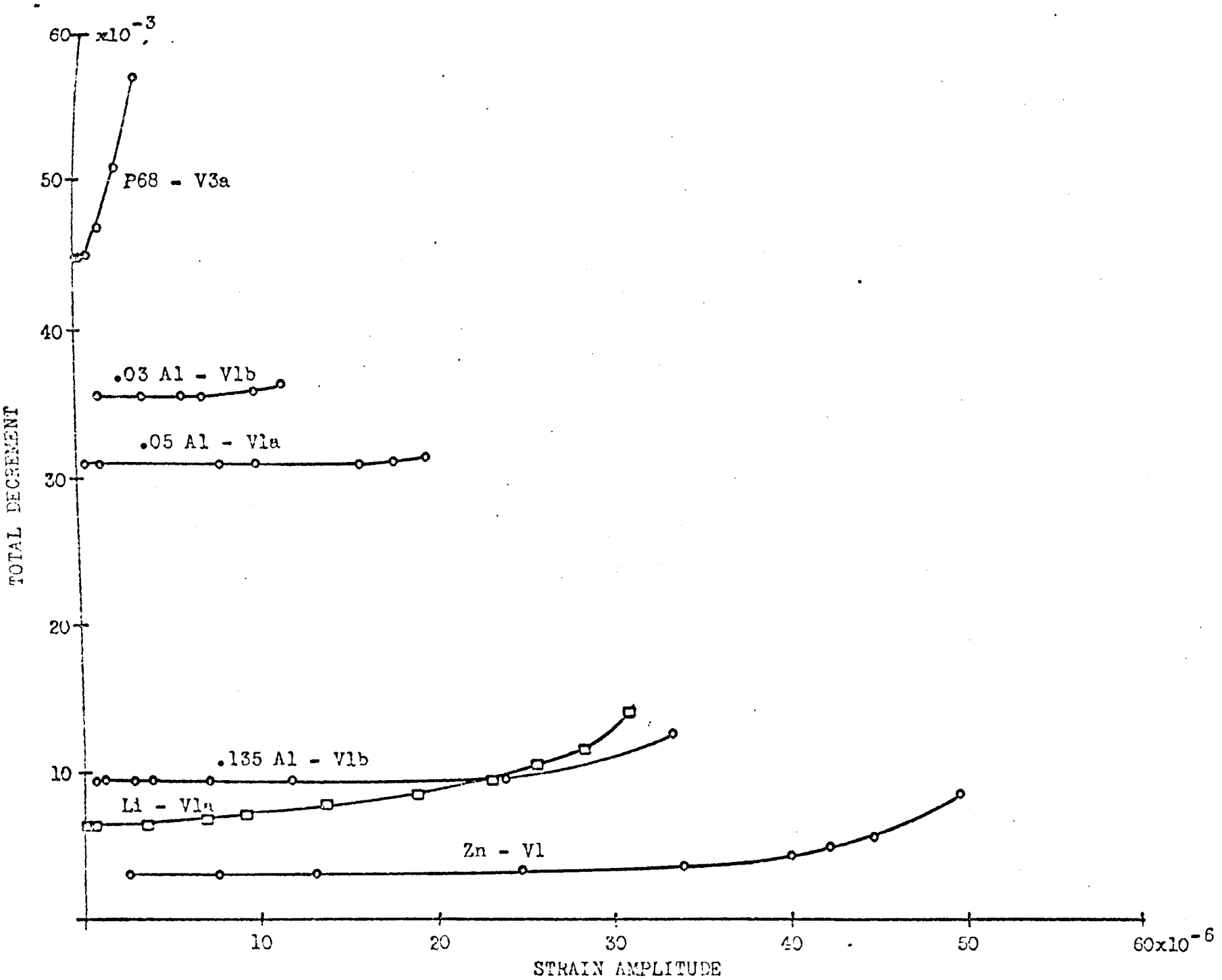

Figure 7. Typical decrement vs strain amplitude curves for pure and doped magnesium crystals

considerable number of them. However, fits for which the average deviation between the calculated and experimental points was greater than 5% were not used. Several typical G-L plots are given in fig. 8.

An unusual strain amplitude dependence effect was observed for the P74 crystal. To the author's knowledge, this effect has not been reported by anyone else. It is usual to find that the damping increases with the duration of vibration for strain amplitudes above breakaway. The rate of increase is somewhat proportional to the strain amplitude. This effect is especially pronounced in magnesium and was reported earlier by the author.[28] However, the P74 crystal exhibited a very unusual strain amplitude dependence which is illustrated in fig. 9. It was found that as the driving voltage to the oscillator was increased, the damping increased with strain amplitude in the normal fashion being slightly time dependent at the higher strain amplitudes (a to b in fig. 9). However, at some critical strain amplitude, ε_c, (point b in fig. 9), the damping suddenly increased to a much larger value (point c in fig. 9) for no increase in driving voltage. This also caused a decrease in strain amplitude (see page 53). The damping then continued to increase with time but much more slowly (c to d) and reached a saturation value (point d). Again, this occurred for no increase in driving voltage and therefore required a decrease in strain amplitude. A subsequent decrease in driving voltage resulted in a decrease in damping and strain amplitude (d to e) but the damping was much larger than before the "jump". At some lower strain amplitude (point e) the damping would rapidly decrease to the same value observed before the increase (e to f).

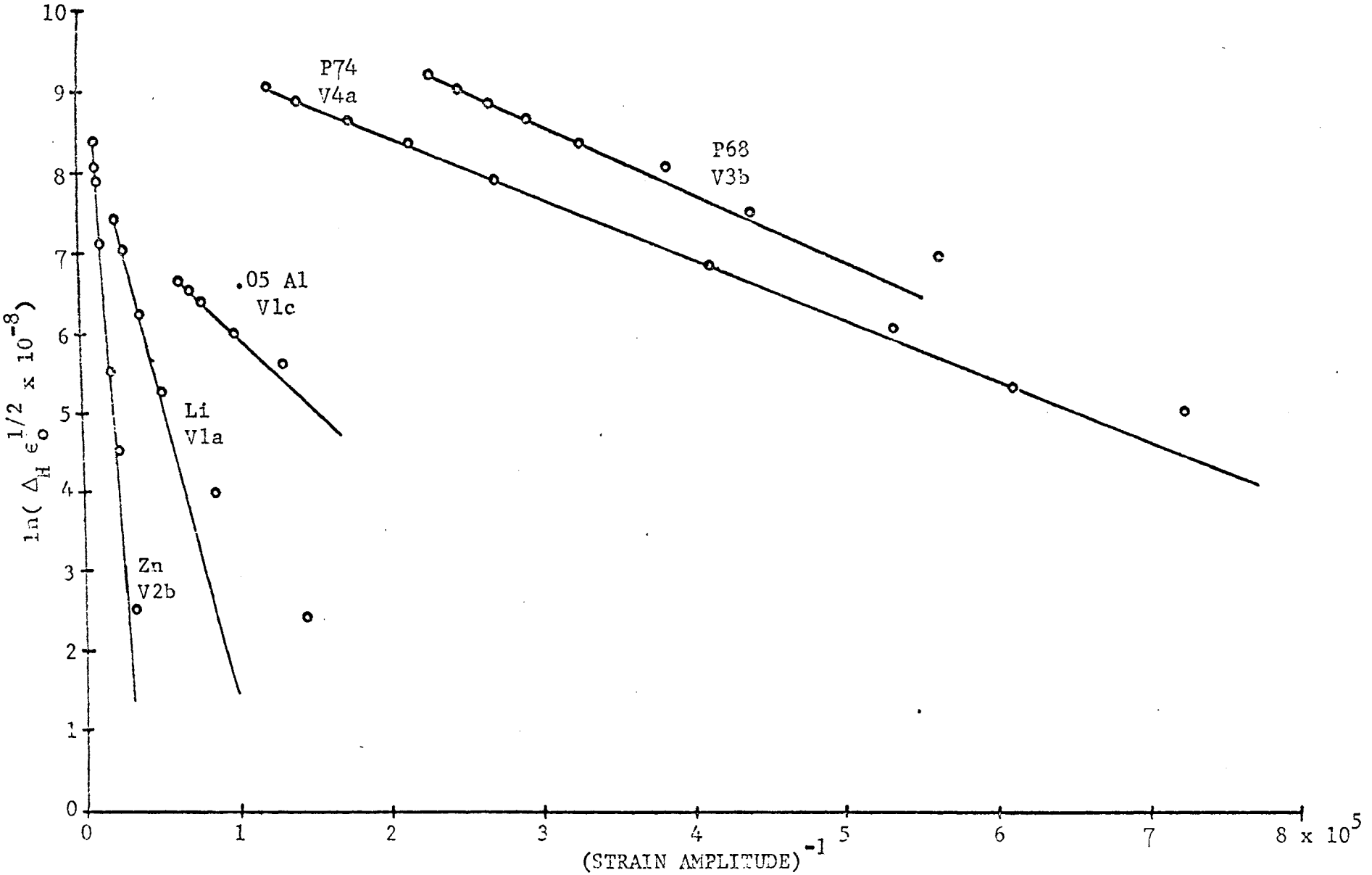

Figure 8. Typical G-L plots

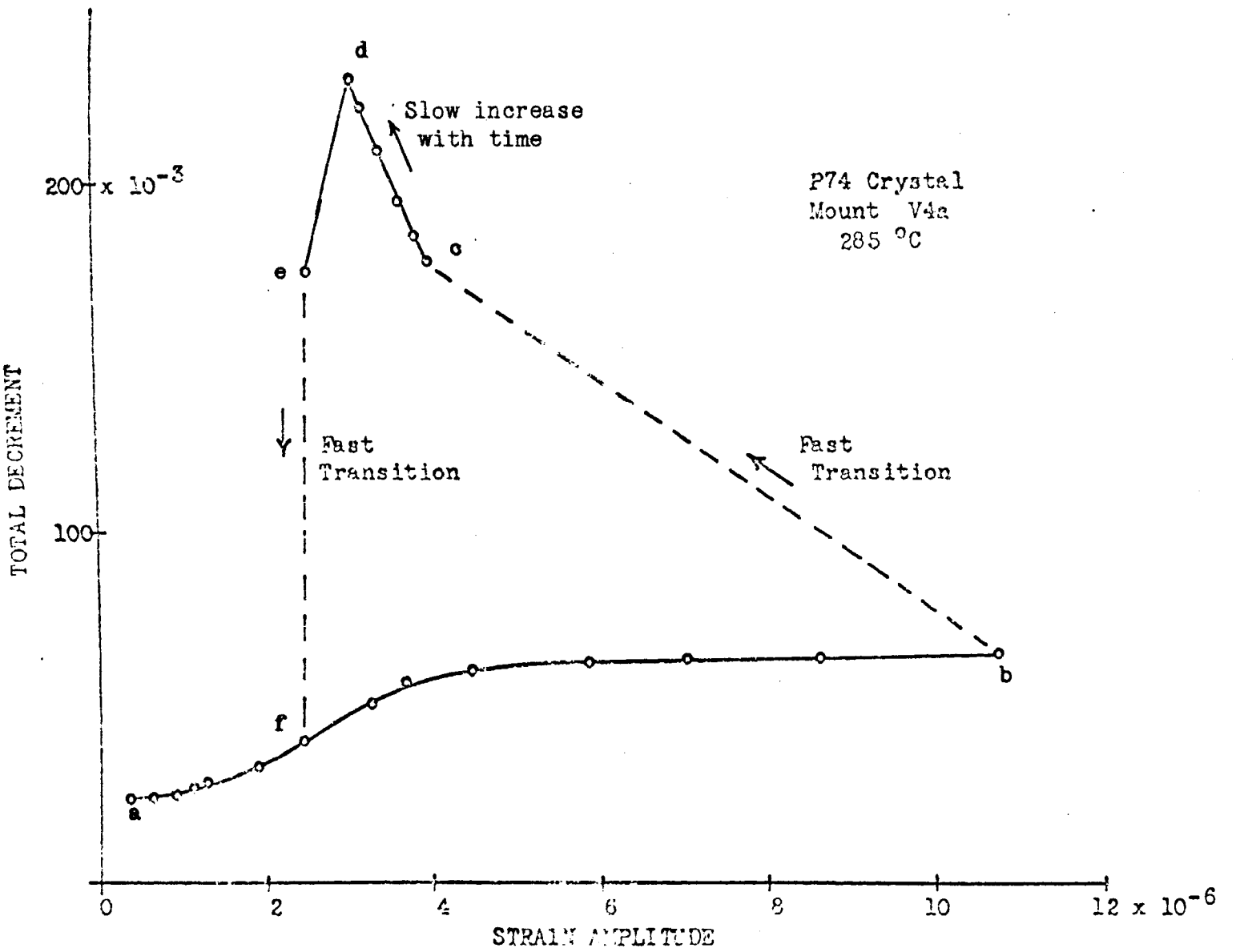

Figure 9. Double strain amplitude dependence exhibited by the P74 crystal

Equally striking was the reproducibility of these measurements. At a temperature of 280° C, the cycle was continued as many as 10 times with no change in the values of Δ_H and Δ_I from their original values. As the temperature was lowered, greater and greater increases in Δ_I after the high excitation were observed.

The critical strain amplitude, ε_c , was also observed to increase with temperature, and at 86° C no break could be obtained. In addition, it was found that a break could be caused at a value of ε_o slightly less than ε_c by a slight tap of the oscillator housing. There was also a critical value of ε_o below which even tapping could not induce the break.

The same effect was also noted for the .03 Al crystal. However, even at 280° C small increases in Δ_I were detectable after a break. Analysis of the strain amplitude dependence of Δ_H before and after the break showed that two separate linear G-L plots were obtained. This is shown in fig. 10. The value of the slope is much smaller after the break than before. These double G-L plots were obtained for several different temperatures down to 147° C.

It is to be emphasized that the above double G-L plot is quite different from other double slope plots obtained by Hasiguti, Igata, and Tanaka,[38] and also obtained by the author for the P68 crystal during an air anneal. These plots are of the type shown in fig. 11 in which lines of two different slopes connect.

It is possible that these type G-L plots can be explained by the activation of an additional slip system at the high stresses. This could cause a change of slope because the orientation factor would be different for the different slip system. However, it is

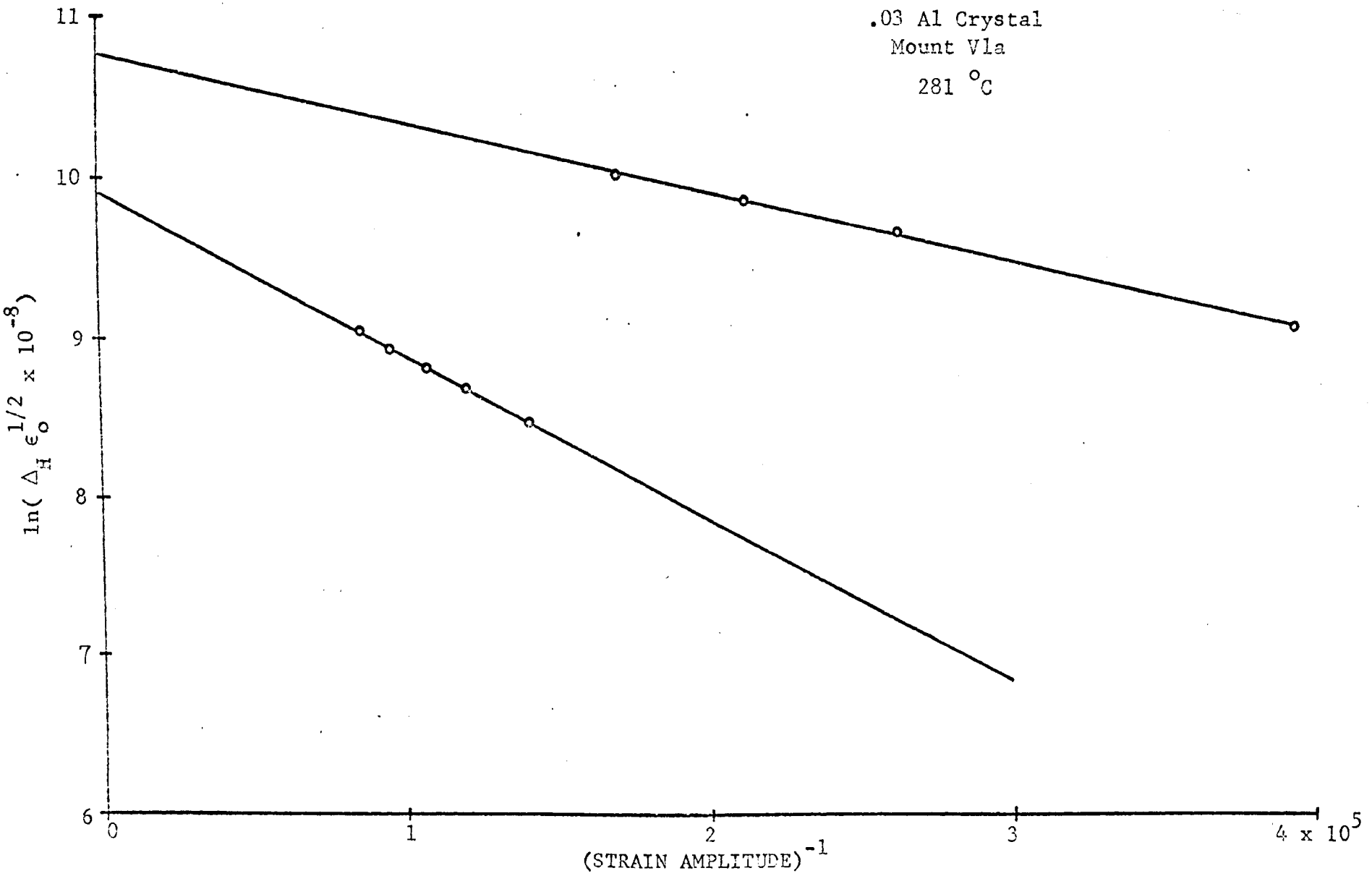

Figure 10. Granato-Lücke plot of double strain amplitude dependence for the .03 Al crystal

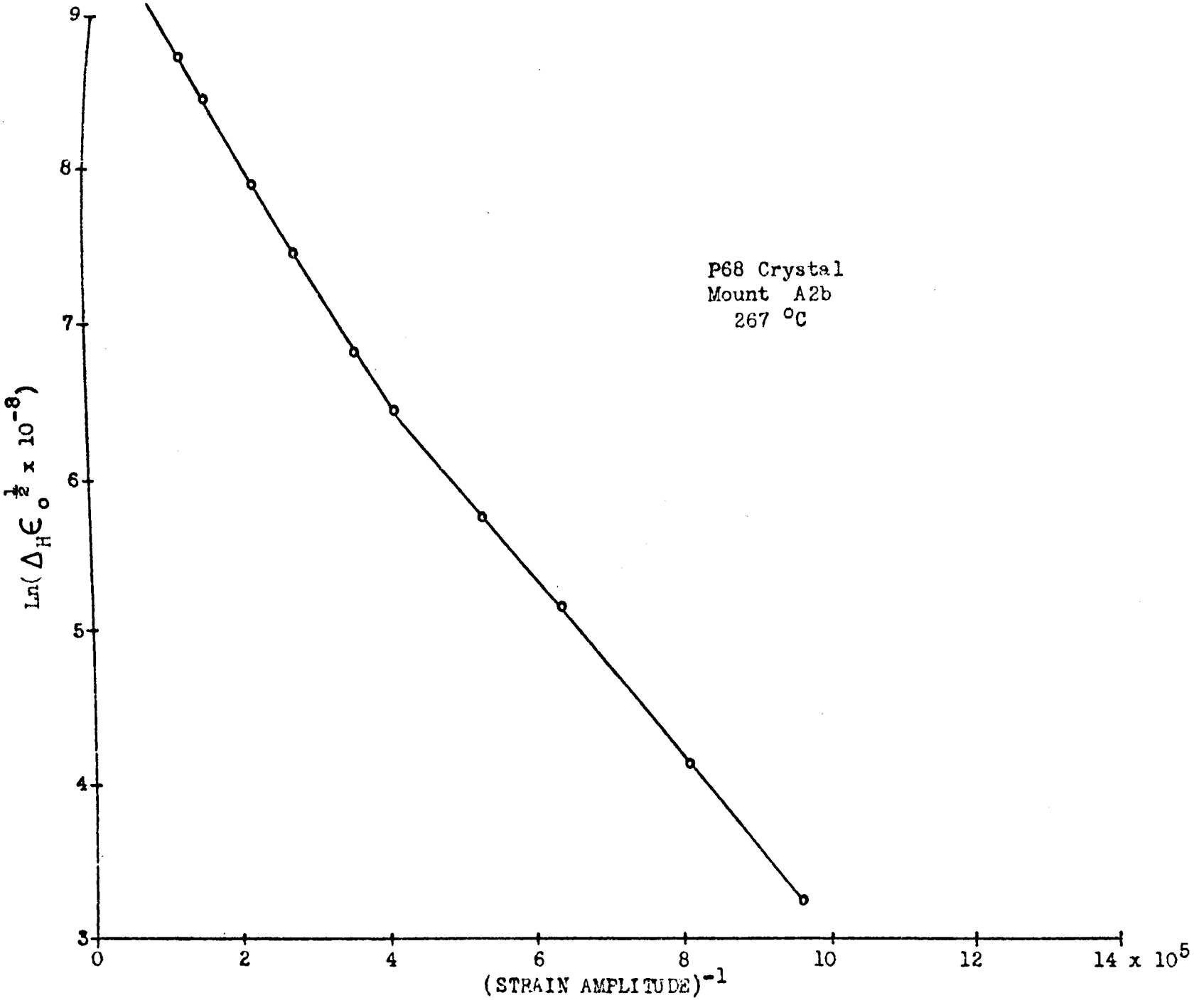

Figure 11. Double slope G-L plot for the P68 crystal

difficult to see how this could explain the double plots of fig. 10, because the decrement exhibits two different values for the same strain amplitude.

B. Dependence on Temperature

In general, an increase in temperature caused an increase in Δ_I, a decrease in ε_b, and an increase in the dependence of Δ_H on the strain amplitude. Plots of $\ln \Delta_I$ vs $1/T$ are available for most specimens and typical ones are shown in fig. 12. The fit is quite linear except for a tail in the low temperature region. This tail is probably due to the fact that the equation, $C = C_o e^{Q/kT}$ is valid only for low concentrations and the concentration at temperatures of the order of room temperature may be too high. Also the diffusion rate may be too slow at room temperature to produce an equilibrium situation in a reasonable time. Table II gives Q and $A_4 a^4/C_o^4$ determined from the above type plot for most of the crystals.

Plots of $\ln S$ vs $1/T$ obtained from the slopes of G-L plots at different temperatures are available for several specimens and are shown in fig. 13. The deviation from linearity begins at temperatures below approximately 150° C. Values of Q and KnC_o determined from these plots are reported in Table II.

C. Dependence on Time

The dependence of the damping and modulus on time can be divided into two areas. The first concerns the dependence of the independent damping, modulus, dependent damping on annealing time following mounting, and an increase in the temperature (usually about 280° C). The second concerns the dependence of the independent damping on recovery time following an excitation at a high strain amplitude.

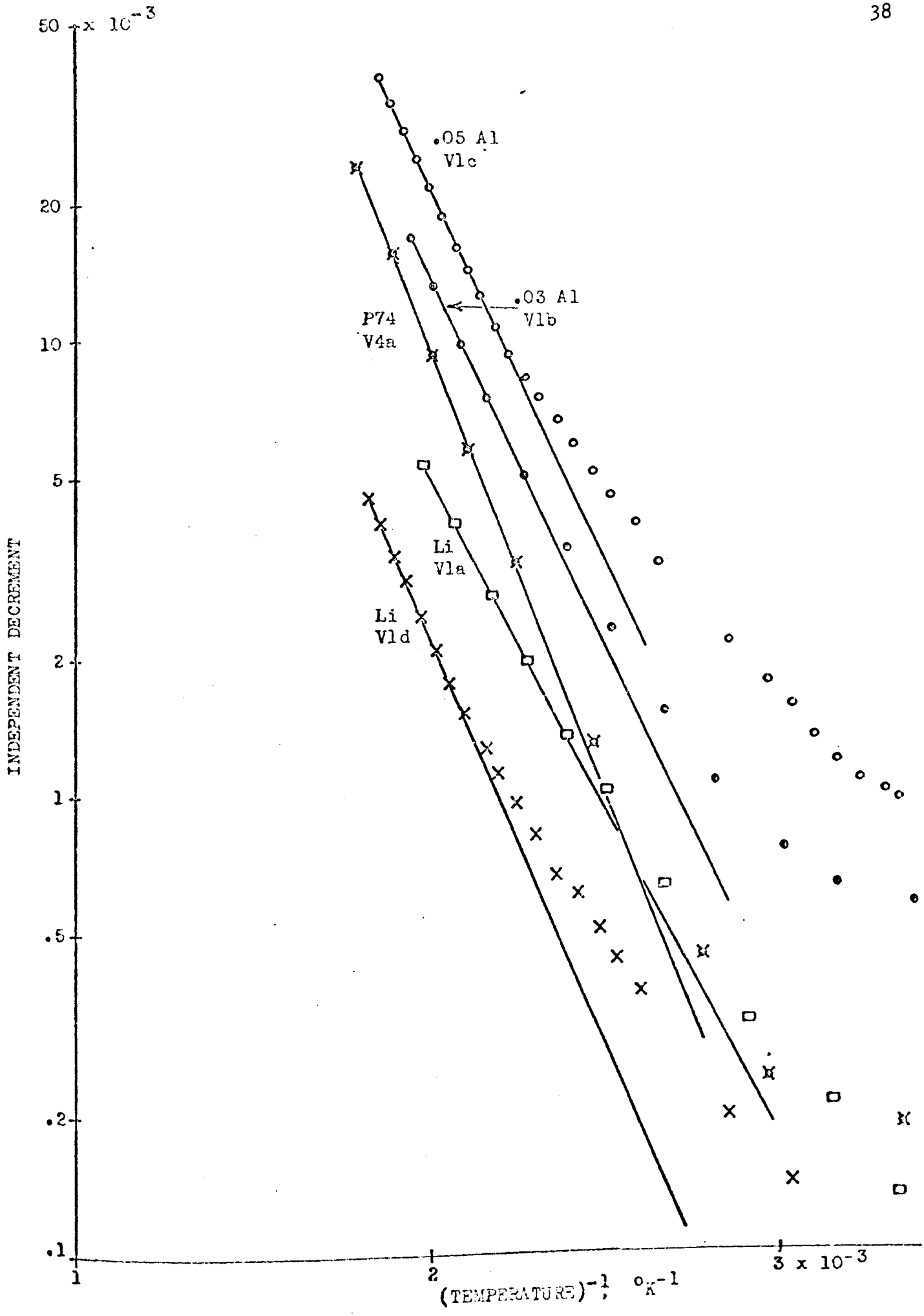

Figure 12. Temperature dependence of the independent decrement

TABLE II

Slopes and Intercepts of $\ln \Delta_I$ vs $1/T$ and $\ln \Delta_H$ vs $1/T$ Plots

Crystal	Mount	$\ln \Delta_I$ vs $1/T$		$\ln \Delta_H$ vs $1/T$		
		Q	Intercept	Q	Intercept	
		Kcal/mole		Kcal/mole	$\times 10^{-7}$	
P14.5	A1a	1.94	39.2			
P44	A1	2.46	200.			
P57	A1	2.55	3017.			
P62.5	A1	1.62	24.6			
P62.5	A2	2.16	96.7	2.48	7.97	
P74	A1	1.63	16.3	2.18	13.8	
P74	V4a	2.38	136.	4.4	1.08	
Li	V1a	1.69	4.63			
Li	V1c	2.31	26.4	5.96	1.13	
Li	V1d	2.18	13.2			
Zn	V2a	2.23*	2.57*	6.33	10.5	
.03 Al	V1b	2.33	163.	9.55	.015	Before "Jump"
.03 Al	V1b			5.02	40.9	After "Jump"
.05 Al	V1c	2.00	67.5			

*Calculated from high temperature part of $\ln \Delta_I$ vs $1/T$ plot before reverse temperature dependence started.

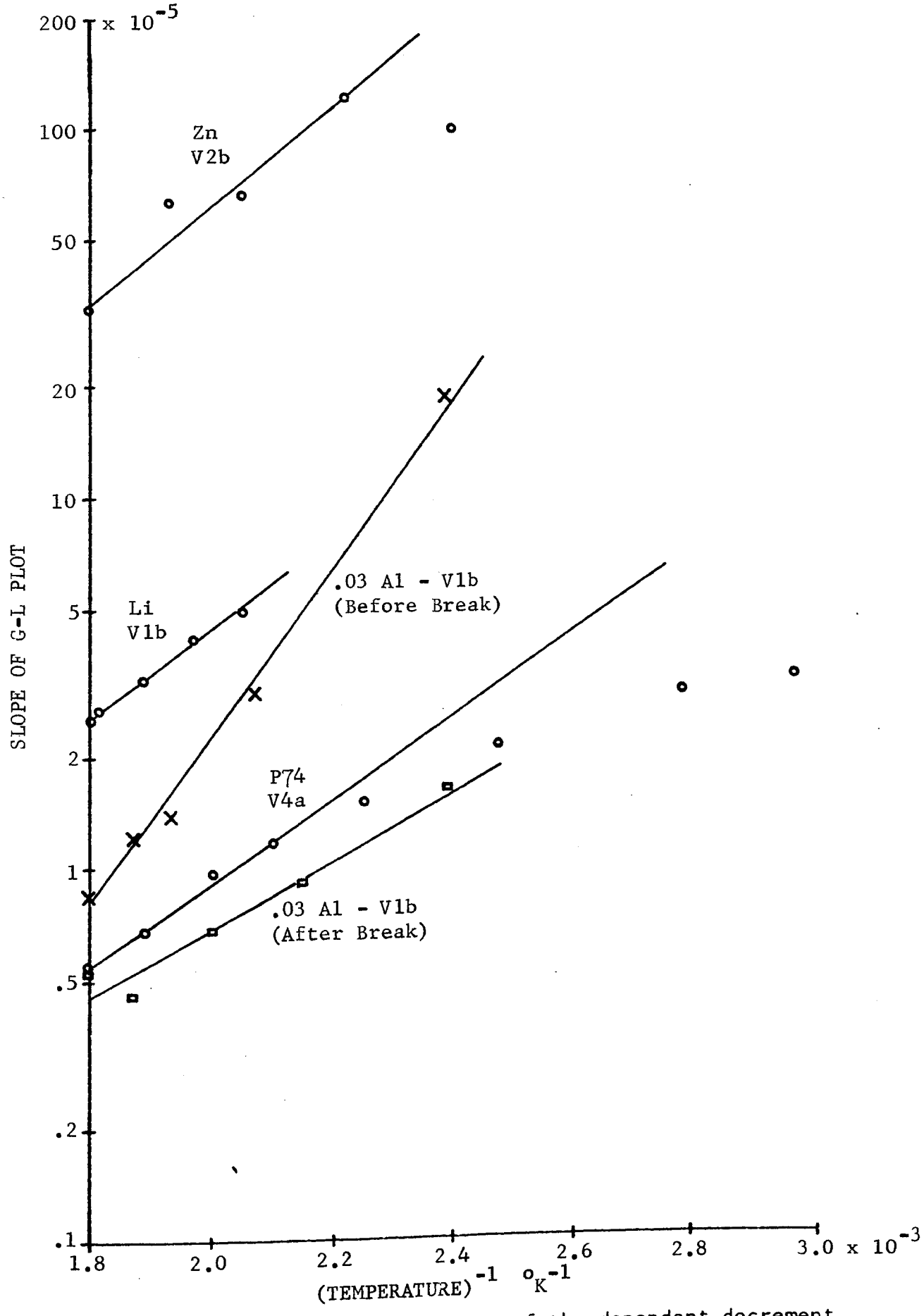

Figure 13. Temperature dependence of the dependent decrement

1. Dependence on Annealing Time

a. Reverse Anneal Effect. Without exception, a certain amount of annealing occurred each time a specimen was mounted and the temperature raised to the annealing temperature. The temperature was kept at the annealing temperature throughout the annealing period. In every case, the independent decrement was observed to decrease with time until a constant value was reached. However, for a number of specimens that were permitted to remain at the annealing temperature for some time after the decrement had leveled off, it was observed that the damping began to increase with time. This effect has not been reported previously by anyone else to the author's knowledge. This effect was observed in both the doped and un-doped crystals and for both air and vacuum anneals and thus it is unlikely to be due to polymerization of the bond. A possible explanation for this will be offered in the last section.

b. Bond Polymerization Effect. In the early studies of the pure crystals, annealing was performed in air. This had the effect of polymerizing the silicone vacuum grease and causing a tight specimen to quartz bond as described earlier. It was found that these crystals were very sensitive to thermal changes. That is, a decrease in the temperature from the annealing temperature and subsequent increase in the temperature back to the annealing temperature would cause an increase in the damping from the value measured before the temperature change. This effect was not observed in some of the same crystals if annealed in vacuum, which did not polymerize the bond. The effect is evidently due to a small deformation in the crystal region next to the bond caused by the difference in the

coefficient of thermal expansion of magnesium and quartz. To check this possibility, a crystal was annealed in vacuum, then annealed in air to allow the grease to polymerize and then returned to vacuum. A subsequent temperature change caused an increase in damping, substantiating the above hypothesis. Although the deformation is small (about 1%)* and occurs at a stress node which would further tend to minimize the effect, the effect is quite striking as shown in the following example. The annealing curve for the P68 crystal is shown as part A in fig. 14. After 169 hours, a power failure caused the temperature to decrease to room temperature. A subsequent return of the temperature to the annealing temperature (267° C) caused the damping to increase to nearly its original unannealed value and decrease again with time, to almost the same previously annealed value (Part B). Part C of fig. 14 shows the subsequent increase of the damping with time as described earlier.

c. Comparison of Annealing Data to the Granato-Hikata-Lücke Theory. The annealing data were compared to the Granato-Hikata-Lücke (G-H-L) theory[14] although there are some questions as

---

* The magnitude of this can be estimated as follows: The coefficient of thermal expansion for fused silica is $.5 \times 10^{-6}\ °C^{-1}$ for 20° to 1000° C while for magnesium it is $27.7 \times 10^{-6}\ °C^{-1}$ parallel to the [0001] axis and $26.6 \times 10^{-6}\ °C^{-1}$ perpendicular to the [0001] axis which gives an average of about $27 \times 10^{-6}\ °C^{-1}$ for any orientation. Thus, if the grease polymerizes at 280° C, for example, and the temperature is lowered to 20° C, the percent difference in the area of the bond end and the free end of the crystal would be given by $\frac{[1 - 27 \times 10^{-6}(260)]^2 - [1 - .5 \times 10^{-6}(260)]^2}{[1 - .5 \times 10^{-6}(260)]^2}$, which equals about 1%.

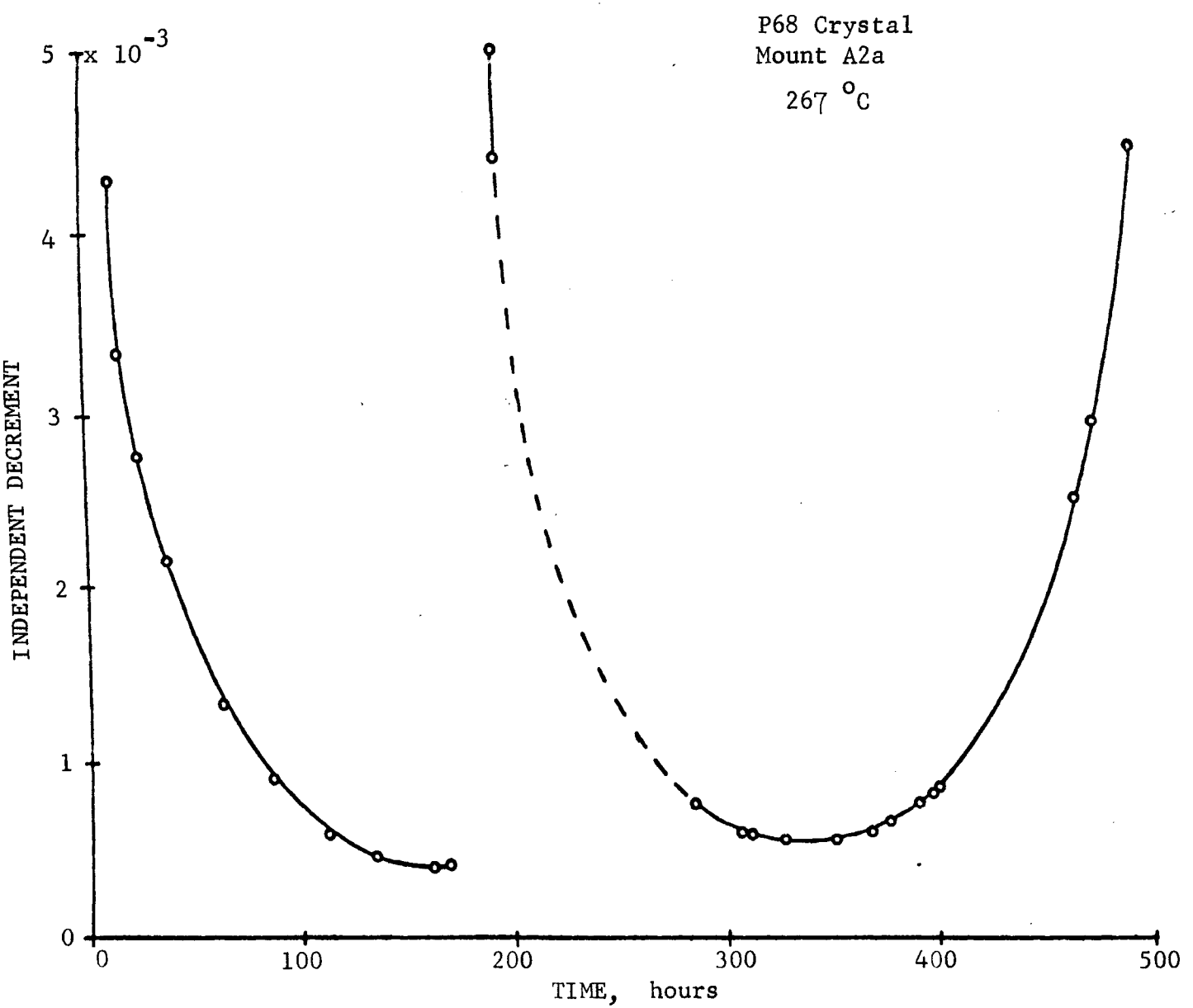

Figure 14. Anneal of the P68 crystal

to the applicability of this type data to the G-H-L theory. First, except for the specimens having polymerized bonds, no plastic deformation occurred. However, the theory assumes that plastic deformation produces point defects and free dislocations which are subsequently pinned. The mechanical state of an unannealed crystal should be very similar to that of a crystal that has been plastically deformed, because the unannealed crystal should also contain free dislocations which during annealing can be pinned by a diffusion of unsegregated point defects. Second, it is usually assumed that annealing reduces the dislocation density, and this is assumed to be constant in the G-H-L theory. However, it seems reasonable that the dislocation density would also decrease following plastic deformation. Therefore, there seems to be just as much reason to apply the G-H-L model to annealing data as to recovery data following plastic deformation.

To apply the G-H-L theory to the annealing data, equation (7), page 12, can be written in the following linear form:

$$(\Delta_1)^{-1/4} = C_{20}(1+\beta t^{2/3})/A_3^{1/4}\, a$$

and a plot of $(\Delta_1)^{-1/4}$ vs $t^{2/3}$ should be a straight line with slope $\beta C_{20}/A_3^{1/4}\, a$ and intercept $C_{20}/A_3^{1/4}\, a$. Figure 15 shows typical annealing data plotted in the above fashion. It will be noticed, that agreement is obtained only at early times. A more convincing plot that does not depend on the power of t is to express equation (7) as:

$$[\Delta_1(0)/\Delta_1(t)]^{1/4} - 1 = \beta t^n$$

where $\Delta_1(0)$ is the value of the decrement at $t = 0$ and equals $A_3 a^4/C_{20}^4$. A plot of $\ln\{[\Delta_1(0)/\Delta_1(t)]^{1/4} - 1\}$ vs $\ln t$ should be linear. Figure 16 shows typical plots of the annealing data in this fashion. They also deviate at longer times.

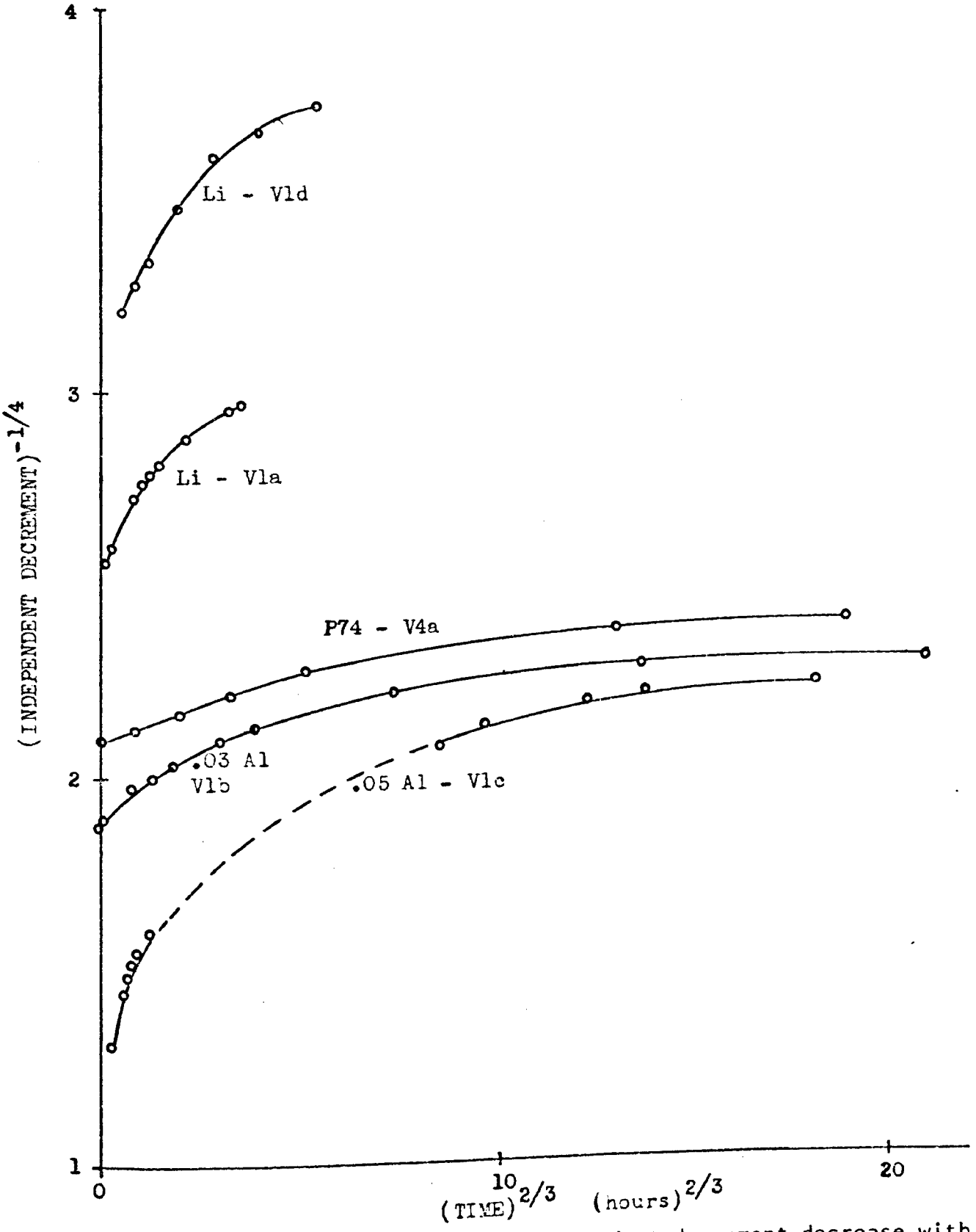

Figure 15. Cottrell-Bilby plot of independent decrement decrease with time during an anneal

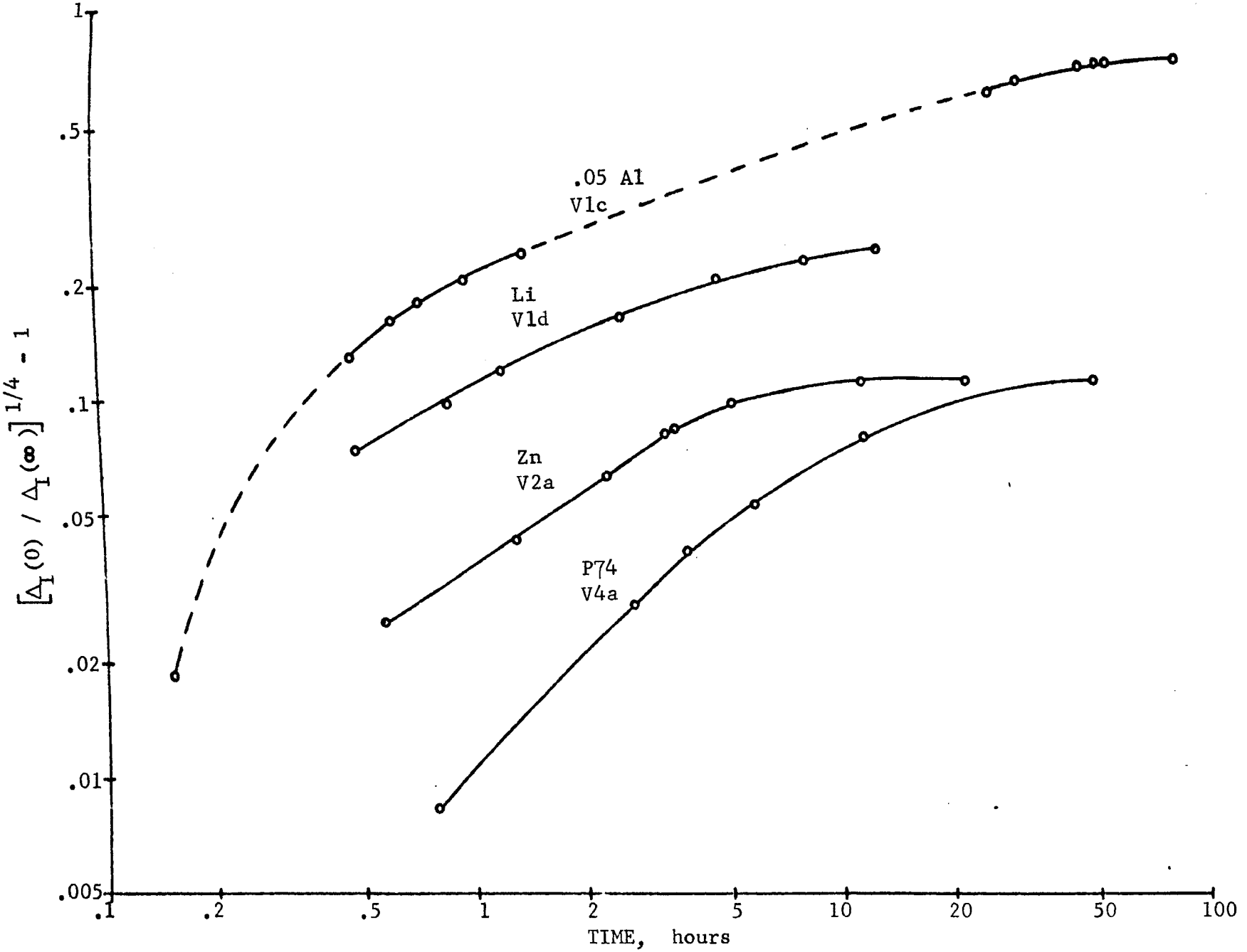

Figure 16. Cottrell-Bilby type plot using t^n for independent decrement decrease with time during an anneal

d. Modification of the G-H-L Theory. In order to correct for longer times, a modification was made in the G-H-L theory. The modification consists of replacing the Cottrell-Bilby law (eq. (4), page 11) by a modified relation derived by Harper[39] to account for longer times. Based on a suggestion by Johnson and Mehl[40], Harper proposed that the rate of precipitation of solute atoms on a dislocation array would decrease in proportion to the fraction, f , of the orginal solute already precipitated. Using this, he obtained:

$$f = n(t)/n_o = 1 - \exp[-\alpha\Lambda(ADt/kT)^{2/3}]$$

where the symbols above have the same meaning as in equation (4).

In terms of concentrations, we have (using the same relations as on page 11):

$$C(t) = (\sqrt{2}C_o/a^2\Lambda)(1 - \exp[-\alpha\Lambda(ADt/kT)^{2/3}])$$

For short times, $e^x = 1 + x$, where $x = -\alpha\Lambda(ADt/kT)^{2/3}$, and the above expression reduces to the Cottrell-Bilby law.

If this expression is substituted for $C_1(t)$ in equation (5), page 12, the modified expression for the loop length L becomes:

$$L = \frac{a/C_{20}}{1 + (C_{10}\sqrt{2}/C_{20}a^2\Lambda)(1 - \exp[-\alpha\Lambda(ADt/kT)^{2/3}])}$$

$$= \frac{a/C_{20}}{1 + \gamma[1 - \exp(-\lambda t^{2/3})]}$$

where $\gamma = C_{10}\sqrt{2}/C_{20}a^2\Lambda$ and $\lambda = \alpha\Lambda(AD/kT)^{2/3}$.

Therefore, the Harper modified G-H-L equations for the damping and fractional modulus change are:

$$\Delta_H = (A_1/\varepsilon_o^{1/2})\exp\{-(Kn C_{20}/\varepsilon_o)(1 + \gamma[1 - \exp(-\lambda t^{2/3})])\} \qquad (8)$$

$$\Delta_1 = \frac{A_3 a^4/C_{20}^4}{\{1 + \gamma[1 - \exp(-\lambda t^{2/3})]\}^4} \qquad (9)$$

$$(\Delta E/E)_1 = \frac{A_3 a^4/C_{20}^4}{\{1 + \gamma[\,1 - \exp(-\lambda t^{2/3})]\}^2} \qquad (10)$$

where the time dependence of A_1 has again been neglected.

e. Comparison of the Independent Decrement Annealing Data to the Harper Modified G-H-L Theory. In comparing the independent decrement annealing data to the above equation, a complication occurs. In order to put equation (9) in a linear form, either the value of Δ_1 at $t = 0$ or $t = \infty$ must be known. Both of these values are difficult to obtain experimentally. There is some question as to when to let $t = 0$ because annealing undoubtedly begins during the temperature increase. Therefore the value of $\Delta_1(0)$ is somewhat unreliable. An approximate value for $\Delta_1(\infty)$ can be obtained by drawing a rough asymptote to the Δ_1 vs t curve. However, this is only an approximation at best. Therefore, the following method was used to fit the data:

Equation (9) was written in the linear form:

$$\ln\{[\Delta_1(\infty)]^{-1/4} - [\Delta_1(t)]^{-1/4}\} = \ln(\gamma C_{20} a/A_3^{1/4}) - \lambda t^{2/3}$$

where $\Delta_1(\infty) = A_3 a^4/C_{20}^4(1 + \gamma)^4$. An approximate value for $\Delta_1(\infty)$ was used as the initial trial value, and a successive approximation routine was employed to find the value of $\Delta_1(\infty)$ which gave the best least squares fit of the equation to the data. The values of $A_4 a^4/C_{20}^4$, γ and λ obtained in this manner were then used as trial values for a generalized least squares fit to the non-linear equation. This latter method was used because of similar reasons given on page 29, viz. a linear least squares fit to a linearized form of a non-linear equation is not always the best fit of the data to the non-linear equation.

Typical fits of equation (9) to the annealing data are shown in figs. 17-19. In general, good agreement is obtained for nearly all of the annealing data of both doped and undoped crystals that were annealed in vacuum. However, annealing data obtained from crystals that were annealed in air could not be fitted by this equation. The fits of the data from the air annealed crystals usually predicted unreasonably low values for $\Delta_1(\infty)$, $(\simeq 10^{-8})$, or negative values for γ or λ.

f. Comparison of the Independent Modulus Data to the Harper Modified G-H-L Theory. The fit of the modulus data to equation (10) is even more complicated. First, as stated earlier, the modulus data are rather scattered due to the extreme sensitivity to temperature changes. Second, the true elastic modulus is unknown. However, a close approximation to its value can be obtained by irradiation because this pins down nearly all the dislocations sufficiently so that they do not contribute to the modulus. This method was used by Gordon and Nowick[23] on their Na Cl measurements. However, irradiation was not practical in this study, so the following method was used to fit the modulus data:

For those crystals which a fit of the independent damping was obtained and which reasonably good frequency data was obtained, the constants γ and λ from the independent decrement fit were used to check the modulus data. In terms of frequencies, $E = 4\rho\ell^2 f^2$ where ℓ and ρ are the specimen length and density respectively.

Thus, $$E = 4\rho\ell^2 2f\Delta f$$

and $$\Delta E/E = 2\Delta f/f_e = 2[f_e - f(t)]/f_e$$

where f_e is the frequency associated with the true elastic modulus.

Thus, $f(t) = f_e - (f_e A_4 a^2/2C_{20}^2)(1 + \gamma[1 - \exp(-\lambda t^{2/3})])^{-2}$ so that a plot of $f(t)$ vs $(1 + \gamma[1 - \exp(-\lambda t^{2/3})])^{-2}$ should be a straight line with slope $-f_e A_4 a^2/2C_{20}^2$ and intercept f_e. The

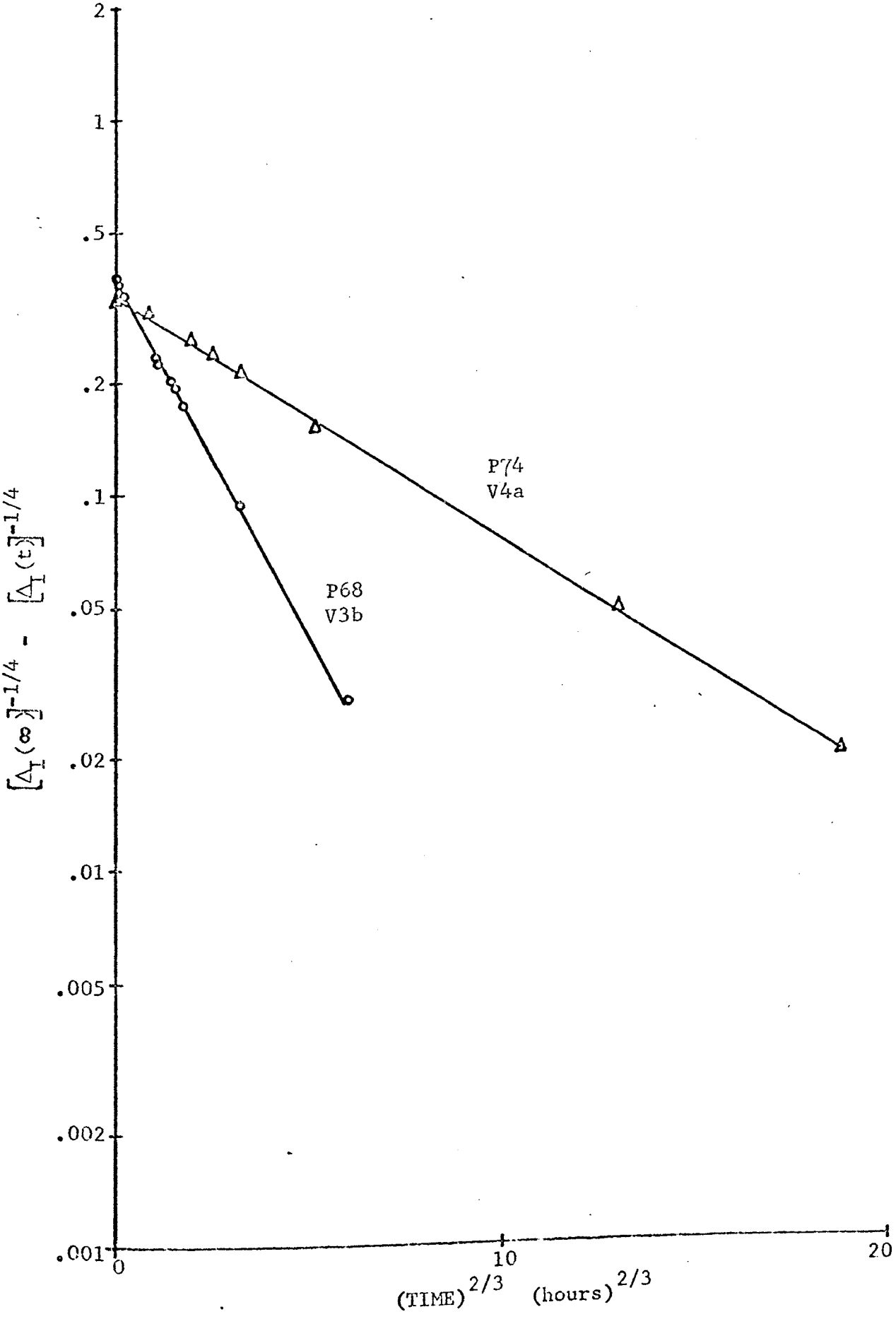

Figure 17. Harper plots of independent decrement decrease with time during an anneal

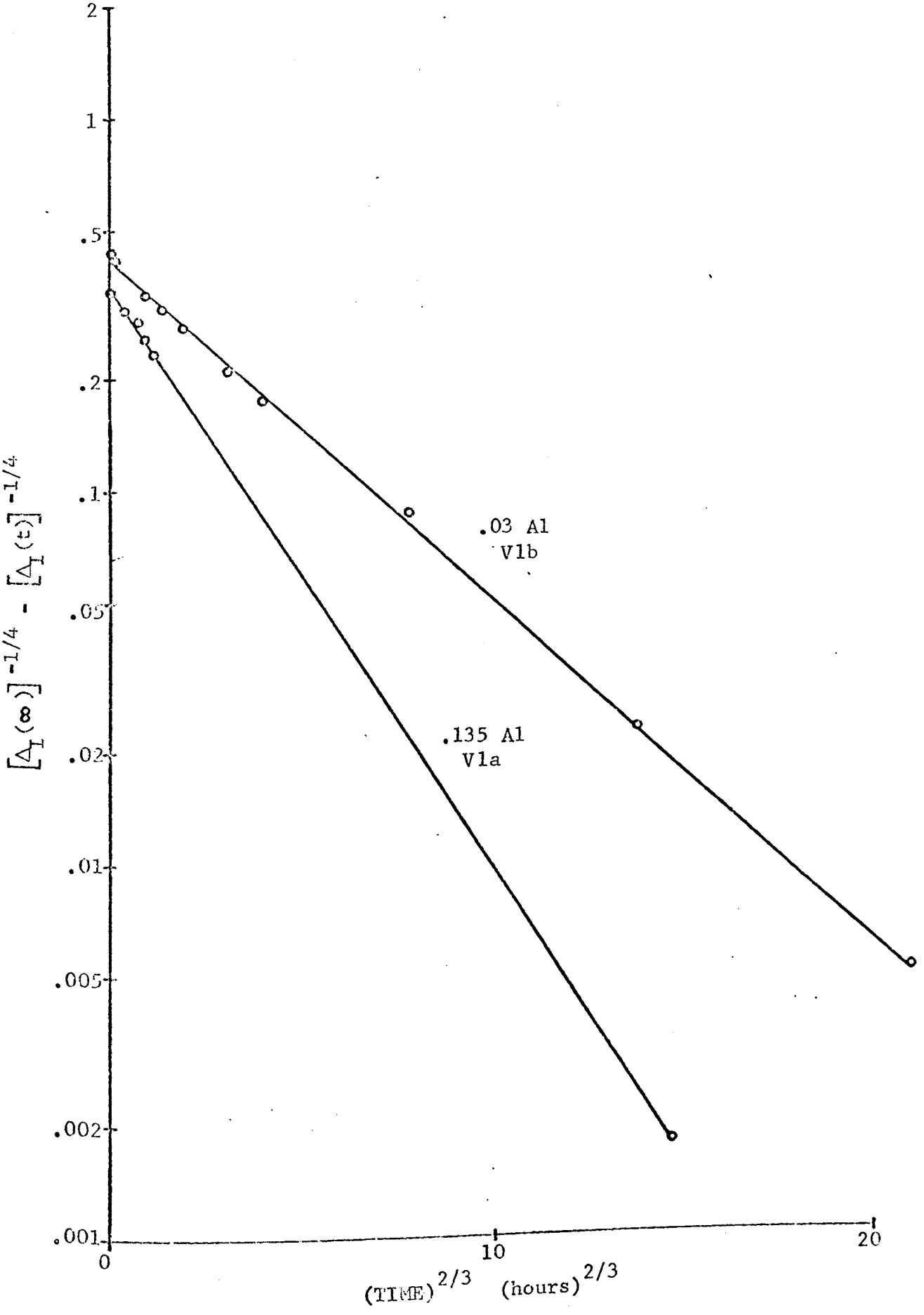

Figure 18. Harper plots of independent decrement decrease with time during an anneal

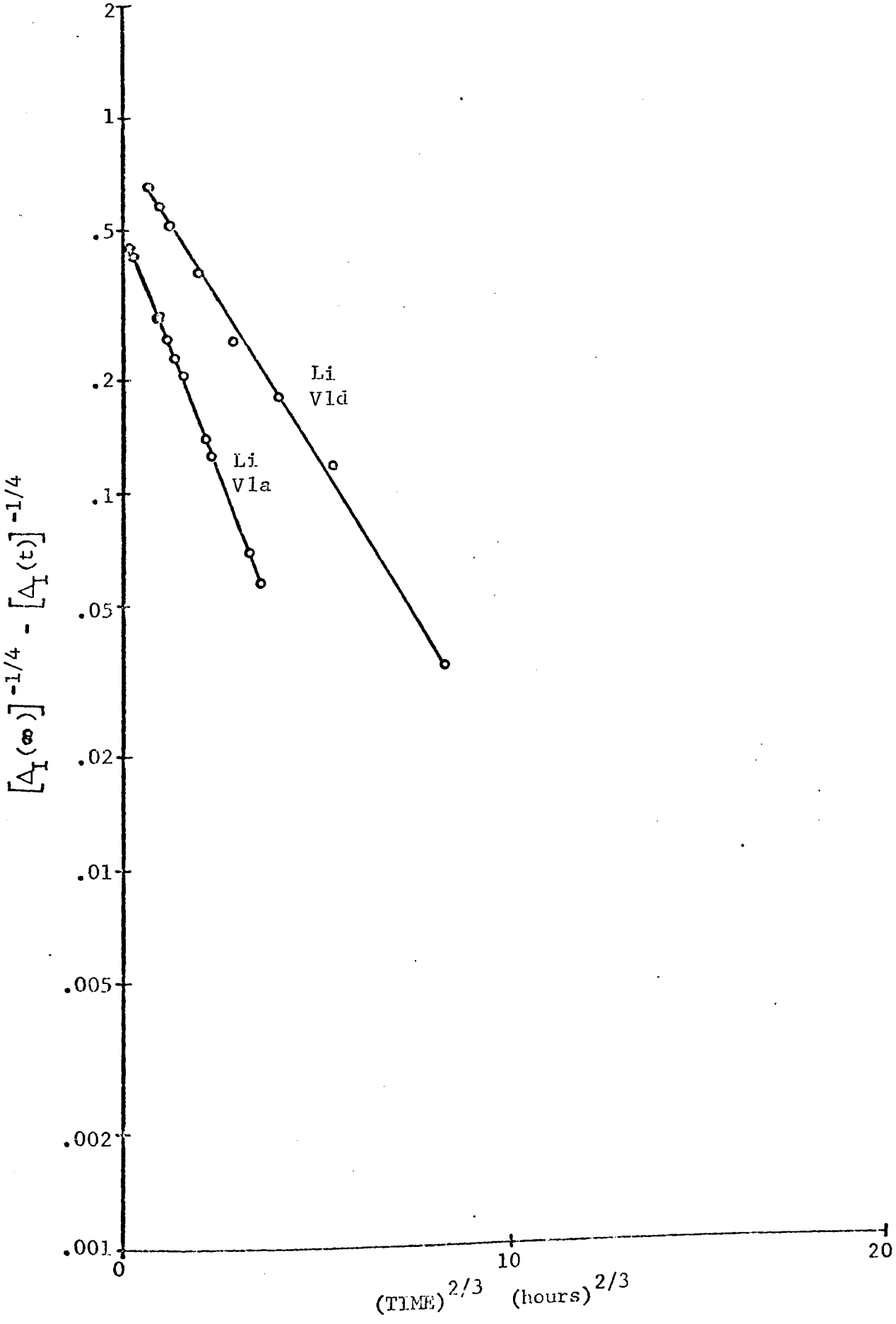

Figure 19. Harper plots of independent decrement decrease with time during an anneal

quantity $A_4 a^2/2C_{20}^2$ will be represented by χ.

Plots of the above type are shown in fig. 20. The agreement is not bad considering the fluctuations in the frequency data. The fact that the plots are approximately linear shows that the assumption stated on page 44 that the dislocation density, Λ, does not vary with time is reasonably valid. If Λ were changing considerably with time, a non-linearity should be noticeable even with scattered data. A generalized least squares fit to the modulus data was attempted, but the points were too scattered to permit the process to converge.

g. Comparison of the Dependent Decrement Annealing Data to the Theory. To check the dependence of Δ_H on t, either the value of Δ_H at constant strain amplitude or the slope of a G-L plot is needed as a function of time during the recovery process. To compare the G-H-L theory with the data, plots of $\ln \Delta_H$ vs $t^{2/3}$ or plots of S vs $t^{2/3}$ could be made which should be linear. Comparison of the data to the Harper modified G-H-L theory is complicated because the equation cannot be conveniently put into linear form. Also, the inherent nature of the composite oscillator,* and the rapid increase of the damping with excitation time makes it extremely difficult to obtain values of Δ_H at a constant strain amplitude.

Table III lists the values of $\Delta_I(0)$, γ, λ, and χ obtained from the fits of the theory to the annealing data.

---

* For a constant input voltage, the product $\Delta\varepsilon_o$ is a constant. Therefore, the input voltage must be adjusted by a trial and error technique to obtain a given ε_o. This is extremely difficult especially if the damping is changing rapidly with the duration of applied vibration.

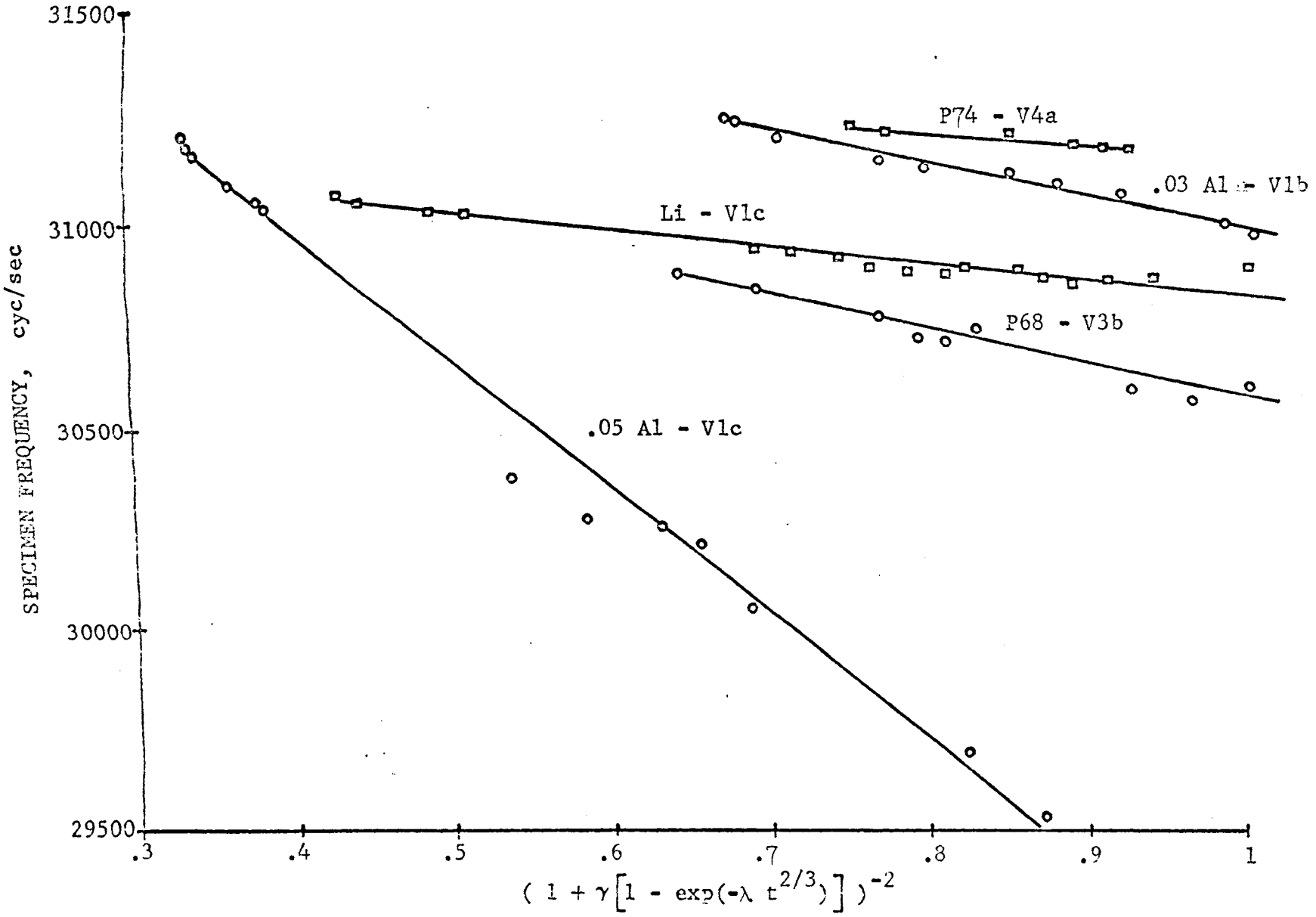

Figure 20. Harper plots of independent modulus increase with time during an anneal

TABLE III

Parameters Obtained from Harper Plots of Δ_l and $(\Delta E/E)_l$ vs Annealing Time

Crystal	Mount	$\Delta_l(0)$ $\times 10^{-3}$	γ	λ $hr^{-2/3}$	χ
P62.5	A2	2.27	.665	.465	
P68	V3a	163.	.330	1.142	.0556
P68	V3b	240.8	.270	.475	.0308
P74	V4a	54.2	.169	.178	.012
Li	V1a	25.3	.202	.665	
Li	V1c	73.1	.552	.234	.013
Li	V1d	12.6	.275	.514	
.03 Al	V1b	80.2	.220	.263	.026
.05 Al	V1a	93.7	.259	.487	.019
.05 Al	V1c	492.3	.815	.477	.098
.135 Al	V1a	46.4	.161	.338	.015
Zn	V1	105.3	1.468	.329	.098
Zn	V2a	1.69	.153	.542	.006

2. Dependence on Recovery Time

a. Experimental Recovery of the Independent Damping Following a High Strain Amplitude Vibration. As described earlier on page , the damping at high strain amplitude was found to increase with the length of time of excitation. When the excitation was turned off, the damping decreased back to its original value. To observe this effect, the measurement times during the recovery should be very short so as not to disturb the crystal again. It was also found that excitation at a high strain amplitude caused the damping to increase over the entire range of strain amplitudes below the excitation strain amplitude. In other words, a long excitation at a high strain amplitude would also increase the independent decrement. Upon removal of the excitation, the independent decrement would decay back to its initial value before excitation.

Figures 21-25 show the recovery of the independent decrement following excitation at high strain amplitude for two specimens. The effect of temperature can be seen in the recovery curves for the Li doped crystal. As can be seen in the graphs, the independent decrement does not return to its initial value at temperatures 235° C and below. However, for the case of the recovery at 235° C, the temperature was increased to 277° C and then decreased to 235° C and the damping was approximately the same value as before the excitation.

b. Interpretation by Chambers and Yamafuji and Bauer. This type of time dependence was first studied in detail by Chambers.[3] He explained the increase in damping during a high amplitude vibration as due to a thinning of the Cottrell atmosphere surrounding the dislocation. Recovery occurs as the atmosphere diffuses back to the dislocation. Chambers quantitatively measured the increase of the damping with time during a large strain amplitude excitation and its subsequent

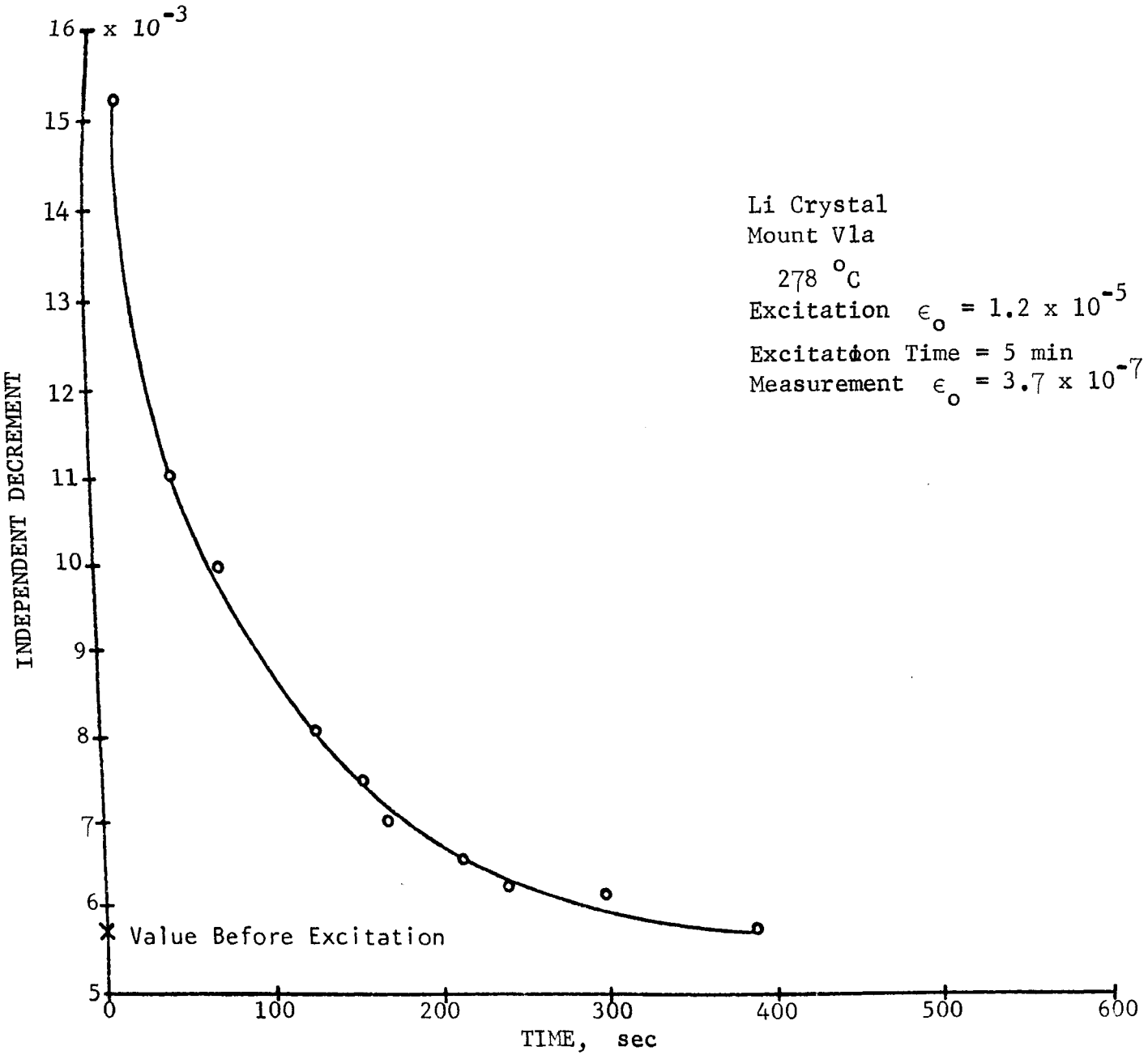

Figure 21. Recovery of independent decrement following excitation at high strain amplitude for the Li doped crystal at 278° C

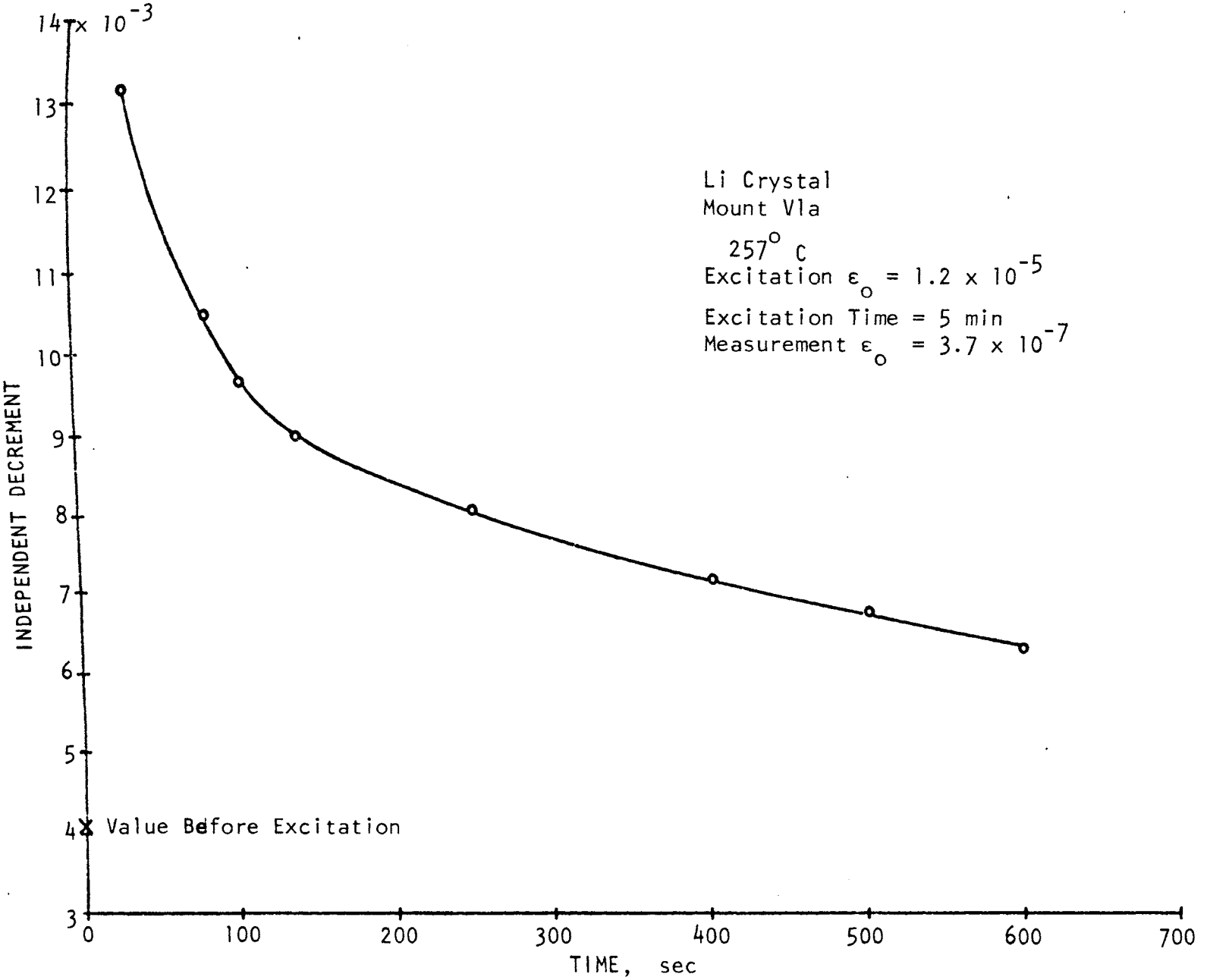

Figure 22. Recovery of independent decrement following excitation at high strain amplitude for the Li doped crystal at 257° C

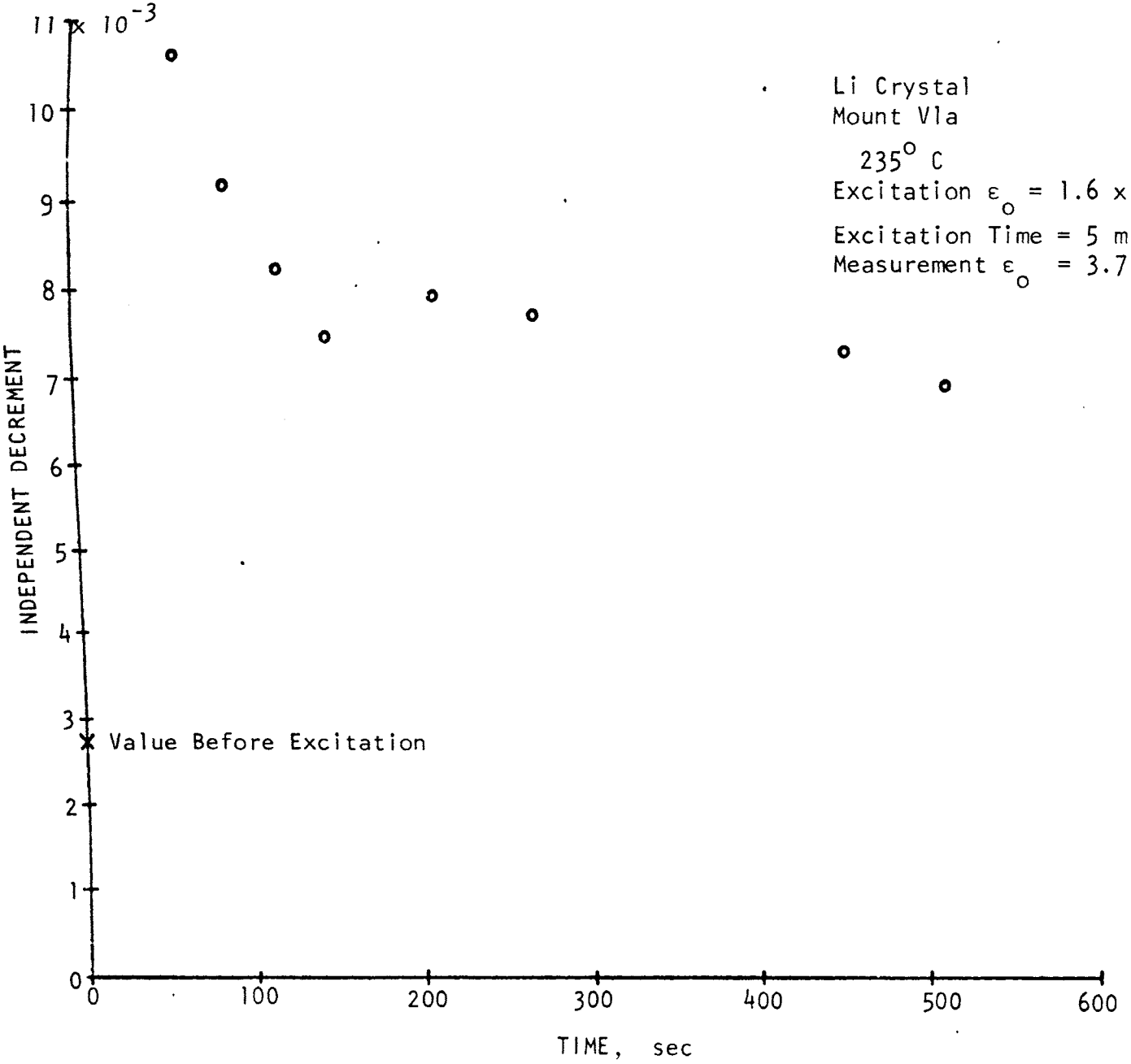

Figure 23. Recovery of independent decrement following excitation at high strain amplitude for the Li doped crystal at 235° C

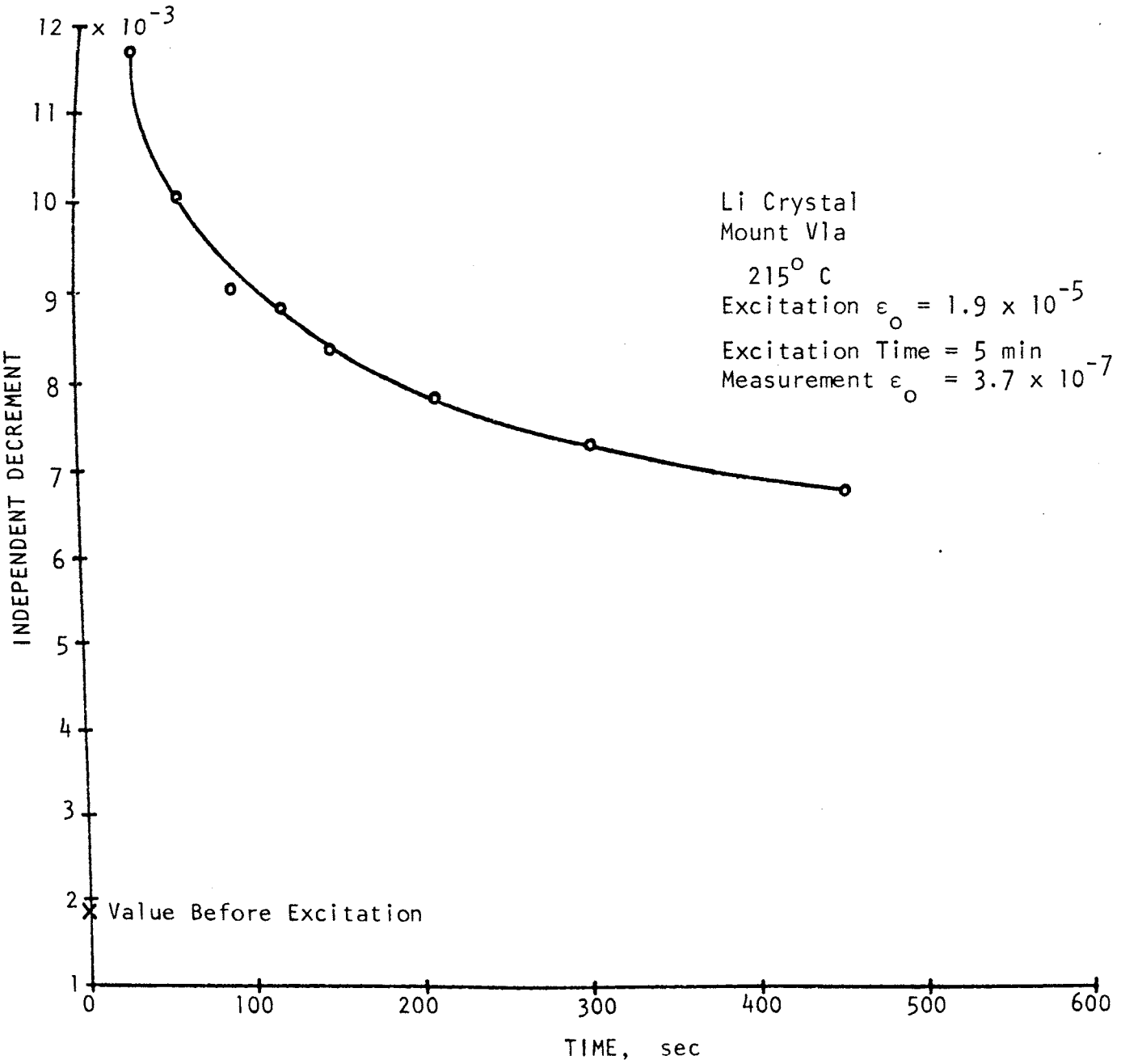

Figure 24. Recovery of independent decrement following excitation at high strain amplitude for the Li doped crystal at 215° C

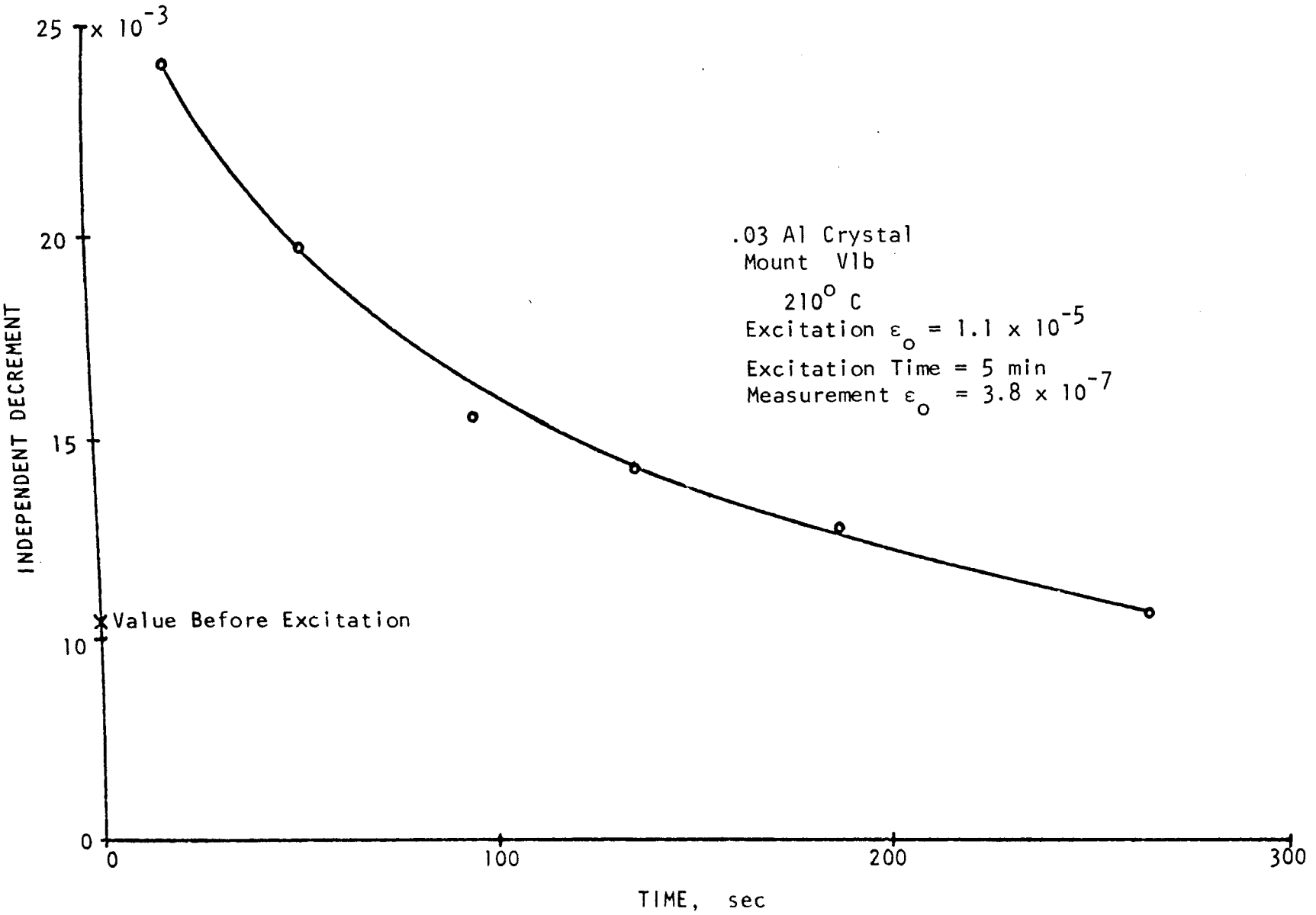

Figure 25. Recovery of independent decrement following excitation at high strain amplitude for the .03 Al doped crystal at 210° C

decrease after removal of the excitation. The measurements of the damping during the decay were made at the same strain amplitude as the excitation amplitude but the excitation periods were kept very short. He did not, however, study the decrease of the independent decrement after removal of the excitation. He found that the decrease in damping was proportional to t^n where n varied from 1/3 to 2/3 depending on the length of excitation time before recovery began.

More recently, Yamafuji and Bauer[41] have reinterpreted the above phenomenon as due to a redistribution of the pinning points along the dislocation during the application of the high excitation amplitude. The recovery is then a return of the pinning points along the dislocation to the original distribution.

c. Comparison of the Recovery Data to the Theory. Comparison of the recovery data to the Harper modified G-H-L theory is shown in fig. 26. The agreement is good, but the predicted values of $\Delta_1(\infty)$ are too low for two cases and too high for the other two cases. If the value of Δ_1 before excitation is used for $\Delta_1(\infty)$ in the Harper plots, the agreement is considerably worse, as shown in fig. 27.

According to the Yamafuji-Bauer theory, the recovery of the independent decrement after the application of a high strain amplitude is given by:

$$\Delta_1(t) = \Delta_1(\infty) + [\Delta_1(0) - \Delta_1(\infty)] \exp(-t/\tau)$$

where τ is the relaxation time. Thus a plot of $\ln[\Delta_1(t) - \Delta_1(\infty)]$ vs t should yield a straight line of slope $1/\tau$ and intercept $\ln[\Delta_1(0)-\Delta_1(\infty)]$.

Plots of the recovery data in this fashion are given in fig. 28. The value of the damping before excitation was used for $\Delta_1(\infty)$. The agreement is good for the two cases where the damping returned to its

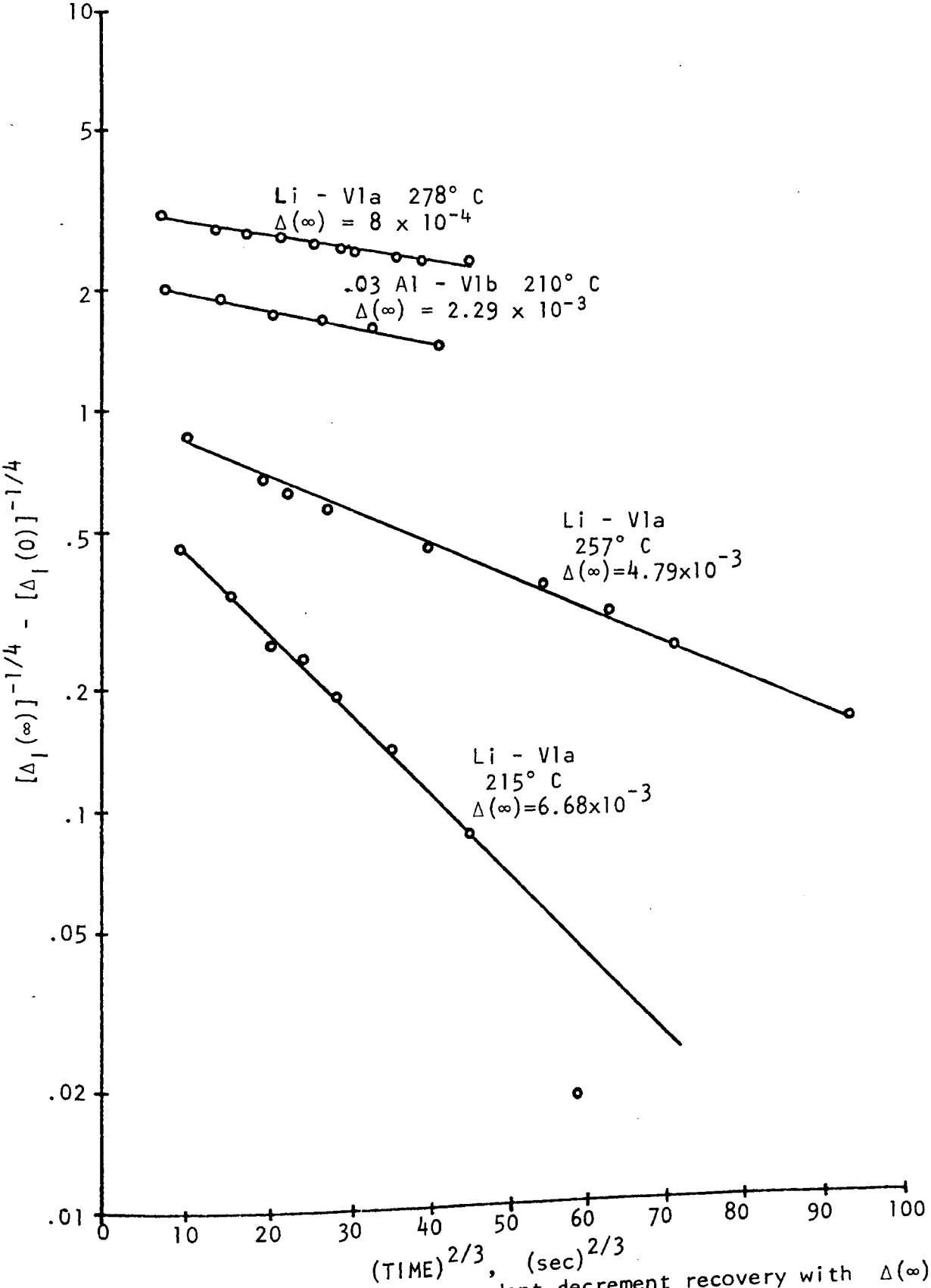

Figure 26. Harper plots of independent decrement recovery with $\Delta(\infty)$ equal to the value that gives the best straight line fit.

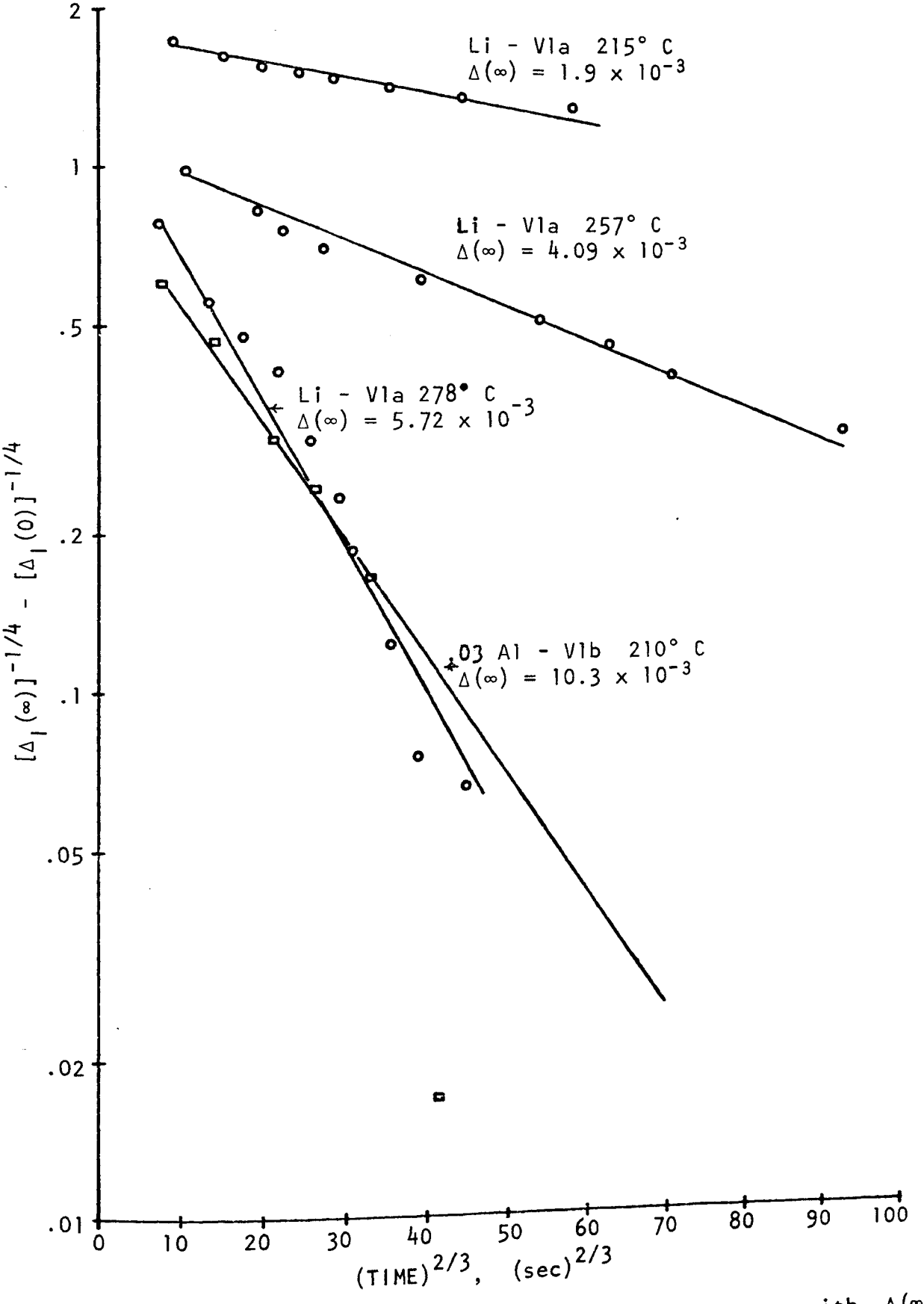

Figure 27. Harper plots of independent decrement recovery with $\Delta(\infty)$ equal to the value of Δ_1 before excitation

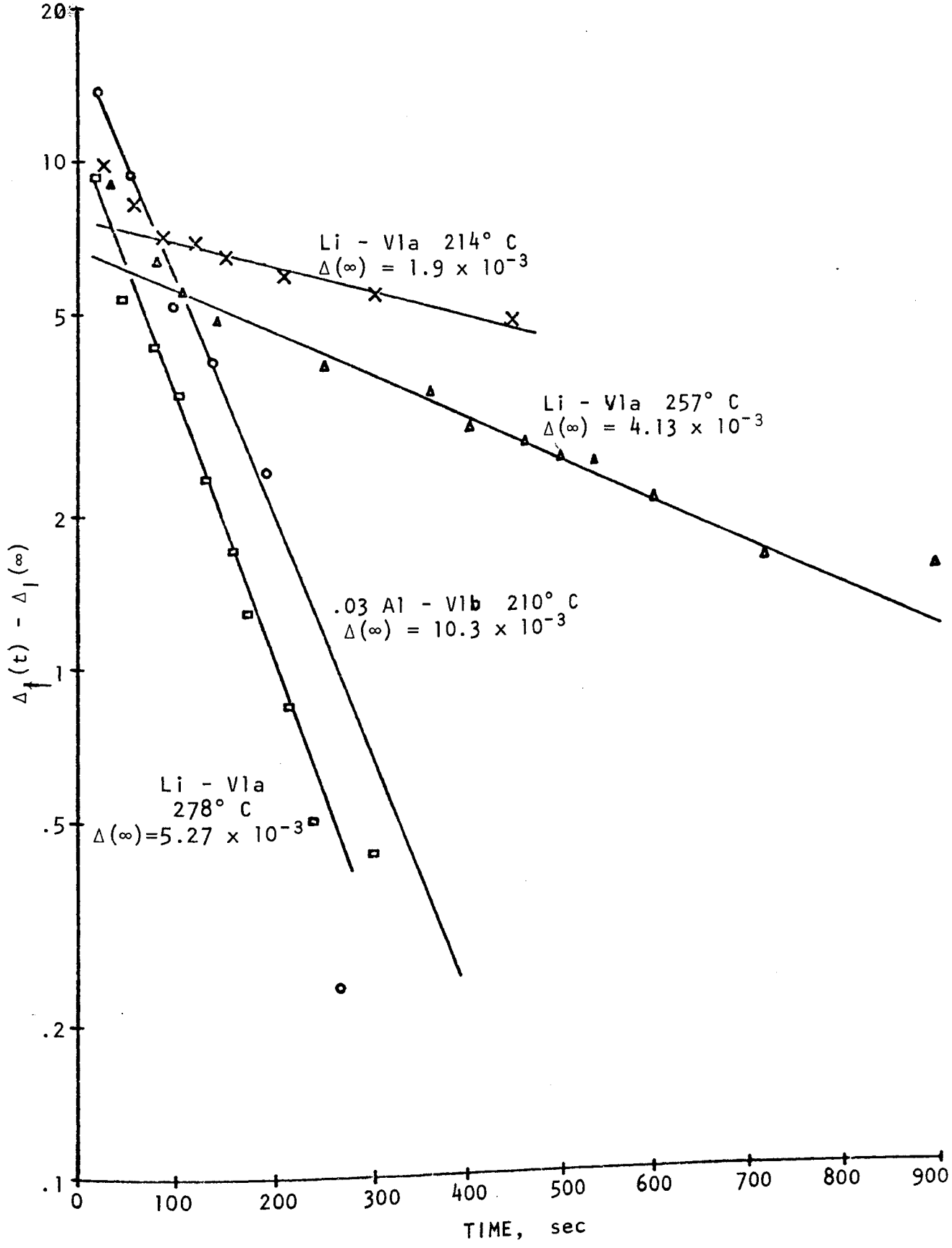

Figure 28. Yamafuji-Bauer plots of independent decrement recovery with $\Delta(\infty)$ equal to the value of Δ_1 before excitation

value before excitation. However, it is evident that a larger value for $\Delta_1(\infty)$ is needed to obtain agreement for the two cases where the decrement appears to approach a larger value for $\Delta_1(\infty)$ than the value before excitation.

The values of $1/\tau$ obtained from the slopes of these plots as well as the values of τ obtained from the Harper plots are given in Table IV.

TABLE IV.

Parameters Obtained from Harper Plots and Yamafuji-Bauer Plots of the Recovery Data

Crystal	Mount	Temp. °C	λ $sec^{-2/3}$	$1/\tau$ sec^{-1}
Li	VIa	278	.077	.013
Li	VIa	257	.014	.0019
Li	VIa	215	.005	.001
.03 Al	VIb	210	.051	.011

D. Dependence on Miscellaneous Parameters

In this section the variation of the damping with regard to mounting history of the specimen, etching, handling, and annealing in air will be presented.

A considerable variation in the damping for the same crystal was observed for different mountings. Some of the undoped crystals were subjected to as many as five different mountings. Table V gives among other quantities the lowest value of Δ_1 observed for each of the separate mountings. Although for reasons given on page 25, variation of the damping between different mountings could be due to the

TABLE V

Annealing Data and Minimum Values of Independent Decrement Observed for All the Crystals

Crystal	Mount ††	Δ_I "Initial" Value After Temp. Inc $\times 10^{-3}$	Time When "Initial" Value Read hours	Δ_I Minimum Value During Anneal $\times 10^{-3}$	Time When Minimum Value Read hours	Anneal Temp. °C
P10	A1	199.8	24	.166	127	276
P10	A2	1.12	67	.882	378	276
P14.5	A2	65.1	0	.161	169	273
P14.5	A3	252.2	1	.152	96	272
P14.5	A4a	107.6	0	.080	408	271
P38	A1a			.408*	264	272
P38	A2	149.3	46	.494*	688	269
P44	A2a	20.5	0	.302	70	271
P44	A3a	70.5	22	.308	193	267
P44	A3b	2.9	72	.23	383	272
P50	A1	.31	22	.154	96	276
P50	A2	4.14	67	.436	378	267
P57	A2a	1.5	20	.153*	164	273
P62.5	A2a	5.11	15	.308	48	273
P62.5	A2b	1.29	0	.292	29	267
P62.5	A3a	37.1	0	6.77*	143	267
P62.5	A4a	17.05	0	.172	500	267
P68	A1	1.59	21	.191	92	272
P68	A2a	4.27	16	.373	145	263
P68	A2b	5.02	0	.583	313	267

Crystal	Mount	Δ_I "Initial" Value After Temp. Inc $\times 10^{-3}$	Time When "Initial" Value Read hours	Δ_I Minimum Value During Anneal $\times 10^{-3}$	Time When Minimum Value Read hours	Anneal Temp. °C
P68	A2c	72.3	13	.574	450	267
P68	V3a	169.2	0	31.79	99	281
P68	V3b	234.7	0	95.9*	15	278
P74	A2	.232	28	.177	72	272
P74	A3a	51.3	18	2.87	332	267
P74	A3c	40.07	24	.297	190	271
P74	V4a	50.8	0	27.8	174	287
P74	A4b	126.	0	.21**	52	288
P84	A1	.63	19	.353*	21	271
P84	A2	77.5	0	.337	646	262
Li	V1a	25.6	0	6.38*	305	280
Li	V1b	6.1	0	5.72	36	278
Li	V1c	70.5	0	11.56*	404	278
Li	V1d	5.47	0	1.64*	178	274
Zn	V1	105.9	0	3.07†	51	277
Zn	V2a	1.57†	0	.956†	34	278
Zn	V2b	1.17†	17	1.097†	65	280
.03 Al	V1a	59.8	0	19.9*	48	279
.03 Al	V1b	115.5	0	34.98	216	281
.05 Al	V1a	105.	0	19.25	280	284
.05 Al	V1b	17.9	0	15.9	0.2	283
.05 Al	V1c	390.8	0	37.8	147	281
.135 Al	V1a	46.2	0	25.95	68	282
.135 Al	V1b	44.2	0	9.46	682	273

(see following page for footnotes)

Footnotes for Table V

††The Mount symbols have the following meaning:

A - Air anneal

V - Vacuum anneal

1,2,··· Designates specimen was etched before mounting

a,b,··· Designates specimen was removed and replaced or a rapid temperature change caused a large increase in Δ_I.

* Anneal was stopped before a definite minimum or constant value was reached.

**Value obtained after an air anneal.

† These values are deceptively low due to the reverse temperature dependence of Δ_I .

condition of the bond, a definite trend is seen for some of the crystals. For the P68 crystal, a definite increase in the damping is evident for successive mountings.

The effects of etching, and handling were studied for the P74 crystal. The results show that etching in general reduces the damping, which is in agreement with earlier work by Marx and Koehler.[42] The effect of handling was complicated by the bond problem, but in general, removing a well annealed crystal, replacing it and heating it to 280° C caused increases as large as 10^3 in the value of Δ_1 from its previously measured value at 280° C before removal.

The effect of annealing in air is shown in fig. 29. These data were obtained for the P68 crystal after it had been annealed in vacuum for 82 hours by opening the oscillator to air. The resulting decrease in the damping was compared to the G-H-L theory and the result is shown in fig. 30. The fit is quite poor and an "S" shaped curve is evident. It is of interest to note that close examination of Harper plots of data obtained while annealing in vacuum show a slight "S" shaped deviation.

E. Unusual Behavior of the Zn Doped Crystal

The behavior of the zinc doped crystal was so unusual, that its measurements will be described separately.

During the first mounting of the zinc doped crystal, the dependent damping was observed to be very sensitive to the duration of the applied vibration. Measurement of the output voltage with the VTVM was virtually impossible and all measurements of the damping above breakaway were performed with the oscillograph method described earlier on page 23. It was found that the decrement increased to over 50% of its initial value within 0.1 sec after application of a high strain

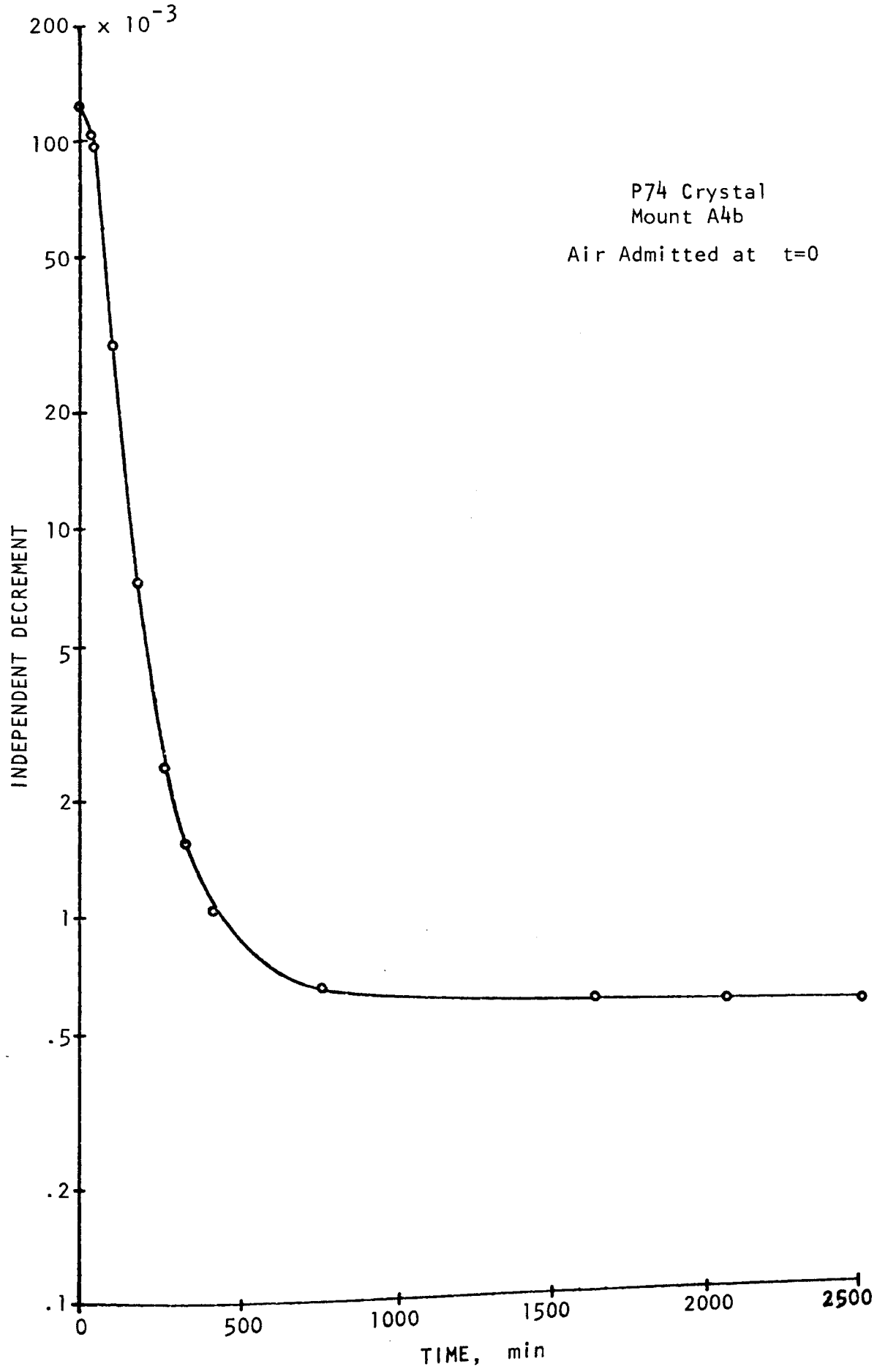

Figure 29. Decrease of damping with time during an anneal in air

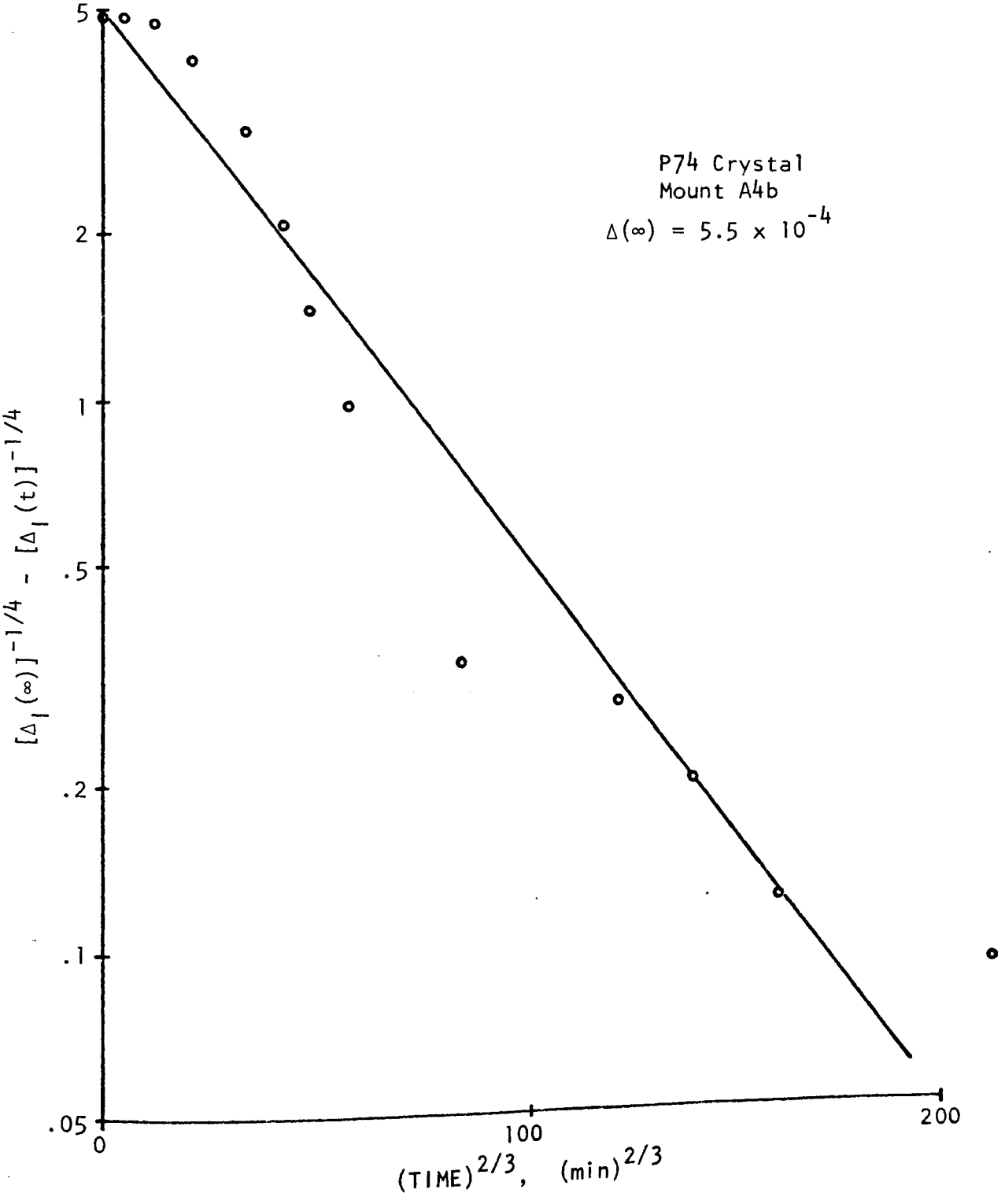

Figure 30. Harper plot of the decrease of independent decrement with time during an anneal in air

amplitude vibration. Actually, because of the reasons given on page 53, the strain amplitude decreased as the damping increased. Thus it is not possible to study the increase of damping as a function of time for a constant strain amplitude. Continued excitation at the high strain amplitude resulted in a saturation of the damping with time.

If the high amplitude vibration was removed and the damping immediately measured at high strain amplitude again, the damping was observed to exhibit the same initial value and increase with time as before. After long excitations at high strain amplitudes, a small increase in the independent damping could be observed. To the author's knowledge, no one has ever reported time effects as rapid and reproducible as the ones described above.

After an anneal of 104 hours at 278° C, measurement of the damping at a high strain amplitude caused the damping to nearly triple in magnitude. Subsequent measurement of the independent damping showed it had increased 28 fold. At this point the crystal was removed from the oscillator.

The second mounting of the zinc doped crystal yielded very low values ($\approx 10^{-4}$) for the damping after the initial increase in temperature. Also, annealing progressed rather slowly. Measurements of the damping as a function of strain amplitude showed the damping was quite strain amplitude dependent, but no time dependence could be detected even at the highest strain amplitudes. Subsequent decrease in temperature showed that the independent damping began to increase with decreasing temperature. This is shown in fig. 31. It should be mentioned that because of the unusual temperature dependence, the independent decrement was measured as a function of temperature several times and

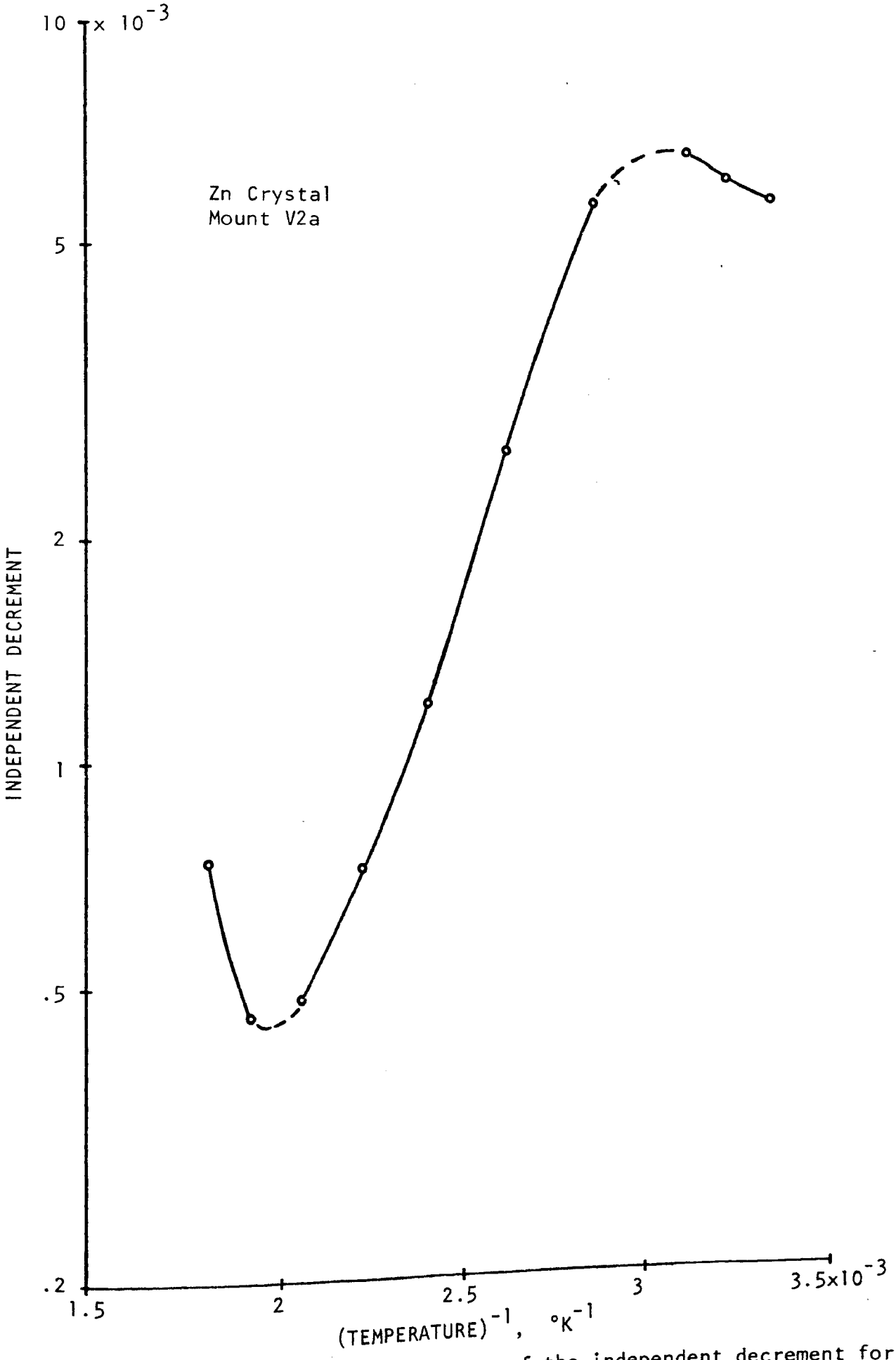

Figure 31. Temperature dependence of the independent decrement for the Zn doped crystal

the data were very reproducible. The damping also became less and less dependent on strain amplitude as the temperature was lowered, but more and more time dependent. In addition, at temperatures of 76° C and below, the damping exhibited a very unusual dependence on strain amplitude. The damping was observed to decrease with increasing strain amplitude for high amplitudes. This is shown in fig. 32.

It was also noted that the independent decrement decreased with annealing time much more rapidly at low temperatures (approximately 25° C) than at high temperatures (280° C). This is the exact reverse of what was observed for the other crystals.

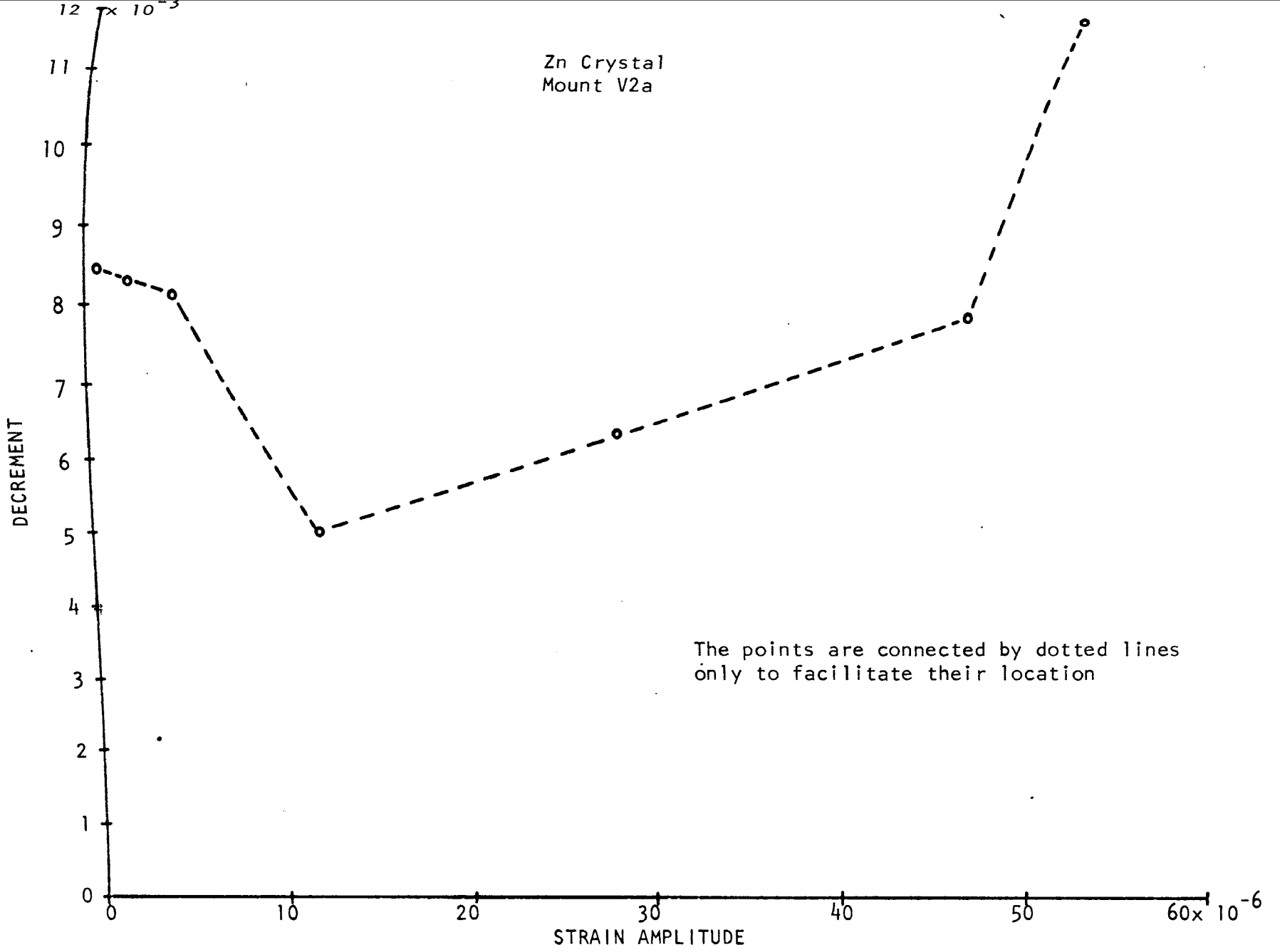

Figure 32. Dependence of the damping on strain amplitude for the Zn doped crystal

V. DISCUSSION

In this section, values for some of the parameters in the theory will be determined from the previous analysis of the data. Also, some of the new phenomena discovered in these experiments will be discussed and possible explanations offered.

A. Discussion of the Analysis of the Annealing Data

1. Reinterpretation of Parameters in the Harper Modified G-H-L Equations. A reinterpretation of some of the parameters in the Harper modified G-H-L equations (given on page 47) for the dependence of the damping and fractional modulus change on annealing time is necessary to have reasonable agreement with the data.

First, in the orginal development of the theory on page 12, it was stated that the concentration of type 2 point defects, C_2 , was equal to the overall concentration of type 2 point defects in the crystal, C_{20} . This was because the orginal theory was developed for room temperature ($\simeq 25°$ C) studies, and for temperatures of this order, the impurity point defects were assumed to be immobile. However, for the annealing experiments in this study, the temperature is high enough that diffusion of these defects is expected. If the mobility of these defects is large enough for thermal equlibrium to be established we would have $C_2 = C_{20}\, e^{Q/kT}$. Since this condition may be subject to question, the concentration of type 2 point defects will be simply represented by C_2, where it is assumed that C_2 is dependent on temperature and definitely larger than C_{20} .

The above change is also necessary to obtain consistency with the other data. If the change is not made, the value obtained for the quantity, $A_4 a^4 / C_{20}^4$, from the value of the damping at time equal zero,

$\Delta_1(0)$, is from 10^{-2} to 10^{-3} times smaller than the value obtained from the theoretically equivalent quantity, A_4a^4/C_o^4, from the intercept of $\ln \Delta_1$ vs $1/T$.

An additional reason for the change, and perhaps the most convincing, is that the value of Δ_1 at $t = 0$ and at 280° C, i.e., immediately after the temperature increase, is much larger than the room temperature value. The only way to explain an increase of the independent damping with temperature is for C_2 to decrease, because the dislocation density, Λ, will certainly not be expected to increase in an unannealed sample. (Excluded from this discussion is the case of the tight quartz-specimen bond for which Λ could increase as a result of the plastic deformation.) If C_2 is given by C_{20} only, then it cannot decrease, and therefore C_2 must be given by $C_{20}e^{Q/kT}$ or some other temperature dependent expression.

Second, the theory assumes that $C_1(t) = (C_{10}\sqrt{2}/a^2\Lambda)(1-\exp[-\lambda t^{2/3}])$. Thus, at $t = \infty$ we would have, $C_1(\infty) = C_{10}\sqrt{2}/a^2\Lambda$. However, if we assume that thermal equilibrium is established after a certain length of time, then C_1 at $t = \infty$ would be given by, $C_{10}e^{Q_1/kT}$. This would require that $C_{10}e^{Q_1/kT} = C_{10}\sqrt{2}/a^2\Lambda$. (11)

If we assume a reasonable value for the dislocation density, Λ, of 10^6 cm^{-2}, equation (11) requires that the interaction energy, Q_1, equal approximately 20 Kcal/mole. This value for Q_1 is in considerable disagreement with the value of approximately 4 Kcal/mole obtained from the slope of $\ln \Delta_1$ vs $1/T$ and $\ln \Delta_H$ vs $1/T$. (See figs. 12 and 13 and Table II.) In order to obtain a value of 4 Kcal/mole from equation (11), it is necessary to have $\Lambda \approx 10^{13}$ cm^{-2} which is unreasonably large. Furthermore, the above relation between Q_1 and Λ

does not depend on the condition of the sample, which is theoretically incorrect. It appears that either one or both expressions for $C_1(t)$ may be incorrect. Therefore, the concentration of type 1 point defects will be given by; $C_1(t) = C_1 \left(1 - \exp[-\lambda t^{2/3}] \right)$, where C_1 is the concentration at $t = \infty$.

Third, the concentration of the network nodes, given by a/L_N, should be added to the concentration of the type 2 point defects, C_2, to be completely correct.

If the above changes are made, the new expressions for $\Delta_1(0)$, γ, and χ, are the following:

$$\Delta_1(0) = A_3 a^4/(C_2 + a/L_N)^4$$

$$\gamma = C_1/(C_2 + a/L_N)$$

$$\chi = A_4 a^2/2(C_2 + a/L_N)^2$$

2. Evaluation of the Parameters K, L, L_N, U, and D. It is immediately evident that values for all the parameters in the theory cannont be experimentally determined from the reported measurements. It is therefore necessary to use the theoretically calculated values for some of the parameters. The dislocation line tension, C', the orientation factor, Ω, and the parameter, A, which is related to the force between a solute atom and a dislocation, will be assumed to equal their calculated values in the Appendix. Although conclusive experimental proof is lacking for the theoretical values of these constants, no contradictory evidence has been found either.

The value of the damping constant, B, is in doubt yet, but recent evidence indicates it agrees with the theoretical estimate by Liebfried.[62] Therefore, a value of 10^{-4} wil be used for B. This value

is close to the Liebfried calculation (see Appendix) and is probably quite reasonable. The parameter, K, which is related to the force required to produce breakaway, is in much greater doubt and therefore it will be left to be determined from the data. The remaining quantities to be determined are the dislocation density, Λ, the average loop length, L, the network node length, L_N, the activation energy for diffusion, U, and the diffusion coefficient, D. The following procedure has been used to obtain values of the above parameters:

From the independent decrement and independent fractional modulus change fits, experimental values for the following quantities have been determined (see Table III).

$$\frac{A_3 a^4}{(C_2 + a/L_N)^4} = \frac{120\Omega\Lambda B\omega a^4}{\pi^3 C' (C_2 + a/L_N)^4} = \Delta_1(0)$$

$$C_1(C_2 + a/L_N) = \gamma$$

$$\alpha\Lambda(AD/kT)^{2/3} = \lambda$$

$$\frac{A_4 a^2}{2(C_2 + a/L_N)^2} = \frac{3\Omega\Lambda a^2}{\pi^2(C_2 + a/L_N)^2} = \chi$$

Thus the ratio, $\Delta_1(0)/\chi^2$ gives a value for B/Λ. If B is assumed to equal 10^{-4}, then Λ can be determined. From the value of either $\Delta_1(0)$ or χ, the value of $C_2 + a/L_N$ is found. The value for C_1 is then calculated from γ. The value of λ determines D, which equals $D_o e^{-U/kT}$. If a value for D_o is picked, then U can be determined. The results of the above procedure are given in Table VI for the crystals possessing reasonable fits of the data to the theory.

The values obtained for the dislocation density, Λ, seem very reasonable and agree with etch pit measurements on well annealed metal crystals which yield values for Λ between 10^4 and 10^6 cm^{-2}. [43]

TABLE VI

Values of Dislocation Density, Point Defect Concentration, and Activation Energy Obtained from the Annealing Data

Crystal	Mount	B/Λ $\times 10^{-10}$	Λ $\times 10^{6}$	$C_2 + a/L_N$ $\times 10^{-5}$	C_1 $\times 10^{-5}$	D $\times 10^{-8}$	U Kcal/mole
P68	V3a	.474	2.11	2.40	.79	53.1	13.28
P68	V3b	2.29	.44	1.47	.40	149.2	12.08
P74	V4a	1.98	.50	1.93	.33	28.5	14.24
Li	V1c	4.33	.23	1.72	.95	135.3	12.27
Zn	V1	.107	9.36	3.97	5.83	.87	17.76
Zn	V2a	.475	2.1	7.64	1.17	16.4	14.61
.03 Al	V1b	1.13	.88	2.35	.52	29.3	14.2
.05 Al	V1a	2.57	.39	1.84	.46	186.	12.05
.05 Al	V1c	.49	2.03	1.84	1.50	14.7	14.76
.135 Al	V1a	1.90	.53	2.37	.38	69.	13.17

In regard to the values obtained for U, Shewmon[44] obtained a value of 32 Kcal/mole for the self diffusion activation energy of magnesium. This would give a value of about 16 Kcal/mole for the activation energy for the migration of vacancies, which is close to the values given in Table VI. This seems to indicate that vacancies or substitutional solute atoms are the segregation point defects.

The values obtained for C_1 and $C_2 + a/L_N$ seem to be rather small. Even if the value of a/L_N is zero, the value of C_2 for the .135 Al doped crystal is much too small. It is only about 24 ppm and if $C_2 = C_{20}\, e^{Q_2/kT}$, this value should be larger than C_o which is about 1.68×10^{-3} from the actual chemical analysis. This difficulty will be discussed more later.

3. Evaluation of the Parameters K, L_N, and C_2. It is possible to determine values of K, and L_N for those crystals for which the damping was measured as a function of strain amplitude after the anneal. Values for the following two quantities are obtained from the slope, S and intercept, I, of a G-L plot:

$$A_2 = K\eta a/L_c = S \tag{12}$$

$$A_1 = (\Omega\Lambda L_N^3/\pi^2)(2K\eta a/\pi L_c^3)^{1/2} = e^I$$

If we assume $a/L_c = C = C_1 + C_2$, then from equation (12) we have

$$C_1 + C_2 = S/K\eta \tag{13}$$

However, values of

$$C_T = C_1 + C_2 + a/L_N \tag{14}$$

were obtained previously (col. 5 plus col. 6 in Table VI). Thus we have from the above two equations:

$$a/L_n = C_T - S/K\eta \tag{15}$$

If we now replace the factor L_c in the expression for A_1 by $K\eta a/S$,

we have:

$$(\Omega \Lambda L_N^3/\pi^2)(2/\pi)^{1/2}(S^{3/2}/K\eta a) = e^1$$

Thus,

$$\Lambda L_N^3 = \pi^2(\pi/2)^{1/2}(e^1 K\eta a/S^{3/2}\Omega)$$

Values for the quantity, $\Lambda L_N^3/K\eta$, are listed in col. 5 of Table VII. If we now use the value of Λ determined earlier, we can find a value for a/L_N in terms of $(K\eta)^{-1/3}$. This relation and equation (15) above can be solved simultaneously (a graphical solution was used) to give values of a/L_N and $K\eta$. These are listed in col. 6 and 8 in Table VII. Then from either equation (13) or (14) a value of $C_1 + C_2$ is found. Using the value of C_1 obtained earlier, the value of C_2 is determined. The values of C_2 are given in col. 10 of Table VII.

The values obtained for L_N are in agreement with the work by Weertman and Salkovitz.[45] In the early tests of the G-L theory, it was thought that L_N would not be expected to be larger than 10^{-4}. However, values of 10^{-3} are now quite commonly found.

Using the values of η in the Appendix, values from 1.6 to 28 are found for the constant K. These values are considered quite large. Theoretical estimates for K as given in the Appendix show it should be of the order of 0.5. Also, we note that the value of K is considerably larger for the .05 Al doped crystal than the .03 Al doped crystal. This is theoretically incorrect because the binding force should be the same for the same type pinning point. The values obtained for C_2 are even smaller than expected, because a/L_N is certainly not negligible. In face, a/L_N exceeds the value for $C_2 + a/L_N$ for the case of the .135 Al doped crystal.

TABLE VII

Values of Network Node Loop Length, Parameter K, and Point Defect Concentration Obtained from the Annealing Data

Crystal	Mount	$\ln(\Delta_H \varepsilon_o^{1/2})$ vs $1/\varepsilon_o$ Slope $\times 10^{-5}$	Intercept $\times 10^{-4}$	$\Lambda L_N^3/K$	a/L_N	L_N $\times 10^{-5}$	L_N $\times 10^{-3}$	Kn	K	C_2	C_{10} $\times 10^{-15}$
P68	V3a	1.22	20.5	.392	.71	4.52	.492	2.46	1.69	12.2	
P68	V3b	.82	6.55	.227	.47	6.83	.586	2.93	1.00	1.3	
P74	V4a	.52	1.89	.225	.61	5.26	.314	1.57	1.32	1.2	
Li	V1c	7.14	3.13	.0038	.80	4.01	3.81	19.	.92	1.6	
Zn	V1	24.8	51.4	.0096	1.85	1.73	3.12	21.5	2.12	400.	
Zn	V2a	32.7	1900.	.244	.41	7.83	3.89	26.8	7.23	18.	
.03 Al	V1a	.39	1.71	.0016	.94	3.41	.20	1.65	1.41	3.3	
.05 Al	V1b	5.04	.04	.00007	-	-	>10	>100	-	1.3	
.05 Al	V1c	1.8	.26	.0025	2.4	1.34	1.9	15.7	<0	22.2	

Finally, col. 11 of Table VII gives the value of C_{10} as calculated from the relation, $C_{10} = \sqrt{2}/a^2\Lambda$. The values obtained are unreasonably small, because estimates of vacancy concentrations are usually of the order 10^{-5} to 10^{-8}. [46]

B. Discussion of the Analysis of the Dependence of the Damping on Temperature.

1. Evaluation of the Parameters K and C_o . If we assume $C_1 = C_{10}\, e^{Q_1/kT}$ and $C_2 = C_{20}\, e^{Q_2/kT}$, and further assume for the moment that $Q_1 = Q_2$ we have:

$$C = C_1 + C_2 = (C_{10} + C_{20})\, e^{Q/kT}$$

or $C = C_o\, e^{Q/kT}$ where $C_o = C_{10} + C_{20}$. Under these assumptions, the intercept of $\ln \Delta_l$ vs $1/T$ yields a value for the quantity, $A_3 a^4/C_o^4$, and the intercept of $\ln \Delta_H$ vs $1/T$ gives a value for $Kn C_o$, where n is the misfit parameter, and C_o is the overall impurity concentration in the crystal. These values have been listed previously in Table II. If the value for C_o is calculated from the intercept of $\ln \Delta_l$ vs $1/T$ and the values determined earlier are used for , then K can be calculated from the intercept of $\ln \Delta_H$ vs $1/T$. The values of C_o and K obtained in this manner are listed in Table VIII.

Again, we see the values of C_o are too small, especially for the Al doped crystal. However, the values of K are in better agreement with the theory.

It should be noted that the factor a/L_N has been neglected in the $\ln \Delta_l$ vs $1/T$ plot. The inclusion of this term would actually invalidate this way of plotting the data. If we assume, however, that the effect of the term would have only a small influence on the plot,

TABLE VIII

Values of Point Defect Concentration and Parameter K Obtained from the Temperature Dependence of the Damping

Crystal	Mount	C_o^* $\times 10^{-6}$	Kn	$C_o^\dagger$ $\times 10^{-4}$	
P74	V4a	2.77	.039	5.86	
Li	V1c	3.91	.029	1.72	
Zn	V2a	18.1	.058	5.1	
.03 Al	V1b	3.5	.0004	.85	Before "Jump"
.03 Al	V1b	3.5	1.16	44.9	After "Jump"

*Calculated from $\ln \Delta_I$ vs $1/T$ and $\ln \Delta_H$ vs $1/T$ intercepts

†Calculated from $\ln \Delta_H$ vs $1/T$ intercept using $C = C_o^2 e^{2Q/kT}$ and previous values of Kn from Table VII

the intercept would then equal $A_3 a^4 / (C_o + a/L_N)^4$. If the term a/L_N is not negligible and the previous discussion shows that it may have a sizable effect, its inclusion would tend to lower the already low value of C_o and also increase the value of K.

A second difficulty has to do with the value of the interaction energy, Q. Table II shows that the values obtained from the Δ_H data are about twice those found from the Δ_I data. This was also found by Hinton and Rider[37] in their study of dilute lead alloys. However, the value for Q depends on the assumption that $Q_1 = Q_2$ and this may not be true. It has been argued that if two types of defects were present with different interaction energies a plot of $\ln \Delta_I$ vs 1/T would not be linear.[47] This is not true in practice, since fig. 33 and 34 show plots of $\ln \Delta_I$ vs 1/T, where Δ_I is calculated from two different defects. A very good straight line is found showing that the deviation from linearity caused by two types of point defects is not great enough to be detected.

A third difficulty is that according to the theory $C = C_o e^{Q/KT}$, the interaction energy, Q, is not dependent on C, i.e., plots of $\ln \Delta_I$ vs 1/T should have the same slope even if C_o is different. Thus, for example, if the interaction energy is due to an Al atom and a dislocation then we would expect the same value of Q for all concentrations of Al. We see a wide variation of Q determined from $\ln \Delta_I$ vs 1/T plots is exhibited for the crystals. If we assume two different defects as above, fig. 34 shows that a change in the concentration of one of the defects can cause a change in the value of Q found from a $\ln \Delta_I$ vs 1/T plots is exhibited for the crystals. If we assume two different defects as above, fig. 34 shows that a

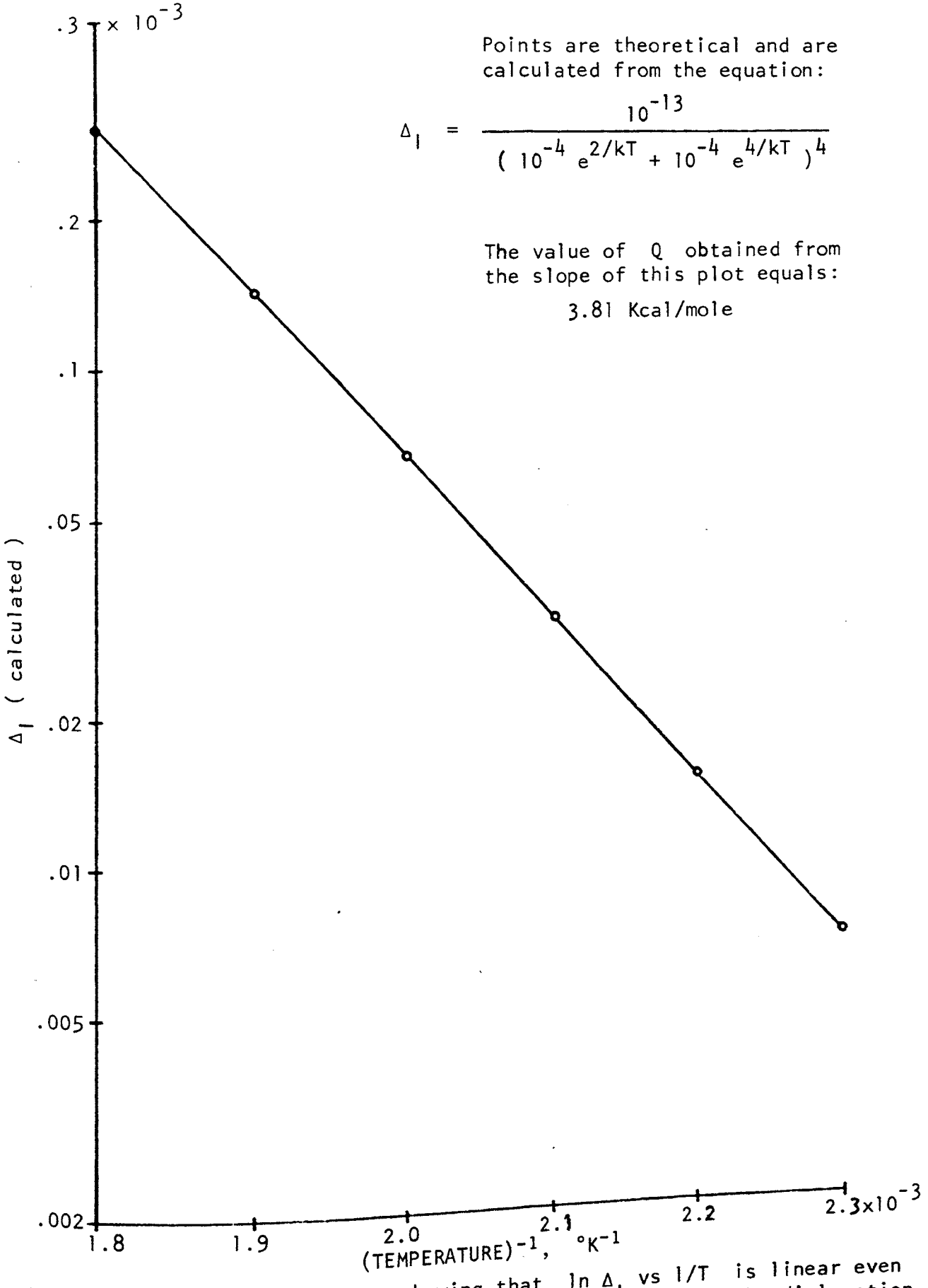

Figure 33. Theoretical plot showing that ln Δ_l vs 1/T is linear even if two types of pinning points interact with the dislocation

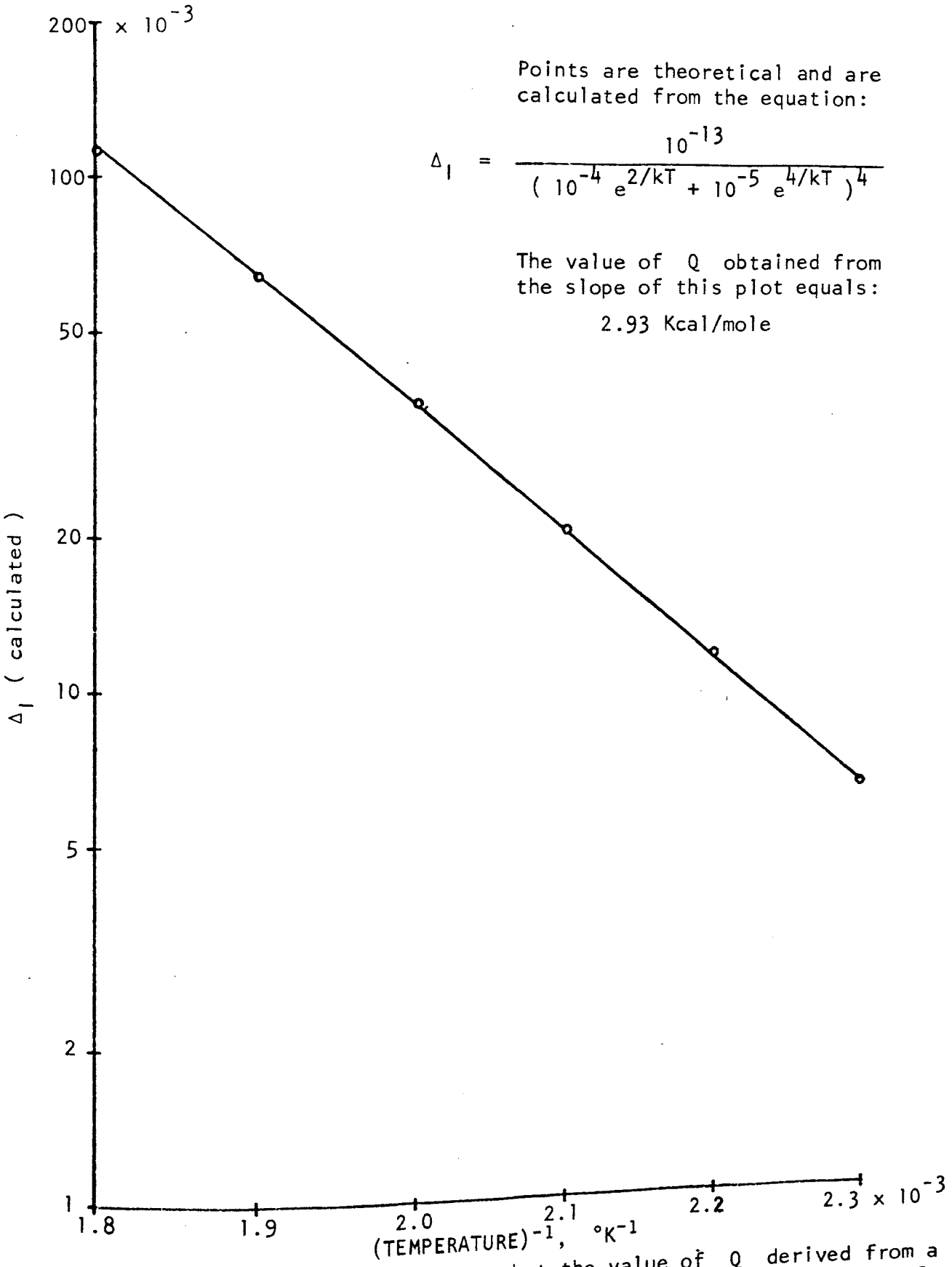

Figure 34. Theoretical plot showing that the value of Q derived from a ln Δ_1 vs 1/T plot can vary with the overall concentration of the pinning points

change in the concentration of one of the defects can cause a change in the value of Q found from a $\ln \Delta_I$ vs $1/T$ plot. Thus these arguments show that a two type defect theory may explain the observed results better than a single defect theory.

2. Interpretation by Bauer. Recently, Bauer[48] has shown that if the entropy contribution of the grouping of pinning points on a dislocation line is taken into account, the expression $C = C_o e^{Q/KT}$ should be replaced by $C = C_o e^{-F_B/kT}$, where F_B is the binding free energy and is equal to $U_B - TS_B$. (Note: U_B is the binding energy and is equal to $-Q$ as used previously.) Bauer has calculated S_B to be approximately equal to $k \ln C^{1/2}$, where k is the Boltzmann constant. In this case, $C = C_o e^{-U_B/kT} C^{1/2}$ or $C = C_o^2 e^{-2U_B/kT}$. This relation would yield the same values of Kn and C_o as obtained in cols. 3 and 4 of Table VIII if the intercepts of the temperature plots of Δ_I and Δ_H are used together. Since the plot of $\ln \Delta_I$ vs $1/T$ intercept alone. The value of Kn, however, is necessary for this calculation. If the values of Kn given earlier in col. 8 of Table VII are used, then the above calculation gives the values of C_o as given in col. 5 of Table VIII. We now see that C_o is too large, especially for the pure crystals. In order to obtain reasonable values for the pure crystals, Kn would need to be as large as 20.

It is possible that the entropy contribution is not quite correct as calculated by Bauer, or the assumptions made in his calculation, namely that mobility along the dislocations is high, do not hold for these crystals. Also, the expression, $C = C_o e^{-F_B/kT}$ is only valid for $C \ll 1$. The more general expression is given by Van Bueren[49] as:

$$C = C_o e^{-F_B/kT} / (1 + C_o e^{-F_B/kT}) \quad (16)$$

If $S_B = k \ln C^{1/2}$ is inserted into eq. (16) above, we obtain:

$$C^{1/2} / (1 + C) = C_o e^{-U_B/kT} \quad (17)$$

Unfortunately, eq. (17) cannot be put into a convenient linear form to permit comparison of the data to it. However, for the approximate values of C_o and U_B found earlier, there would be very little difference between the more general expression (eq. (17)) and the Boltzmann form. The only result would be to lower the deviation of the tail slightly in the low temperature region of the $\ln \Delta_I$ vs $1/T$ plots, thereby extending the linear range of these plots.

In view of the previous considerations, it is concluded that plots of $\ln \Delta_I$ vs $1/T$ and $\ln \Delta_H$ vs $1/T$ are questionable in their theoretical correctness.

C. Discussion of Difficulties Appearing in Sections V-A and V-B.

1. Incompatibility of the Independent Decrement and Dependent Decrement Predictions. From the previous discussions, it appears that the independent and dependent decrement data are incompatible in several ways. There are two possible reasons for this. First, the G-L theory neglects thermal assistance to breakaway. Recent estimates[11] of the effect of including thermal assistance show that it will not alter the strain amplitude dependence of the damping, but the value of the slope of a G-L plot will include a temperature dependent term. It is apparent that a proper change in the values of the obtained slopes could remove all of the previous difficulties. However, the theory is not developed completely enough to allow a comparison with the data. Second, the assumption that $\Delta = \Delta_I + \Delta_H$, where Δ_I remains constant

even into the strain amplitude dependent region, may not be valid. It seems likely that after breakaway Δ_I should originate from the damping of loop lengths of the order L_N. This requires additional theoretical consideration.

2. Incorrect Predicted Concentration of Solute Atoms. The most serious problem which exists for both dependent and independent decrement separately, is that the magnitude of C as well as C_o is too small, especially for the doped crystals. Also, the predicted values of the concentration do not vary with the amount of added impurity. Even glue joint variations would not be expected to be responsible for the tremendous discrepancy existing for the .135 Al crystal. Although the impurity concentration, C, depends on the value chosen for the damping constant, B, an increase of 10^{-4} in the magnitude of B would be necessary to increase C by 100. This has the consequence of causing the dislocation density to become 10^{10}, which is considered unreasonably large. Even so, this could not account for the lack of concentration dependence. In addition, the background (non-dislocation) damping, Δ_b is not known for these crystals. Its inclusion would have the effect of increasing the value for C. However, the air anneal data show that the dislocations are far from being saturated, and Δ_b would not be any larger than 10^{-4}. This value would not be large enough to reduce the value of Δ_I observed for the .135 Al crystal to the value of 10^{-8} that is necessary to obtain the correct value for C.

Nevertheless, much closer agreement is found here than Fiore[50] obtained for Cu-Ge alloys. He calculated the magnitude of Δ_I to be about 10^{-15} for a crystal containing 60 ppm of added impurity. He did

not, however, determine any parameters experimentally, but only estimated their values. The value for the loop length, L, was calculated on the basis that $C = C_o e^{Q/kT}$, and it is apparent that the calculated value depends considerably on the choice of the values for Q. Since $\Delta_I \propto L^4$, a small error in the choice of the value for Q would have a tremendous effect on the calculated value of Δ_I. In addition, there seems to be reason to doubt the relation $C = C_o e^{Q/kT}$.

Recently, Hinton and Rider[37] as well as Fiore have not found agreement with the predicted dependence of the damping on concentration. Fiore finds Δ_I varies as C to the first power rather than the fourth power, while Hinton and Rider do not find a constant power dependence at all. Since it has been conclusively verified by Thompson and Holmes[51] as well as others[14,52] that Δ_I varies as L^4, it is doubtful that the power dependence is what is causing the discrepancy. What seems to be more reasonable is that the impurity atoms are simply not reaching the dislocations in the predicted amount. This could be due to the fact that the impurity atoms largely move as a result of vacancy diffusion. It also seems reasonable that it is possible for a greater number of vacancies to reach the dislocation lines in a given length of time than substitutional impurities. This is illustrated by the following figure of a one dimensional line of atoms.

o ● o o o o o o o o o o

Let the black dot represent a substitutional impurity atom. In order for the solute atom to move 10 lattice parameters to the right, 10 vacancies must migrate to the left. Thus, if this is the case, it is possible that the vacancy concentration in the lattice is depleted during an anneal to the point where solute atom migration becomes difficult

before the concentration of impurity atoms has reached its theoretical value. If this is true, a small deformation of the crystal should cause the final value of Δ_1 observed after the anneal following the deformation to be smaller than the value observed prior to deformation. This is because the increase in vacancy population would allow more solute atoms to migrate to the lines. However, this effect may be masked by the increase in dislocation density.

It should be noted that although the values of the solute atom concentration obtained from the data analysis do not agree with the amount of added impurities, Table V shows that the minimum value of Δ_1 ever observed for each of the three Al doped crystals is at least in qualitative agreement with the known concentrations. That is, the damping is smaller for the more impure crystals. Again it should be emphasized that comparison of decrement magnitudes between different crystals is quite unreliable, primarily because of the quartz-specimen bond problem.

D. Evaluation of Parameters Obtained From the Analysis of the Recovery Data.

The parameter, λ, as determined by the recovery data is equal to $\alpha\Lambda(AD_o/k)^{2/3}\, e^{-2U/3kT}/T$. Thus, if the dislocation density remains constant during the recovery process, a plot of $\ln T_\lambda$ vs $1/T$ would give values of U and D_o. Unfortunately, the data are not good enough to obtain a plot of this type. If we assume a value of 1 cm^2/sec for D_o, then values for the activation energy U can be calculated at the different temperatures for the recovery data. These values are given in Table IX. (The values for the dislocation density, Λ, were obtained from Table VI.)

The variation in the obtained values for U is considerable, but the values are about half as large as those obtained from the anneal data. This would imply a more mobile defect is being dispersed by the high strain amplitude vibration than that which originally diffused to the dislocations. Since this seems unrealistic, the interpretation by Yamafuji and Bauer[41] is probably more correct. The parameter $1/\tau$ as determined from the Yamafuji-Bauer plots is related to the pipe diffusion coefficient by, $D^d = 2L_c^2/\tau$, where L_c is the average distance between minor pinning points and $D^d = D_o^d e^{-U^d/kT}$. If we use the values of L_c as obtained from the slopes of the G-L plots, we obtain the values of D^d given in col. 5 of Table IX. If we assume values of D_o^d of .1 and .01 cm^2/sec, we find the values of U^d given in cols. 6 and 7 of Table IX. These values can be compared to 28 Kcal/mole as obtained by Oren and Bauer[53] for Cu-Ge crystals. Not much confidence can be placed in these results, however, because the recovery data are visibly poor.

TABLE IX

Values of Activation Energy, and Pipe Diffusion Coefficient Obtained From the Recovery Data

Crystal	Mount	Temp. °C	G-H-L Harper Theory U Kcal/mole	D^d $\times 10^{-8}$	Yamafuji-Bauer Theory U^d Kcal/mole	
					$D_o^d = .1 cm^2/sec$	$D_o^d = .01 cm^2/sec$
Li	VIa	278	7.7	7.5	15.5	12.9
Li	VIa	257	10.	1.1	16.9	14.5
Li	VIa	215	10.8	.6	16.1	13.9
.03 Al	VIb	210	9.5	5.7	13.3	11.6

E. Discussion of the Reverse Anneal Data

It was stated earlier that the independent decrement was observed to decrease with annealing time at first, then reach a constant value, and, if held at the same temperature long enough, it was observed to increase again. This was observed for doped as well as pure crystals and in the case of both air and vacuum anneal.

In order to account for this with the G-L model, the loop length, L, must begin to increase with time. This can only occur by a net migration of points away from the line, or a redistribution of the points along the line so as to reduce the average value of L, or a disappearance of pinning points. The latter possibility is a very real one for the case of vacancies, since dislocation jogs are known to readily annihilate vacancies and, in addition, mutual annihilation can also occur. Thus the reverse anneal would begin when the net flux of vacancies to the lines is less than the rate of annihilation.

This situation would require a reconsideration of equation (9) on page 47, since no account of this was taken in the theory. Although good agreement was obtained with the predicted rate of decrease, it cannot be said that the addition of an annihilation term would cause disagreement. In fact, this may be the reason a more exact treatment of the precipitation equation by F. S. Ham[54] did not agree as well with the data as the supposedly incorrect form of the Harper equation. It is possible that the addition of an annihilation term in Ham's equation could bring it into better agreement.

It would be expected that the damping would eventually stop increasing and level off at a value governed by the equilbrium number of solute atoms and unannihilated vacancies. Unfortunately the anneal

was not permitted to progress long enough to determine if the damping would eventually reach a plateau.

F. Discussion of the Large Decrease of Damping Observed During an Air Anneal.

It is possible that the large decrease of the damping during the air anneal described on page 70 and shown in fig. 29 is due to the influx of gas atoms which further pin the dislocations and reduce the average loop length, L. Marx and Koehler[42] found that an anneal of a copper single crystal in hydrogen caused the independent decrement to be an order of magnitude smaller than the value observed for a vacuum anneal. Although it is doubtful that oxygen or nitrogen atoms can enter magnesium interstitially, it is known that exposure to moisture can introduce hydrogen into magnesium through the reaction:

$$Mg + 2H_2O \rightarrow Mg(OH)_2 + H_2$$

Raynor[55] states that "heat treatment of magnesium alloys under conditions where they are exposed to the atmosphere results in considerable hydrogen "pick up", especially if the atmosphere is humid."

It may be argued that the polymerization of the vacuum grease at the specimen-quartz interface is the cause of the decrease in damping during the air anneal. However, the rate of polymerization is found experimentally to be much slower than the observed rate of decrease of the damping. Because interstitial hydrogen has a high mobility, this would agree more favorably with the rather rapid rate of decrease of damping.

It is important to note that the minimum values of Δ_1 obtained for the P68 and P74 crystals during the vacuum anneal are much larger than the values obtained for the air anneals. Although

this seems to support the above explanation, a question arises as to why the decrement is larger for the later vacuum measurements. In order for this to occur, the concentration of hydrogen must decrease. It is possible that a certain amount of degassing occurs in vacuum, but whether this process would be able to pull the hydrogen away from the dislocation lines is questionable. It is possible that the increase of dislocation density due to the handling before each mounting causes the observed increase in damping. An additional air anneal would then be required to pin these new dislocations. This would mean that the dislocation density increases for each mounting. Techniques such as etch pit counts would be required to check this point, since the damping is not sensitive to completely pinned dislocations.

It was found that an air anneal of the Li doped crystal did not produce any greater decrease in Δ_1 than would have been expected for a vacuum anneal of the same length. Since the impurity content of the Li doped crystal is about the same as the P74 crystal, it is difficult to explain this behavior. Of course, the surface condition (oxide layer) could have considerable influence on the rate of formation of magnesium hydroxide. Further study of this factor would be of interest.

It is interesting to observe that the only data for the decrease of the damping with time during an air anneal which was able to be fitted to the Harper equation was that for the P62.5 crystal. The conditions for this anneal were somewhat unique however. It had already been subjected to a long air anneal at 200° C, and then the temperature was increased to 280° C. The resulting increase in

damping and subsequent anneal was probably caused by the deformation produced by the tight specimen-quartz joint, since the grease had certainly enough time to polymerize. It is believed that the reason this air anneal data agrees with the Harper equation is that the influx of hydrogen had probably saturated during the long 200° C anneal so that no additional influx of hydrogen was present during the 280° C anneal.

G. Discussion of the Double Strain Amplitude Dependence

On page 31 an unusual phenomena called "double strain amplitude dependence" was described. It was found that G-L plots of this resulted in two separate linear regions (see fig. 10).

It is possible that this type of G-L plot can be explained by two types of intermediate pinning points, one being much more strongly bound than the other. The first strain amplitude dependent region would correspond to the breakaway of the less strongly bound intermediate pinning points and the second region, to the breakaway of the more strongly bound points. However, since a distribution of loop lengths would be expected for the strong as well as the weak pinning points, we would expect the breakaway of the strong points to be a gradual process. Thus, the suddeness of the process presents a problem with this interpretation.

Another possibility is that Frank-Read multiplication has begun. Although this may explain a sudden increase in the damping, it would certainly not be expected to support a rapid decrease to the original value.

It is also possible that a redistribution of pinning points occurs at a critical amplitude above the breakaway amplitude. It

is not known if this would be a sudden process, but rapid recovery would be possible with this interpretation. Also, it was noted that although the damping suddenly increased to a much higher value, continued vibration at this high amplitude caused the damping to increase further with time until a relatively constant value was obtained. This would also be in agreement with a redistribution model. Recent theoretical treatment of this type model by Bauer and Yamafuji[38] has shown that the critical stress for redistribution is smaller than the breakaway amplitude, ie, redistribution starts before breakaway and is the necessary condition for breakaway to occur. However, no second redistribution after breakaway is predicted by Bauer. Whether the above could be explained by this type model requires further study.

A final possibility is that the sudden increase in damping is caused by a micro-crack opening up. Although this could explain a sudden increase, it is somewhat doubtful that it could explain why the decrement continues to increase with time after the "jump" has occured. Also, it would seem that the strain amplitude at which the micro-crack opens up should not depend on temperature. Finally, it seems rather unusual that a micro-crack would appear in two different crystals. In any case, it would be extremely difficult to prove or disporve this possibility experimentally.

H. Discussion of the Unusual Behavior of the Zn Doped Crystal

The G-L theory in its present form is unable to explain the unusual behavior of the zinc doped crystal as described on pages 70 and 73. Although a reverse temperature dependence of the independent damping has been observed earlier by D. N. Beshers[56] for an unannealed copper crystal, this dependence disappeared with annealing. This

behavior can be explained by assuming the defects are quite immobile at room temperature and in the unannealed crystal are unable to segregate to the dislocations. As the temperature is increased, segregation begins which decreases the average loop length L, and therefore the damping decreases with increasing temperature. A subsequent decrease in temperature would then cause a decrease in damping. Since this subsequent return to a normal temperature dependence after an anneal is not observed for the zinc doped crystal, it is evident that a different mechanism is responsible for the increase of damping with decreasing temperature. Even more mystifying is why the dependent damping seems to follow a normal temperature dependence. This would mean that while the average loop length, L, increases with decreasing temperature, the average distance between pinning points, L_c, decreases. If the relation $1/L = 1/L_N + 1/L_c$ is assumed to hold, then as the temperature decreases, the network node loop length, L_N, must increase faster than L_c decreases. This condition is nearly impossible to believe.

The G-L model also can not explain the decrease of the damping with strain amplitude at room temperature. Although the G-L theory predicts a maximum in the damping as very high strain amplitudes are reached, it is very difficult to see how a minimum could be explained.

It is apparent, that further study of several zinc doped crystals is desirable to determine if the phenomena observed are associated with the zinc additive or only this one particular crystal. It might be mentioned that, unfortunately, the temperature dependence of the damping was not measured for the first mounting of the crystal. It is therefore quite possible that the unusual phenomena were unique to the second mounting.

VI CONCLUSIONS

1. Reasonable qualitative agreement is obtained between the G-L theory and the observed dependence of the damping and modulus on strain amplitude, temperature, and time for most of the magnesium crystals studied.

2. The time dependence of the segregation of pinning points to dislocations is adequately described by the Harper modified Cottrell-Bilby equation. However, it cannot be stated that all future theories would have to be of this form to obtain agreement with these data.

3. It is possible to predict from the data reasonable values of the dislocation density, network node length, and migration energy for the diffusion of vacancies in magnesium.

4. There is evidence that the primary point defects that interact with the dislocations are vacancies with added impurity atoms as secondary. In the case of air annealed crystals, interstitial hydrogen atoms also contribute to dislocation pinning.

5. The magnitude of the independent decrement does not agree with the amount of added impurities. However, there seems to be reasons why this could happen for substitutional impurities.

6. The observed temperature dependence of the independent decrement seems to be better explained by assuming the pinning points are of two types having different interaction energies.

7. An unusual "double" stress dependence has been observed that does not seem to be explainable with present theories.

BIBLIOGRAPHY

1. T. A. Read, Phys. Rev. 58, 371 (1940).

2. A. Granato and K. Lücke, J. Appl. Phys. 27, 583 (1956).

3. R. H. Chambers, Carnegie Inst. of Tech. Report AT(30-1)-1193 (1957).

4. A. V. Granato, Internal Friction, Damping, and Cyclic Plasticity, Special Technical Publication No. 378, American Society for Testing and Materials (1965).

5. A. Seeger, Phil. Mag. 1, 651 (1956).

6. J. S. Koehler, Imperfections in Nearly Perfect Crystals, p. 197, John Wiley (1952).

7. A. S. Nowick, Symposium on Plastic Deformation of Crystalline Solids, Office of Naval Research (1950).

8. J. Weertman, J. Appl. Phys. 26, 202 (1955).

9. D. H. Wilks and J. Wilks, Adv. in Phys. 9, 1 (1960).

10. K. Lücke and A. Granato, Dislocations and Mechanical Properties of Crystals, p. 425, John Wiley (1957).

11. A. V. Granato and K. Lücke, Physical Acoustics Vol. 4a, p. 225, Academic Press (1966).

12. A. Granato and K. Lücke, J. Appl. Phys. 27, 789 (1956).

13. Reference 13, p. 805.

14. A. V. Granato, A. Hikata and K. Lücke, Acta Met. 6, 470 (1958).

15. H. L. Caswell, J. Appl. Phys. 29, 1210 (1958).

16. T. S. Hutchison and D. H. Rogers, J. Appl. Phys. 33, 792 (1962).

17. A. H. Cottrell, Report of a Conference on the Strength of Solids, p. 30, University of Bristol, England, Physical Society, London (1948).

18. J. Weertman and E. J. Salkovitz, Acta Met. 3, 1 (1955).

19. J. Friedel, C. Boulanger and C. Crussard, Acta Met. 3, 380 (1955).

20. A. D. N. Smith, Phil. Mag. 44, 453 (1953).

21. A. S. Nowick, Acta Met. 3, 312 (1955); J. Appl. Phys. 25, 1135 (1954).

22. A. H. Cottrell and B. A. Bilby, Proc. Phys. Soc. A 62, 49 (1949).

23. R. B. Gordon and A. S. Nowick, Acta Met. 4, 514 (1956).

24. G. Alers, Phys. Rev. 97, 863 (1955).

25. A. Hikata, R. Truell, A. Granato, B. Chick, and K. Lücke, J. Appl. Phys. 27, 396 (1956).

26. A. Hikata and R. Truell, J. Appl. Phys. 28, 522 (1958).

27. W. Köster, Z. Metallk. 32, 282 (1940).

28. R. R. Nothdurft, Thesis, University of Missouri at Rolla (1964).

29. Mikio Ueki, Thesis, Cornell University, NYO-2471-19 (1966).

30. D. R. Secrist and L. G. Wisnyi, Acta Crystallographica 15, 1042 (1962).

31. A. E. Schwaneke, BuMines Rept. of Inv. No. 6419 (1964).

32. J. Marx, Rev. Sci. Instr. 22, 504 (1951).

33. A. E. Schwaneke, Private communication.

34. N. F. Fiore and C. L. Bauer, Acta Met. 12, 1329 (1964).

35. C. A. Wert, J. Appl. Phys. 20, 29 (1949).

36. J. Weertman and J. S. Koehler, J. Appl. Phys. 24, 624 (1953).

37. T. Hinton and J. G. Rider, J. Appl. Phys. 37, 582 (1966).

38. R. R. Hasiguti, N. Igata and K. Tanaka, Acta Met. 13, 1083 (1965).

39. S. Harper, Phys. Rev. 83, 709 (1951).

40. W. A. Johnson and R. F. Mehl, Trans. Am. Inst. Min. Metall. Engrs. 135, 416 (1939).

41. K. Yamafuji and C. L. Bauer, J. Appl. Phys. 36, 3288 (1965).

42. J. W. Marx and J. S. Koehler, Symposium on the Plastic Deformation of Crystalline Solids, Office of Naval Research (1950).

43. J. Friedel, Dislocations, p. 214, Pergamon Press Ltd. (1964).

44. P. G. Shewnon, Trans. Am. Inst. Min. Metall. Engrs. 206, 918 (1956).

45. J. Weertman and E. I. Salkovitz, J. Appl. Phys. 27, 1251 (1956).

46. F. Seitz, Adv. in Phys. 1, 43 (1952).

47. J. Frankel and L. V. Meisel, J. Appl. Phys. 38, 641 (1967).

48. C. L. Bauer, Phil. Mag. 11, 827 (1965).

49. H. G. Van Bueren, Imperfections in Crystals, p. 188, Interscience Publishers Inc., New York (1961).

50. N. F. Fiore, J. Appl. Phys. 37, 878 (1966).

51. D. O. Thompson and D. K. Holmes, J. Appl. Phys. 27, 713 (1956).

52. R. M. Stern and A. V. Granato, Acta Met. 10, 358 (1962).

53. E. C. Oren and C. L. Bauer, Acta Met. 15, 773 (1967).

54. F. S. Ham, J. Appl. Phys. 30, 915 (1959).

55. Reference 57, p. 453.

56. D. N. Beshers, J. Appl. Phys. 30, 252 (1959).

57. G. V. Raynor, The Physical Metallurgy of Magnesium and its Alloys, Pergamon Press Ltd. (1959).

58. D. Hardie and R. N. Parkins, Phil. Mag. 4, 815 (1959).

59. E. G. Henneke, II, and R. E. Green, Jr., Trans. Met. Soc. AIME 239, 231 (1967).

60. N. F. Mott and F. R. N. Nabarro, Report of a Conference on Strength of Solids, Physical Society, London, p. 1 (1948).

61. J. D. Eshelby, Proc. Roy. Soc. (London) A197, 396 (1949).

62. G. Leibfried, S. Physik 127, 344 (1950).

63. W. P. Mason, J. Acoust. Soc. Am. 32, 458 (1960).

APPENDIX

Definition and Evaluation of Some of the Parameters Appearing in the Granato-Lücke Theory

a - Burger's vector, which is equal to the lattice parameter in the basal plane for magnesium.

= 3.209 A° for pure Mg

= 3.186 A° for .05% Zn in Mg

= 3.197 A° for .03% Al in Mg

= 3.190 A° for .05% Al in Mg

= 3.151 A° for .15% Al in Mg

η - Misfit parameter, which is the fractional change in the lattice constant, a, with a change in solute concentration, C.

$= (1/a)\partial a/\partial c$

The change in the lattice parameter of magnesium with additions of Zn and Al has been measured by Raynor[57] and Hardie and Parkins,[58] and their results give the following values for η:

= -.145 for Zn

= -.121 for Al

For additions of iron, copper, and calcium, the following approximation for η will be used:

$= (d - d_o)/ d_o$ where d_o is the atomic diameter of the added element. In this manner the following values of η are obtained:

= .20 for Fe and Cu

= .23 for Ca

G - Shear modulus, which is isotropic in the basal plane for magnesium and equals $1/ S_{44} = C_{44}$

$= 1.658 \times 10^{11}$ dyne/cm^2

ν - Poisson's ratio

= .33 approximately

E - Young's modulus

= $(22.1 \sin^4\theta + 19.7 \cos^4\theta + 50.5 \sin^2\theta\cos^2\theta)^{-1} \times 10^{13}$ dyne/cm^2

= 4.74×10^{11} dyne/cm^2 for $\theta = 22°$

Ω - Orientation factor

By a comparison of equation (67) in the first article by Granato and Lücke and equation (8) in their first review article[10] we find:

$\Omega = [4(1-\nu)/\pi G]\, E(\theta)\, \Sigma_{i=1}^{3} R_i^2 \Lambda_i / \Lambda$, where R_i is the resolved shear stress factor for the ith slip system, Λ_i is the dislocation density for the ith slip system, and the other symbols have been defined above. Also, $R_i = \sin\theta\cos\theta\cos\phi$, where ϕ is the angle between the slip direction and the projection of the cylinder axis on the basal plane. If the dislocation density is assumed to be equal for all three slip systems, we have $\Lambda = 3\,\Lambda_i$, and in this case we find:

$\Omega = [4(1-\nu)/\pi G]\, E(\theta)\, \Sigma_{i=1}^{3} R_i^2/3$

If only one slip system operates, then we have $\Sigma R_i^2 = \sin^2\theta\cos^2\theta\cos^2\phi$. If all three slip systems operate, Henneke and Green[59] show that $\Sigma R_i^2 = \sin^2\theta\cos^2\theta\,/\,2$. We will assume for convenience that all three systems operate. Using the above values for G and ν, we have:

$\Omega = 9.215 \times 10^{13}\ E(\theta) \sin^2\theta\cos^2\theta$

= .0525 for $\theta = 22°$

= .0285 for $\theta = 74°$

C' - Dislocation line tension. Mott and Nabarro[60] have calculated this to be given as:

$C' = 2Ga^2/\pi(1-\nu)$

$= 1.51 \times 10^{-4}$ dyne

A - Parameter measuring the strength of the interaction between a solute atom and a dislocation. It is calculated by Cottrell[17] to have the following form:

$= (4/3)G\eta r_o^3 a (1+\nu)/(1-\nu)$, where r_o is the atomic radius of the solvent atom and equals 1.76 A° for magnesium.

$= 2.17 \times 10^{-20} \eta$ dyne cm^2

B - Damping constant for the moving dislocation.

Three separate theoretical calculations have been made for the constant B. Eshelby[61] assumes the damping arises from irreversible heat flow in the region about the vibrating dislocation. Eshelby's formula for B is:

$= (Ga^2/10\kappa)(c_p - c_v/c_p) \ln(\kappa/\omega\ell_o^2)$, where G is the shear modulus, a, the lattice parameter, κ , the thermal diffusivity, c_p and c_v, the specific heat at constant pressure and volume respectively, , is the circular frequency, and ℓ_o, is a cut off length taken to be approximately 10^{-7} cm. For magnesium we have; $\kappa = .932$ cm^2/sec, $c_p = .235$ cal/gm °K for T = 300° K, and $c_p - c_v = 9\alpha_o^2 T\beta_o/\rho$, where β_o is the bulk modulus, α_o is the coefficient of linear expansion, T is the absolute temperature and ρ is the density. It is found that $c_p - c_v = 9 \times 10^{-3}$ cal/gm°K for T = 300° K. Thus for $\omega = 2\pi(31{,}000)$ rad/sec, we find:

$B = 1.4 \times 10^{-5}$ dyne sec / cm^2 for T = 300° K

$= 3.0 \times 10^{-5}$ dyne sec / cm^2 for T = 558° K

Liebfried[62] assumes the damping arises from the scattering of thermal phonons by the stress field of the dislocation.

Liebfried's formula is given as:

$B = 3kTZ/10v_s a^2$, where Z is the number of atoms per unit cell, v_s is the shear wave velocity, a is the lattice parameter, and kT has its usual meaning. For magnesium, $v_s = (C_{44}/\rho)^{1/2} = 3.08 \times 10^5$ cm/sec, and $Z = 2$.

Thus, using Liebfried's formula we find:

$B = 7.81 \times 10^{-5}$ for $T = 300°$ K

$= 1.45 \times 10^{-4}$ for $T = 558°$ K

Recently, Mason[63] interpreted the thermal waves in a crystal as a gas of phonons and calculated the energy loss of a dislocation moving through the gas from classical viscous-fluid flow theory. Mason's formula for B is:

$B = 1.43\ E'\ K_e/\beta'\ T\ \bar{c}$, where E' is the internal energy calculated from the Debye theory, β' is the electronic heat capacity coefficient equal to 3.15×10^{-4} cal/mole $°K^{-2}$ for magnesium, $\bar{c}$ is the Fermi velocity of electrons given by $\bar{c} = 2\pi h(3\pi^2 N_o)^{1/2}/m$ where N_o is the number of electrons per unit volume usually taken as the number of atoms per unit volume, m is the mass of the electron, K_e is the thermal conductivity due to electrons, and h is Planck's constant. For magnesium we find, $E'/T = 3.62$ cal/mole for $T = 300°$ K and $E'/T = 4.7$ cal/mole for $T = 558°$ K. These values are taken from the table of E'/T values as a function of Θ/T where Θ , the Debye temperature for magnesium, is $342°$ K. We also have $\bar{c} = 1.25 \times 10^{-8}$ cm/sec and $K_e = .376$ cal/sec cm °K. With these values, we find using Mason's formula:

$B = 1.67 \times 10^{-5}$ for $T = 300°$ K

$= 2.1 \times 10^{-5}$ for $T = 558°$ K

K - Parameter related to the force required to pull a pinning point from a dislocation. In the Granato-Lücke theory it is given by:

$K = \pi f_m/(4\eta a^2 RE)$, where f_m is the force required to produce breakaway, R is the resolved shear stress factor and the other symbols have been defined earlier. Cottrell[17] calculated f_m to be given by $4G\eta a^4/X_b^2$, where X_b is the distance the impurity atom is from the dislocation when breakaway occurs. Using this relation for f_m we find:

$K = \pi G/[X_b/a)^2 RE]$

If we assume X_b is equal to 2 or 3 lattice parameters when breakaway occurs, we fing:

$K = .78$ to $.35$ for $\theta = 22°$